

**SYNTHESIS AND CHARACTERIZATION OF UiO-66 (Zr-MOF) FOR
THE ADSORPTIVE REMOVAL OF MALATHION AND 2, 4-D FROM
AQUEOUS SOLUTION**

MSc THESIS

BANE KEBEDE GURMESSA

November 2018

HARAMAYA UNIVERSITY, HARAMAYA

**Synthesis and Characterization of UiO-66 (Zr-MOF) for the Adsorptive
Removal of Malathion and 2, 4-D from Aqueous Solution**

**A Thesis Submitted to the Department of Chemistry, Postgraduate Program
Directorate**

HARAMAYA UNIVERSITY

**In Partial Fulfillment of the Requirements for the Degree of
MASTER OF SCIENCE IN ANALYTICAL CHEMISTRY**

Bane Kebede Gurmessa

November 2018

Haramaya University, Haramaya

HARAMAYA UNIVERSITY

POSTGRADUATE PROGRAM DIRECTORATE

I hereby certify that we have read and evaluated this Thesis titled ‘Synthesis and Characterization of UiO-66 (Zr-MOF) for the adsorptive removal of Malathion and 2, 4-D from Aqueous Solution’ prepared under our guidance by Bane Kebede. We recommend that it be submitted as fulfilling the thesis requirement.

Abi Tadesse (PhD)

Major Advisor

Signature

Date

Endale Teju (PhD)

Co-Advisor

Signature

Date

Isabel Diaz (Prof.)

Co-Advisor

Signature

Date

As a member of the Board of Examiners of the MSc Thesis Open Defense Examination, we certify that we have read and evaluated the thesis prepared by Bane Kebede and examined the candidate. We recommend that the thesis be accepted as fulfilling the Thesis requirement for the degree of Master of Science in Analytical chemistry.

Chairperson

Signature

Date

Internal Examiner

Signature

Date

External Examiner

Signature

Date

STATEMENT OF THE AUTHOR

By my signature below, I declare and affirm that this Thesis is my own work. I have followed all ethical and principles of scholarship in the preparation and compilation of this Thesis manuscript. Any scholarly matter that is included in the Thesis has been given recognition through citation.

This Thesis is submitted in partial fulfillment of the requirements for MSc degree at the Haramaya University. The Thesis is deposited in the Haramaya University Library and is made available to borrowers under the rules of the Library. I solemnly declare that this manuscript has not been submitted to any other institution anywhere for the award of any academic degree, diploma, or certificate.

Brief quotations from this Thesis may be made without special permission provided that accurate and complete acknowledgement of the source is made. Requests for permission for extended quotations from or reproduction of this manuscript in whole or in part may be granted by the Head of the Department or Director of Postgraduate Program Directorate when in his or her judgment the proposed use of the material is in the interest of scholarship. In all other instances, however, permission must be obtained from the author of the Thesis.

Name: Bane Kebede Gurmessa

Signature: _____

Date: November 2018

Department: Chemistry

BIOGRAPHICAL SKETCH

The Author was born on September 2, 1992 GC at Horro Guduru Zone, Abbay Chomman Woreda, Dino Berama Kebele. He attended his elementary school Ficha Kolobo Primary School. As well as he finished his secondary and preparatory school at Fincha Senior Secondary and Preparatory School. Then after he joined Jimma University 2011/2012 GC in regular program and received Bsc degree in Chemistry with great distinction in July 2014. After graduation, he was employed at Haramaya University Laboratory Management Directorate as senior technical assistant and served as Soil, plant and water analysis until he joined postgraduate program at the Haramaya University to pursue his MSc study in Analytical Chemistry in 2017.

ACKNOWLEDGMENTS

First I would like to express my deepest gratitude to Haramaya University Laboratory Management Directorate Director, Dr. Nigussie Bussa for opening the closed road to the right direction of learning and as he no one can heartily support whatever he has at hand, but partially. I really express my deep sense of indebtedness, gratitude and thanks to my supervisors, Dr. Abi Taddesse, Dr. Endale for their encouragement with critical comments, genuine guidance which provided me a chance to explore further from the very beginning of the selection of the research topic until the completion of this work. I don't forget to thank Dr. Meseret Amde for giving comments.

I want to thank the Ministry of Education for providing me financial support to accomplish this work. I gratefully acknowledge Addis Ababa University, Addis Ababa and Adama science and Technology University.

ACCRONYMS AND ABBREVIATIONS

2,4- D	2, 4-Dichlorophenoxyacetic Acid
BET	Brunauer–Emmet-Teller
EDX	Energy dispersive X-ray Spectroscopy
EPA	Environmental Protection Agency
FTIR	Fourier Transforms Infrared Spectrometry
LAG	Liquid-Assisted grinding
MIL	Materials Institute of Lavoisier
MOFs	Metal-Organic Frameworks
OP	Organophosphorus pesticides
SEM	Scanning electron microscopy
SOCs	Synthetic organic chemicals
UiO	University of Oslo
UV-Vis	Ultra violet visible spectrophotometer
XRD	X-ray diffractometer

TABLE OF CONTENTS

STATEMENT OF THE AUTHOR	iii
BIOGRAPHICAL SKETCH	iv
ACKNOWLEDGMENTS	v
ACCRONYMS AND ABBREVIATIONS	vi
LIST OF TABLES	x
LIST OF FIGURES	xi
LIST OF TABLE IN THE APPENDIX	xii
LIST OF FIGURE IN THE APPENDIX	xiii
ABSTRACT	xiv
1. INTRODUCTION	1
2. LITERATURE REVIEW	5
2.1. Pesticides	5
2.2.1. <i>Malathion</i>	6
2.2.2. <i>2, 4-D (2, 4-Dichlorophenoxyacetic acid)</i>	7
2.3. Environmental Impacts of Pesticides (Malathion and 2, 4-D)	8
2.4. Removal of Pesticides (Malathion and 2, 4-D)	10
2.5. Metal Organic Frameworks	11
2.6. Synthesis Methods of MOFs	13
2.6.1. <i>Hydro or Solvothermal Synthesis</i>	13
2.6.2. <i>Microwave Assisted Synthesis</i>	14
2.6.3. <i>Ionothermal Synthesis</i>	14
2.6.4. <i>Solvent-Free/ Mechanochemical Synthesis</i>	15
2.6.5. <i>Electrochemical Synthesis</i>	16
2.7. Applications of MOFs	17
2.7.1. <i>Hydrogen Storage</i>	17
2.7.2. <i>Catalysis</i>	18
2.7.3. <i>Energy Storage</i>	18
2.7.4. <i>Sensors</i>	19
2.7.5. <i>Drug Delivery</i>	19
2.8. Adsorption	19

2.9. Fundamentals of Adsorption	20
2.9.1. Langmuir Isotherm Model	21
2.9.2. Freundlich Isotherm Model	22
2.10. Kinetics Studies	23
2.10.1. Pseudo-First-Order	24
2.10.2. Pseudo-Second Order	24
3. MATERIALS AND METHODS	25
3.1. Experimental Sites	25
3.2. Apparatus, Instruments and Chemicals	25
3.2.1. Apparatus and Instruments	25
3.2.2. Chemicals and Reagents	25
3.3. Experimental Procedure	26
3.3.1. Synthesis of UiO-66(Zr-MOFs)	26
3.3.2. Characterization of UiO-66 MOFs	26
3.3.3. Preparation of Malathion and 2, 4-D Standard Solutions	26
3.3.4. Batch Adsorption Studies	27
3.4. Optimization of Experimental Parameters	27
3.4.1. The Effect of pH	27
3.4.2. Effect of Adsorbent Dose	27
3.4.3. Effect of Contact Time	28
3.4.4. Effect of Agitation Speed	28
3.4.5. Effect of Initial Concentration	28
3.5. Kinetics Studies	28
3.6. Adsorption Isotherms	29
3.7. Thermodynamic Studies	29
3.8. Determination of pH of Zero Charge (pH _{PZC})	29
3.9. Desorption Studies	29
3.10. Recyclability	30
3.11. Real Sample Analysis	30
4. RESULT AND DISCUSSION	31
4.1. Characterization of UiO-66(Zr) Adsorbent	31
4.1.1. FTIR Spectra Analysis	31

4.1.2. <i>PXRD Analysis</i>	32
4.1.3. <i>TGA Analysis</i>	34
4.1.4. <i>Determination of pH point Zero Charge</i>	35
4.2. Optimization of Experimental Conditions	36
4.2.1. <i>The Effect of pH</i>	36
4.2.2. <i>Effect of Adsorbent Dose</i>	38
4.2.3. <i>Effect of Contact Time</i>	39
4.2.4. <i>Effect of Agitation Speed</i>	40
4.2.5. <i>Effect of Initial Concentration</i>	41
4.3. Adsorption Isotherms Study	43
4.4. Adsorption Kinetics	47
4.5. Adsorption Thermodynamics	50
4.6. Desorption and Reusability	53
4.7. Real Sample Analysis	56
5. CONCLUSION AND RECOMMENDATION	57
5.1. Conclusion	57
5.2. Recommendation	58
6. REFERENCES	60
7. APPENDICES	71

LIST OF TABLES

Table	Page
1. The physico chemical properties of Malathion	7
2. Structural and some properties of 2, 4-D	8
3. Criteria for Langmuir adsorption isotherm	22
4. Langmuir and Freundlich isotherm constants for adsorption of Malathion, 2, 4-D and Mixture on UiO-66 (Zr)	45
5. The values of parameters and correlation coefficients of kinetic models	49
6. Thermodynamic parameters for 2, 4-D and Malathion adsorption onto UiO-66(Zr)	52
7. Recovery (%) values of UiO-66(Zr) based analysis of real sample	56

LIST OF FIGURES

Figure	Page
1. Classes of Pesticides.	5
2. Structures of different MOFs with the terephthalate (BDC) as a linker.	12
3. Hydro/solvothermal synthesis of MOFs.	13
4. Microwave-assisted solvothermal synthesis of MOFs.	14
5. Mechanochemical synthesis of MOFs.	15
6. Electrochemical synthesis of MOFs.	16
7. Summary of the various methods employed for the synthesis of crystal MOFs.	17
8. FTIR spectra of as synthesized UiO-66(Zr).	31
9. FTIR spectra of UiO-66 before and after adsorption of Malathion and 2, 4-D.	32
10. PXRD pattern of as synthesized UiO-66(Zr).	33
11. TGA of UiO-66(Zr) before (a), after adsorption of Malathion (b) and 2, 4-D (c).	35
12. pH point zero charge (pH _{PZC}) of UiO-66.	36
13. Effect of pH on the removal of Malathion, 2, 4-D and mixture (at Co = 5 mg/L; adsorbent dose = 0.1 g; contact time = 60 min; agitation speed = 150 rpm).	38
14. Effect of Adsorbent dose on the removal of Malathion, 2, 4-D and Mixture onto UIO-66 (at Co = 5 ppm; Contact time = 1h; Agitation speed = 150 rpm and optimized pH = 4, 3, 4 respectively).	39
15. Effect of Contact time on the removal of Malathion, 2, 4-D and mixture (at Co = 5 mg/L; Agitation speed = 150 rpm and optimized pH = 4, 3 and 4; Adsorbent dose = 0.1 g respectively).	40
16. Effect of Agitation speed on the removal of Malathion, 2, 4-D and mixture onto UIO-66 (at Co = 5 ppm and optimized pH = 4, 3 and 4; Adsorbent dose = 0.1 g; Contact time = 1 hr respectively).	41
17. Effect of Initial concentration on the removal of Malathion, 2, 4-D and mixture onto UIO-66 (at optimized pH = 4, 3 and 4; Adsorbent dose = 0.1 g; Contact time = 1 hr; Agitation speed = 125,100,150 rpm respectively).	43
18. Langmuir (a ¹ , b ¹ and c ¹) and Fredliuch (a ¹¹ , b ¹¹ and c ¹¹) isotherm for Adsorption of Malathion, 2, 4-D and mixture on UiO-66(Zr), respectively	46
19. Graph for the pseudo-first order (a, b and c) and pseudo-second order (a ¹ , b ¹ and c ¹) of the adsorption of Malathion, 2,4-D and mixture on to UiO-66(Zr) respectively.	49
20. Thermodynamic graph of the lnK against 1/T of 2, 4-D (a) and Malathion (b).	51
21. Desorption of Malathion and 2, 4-D using different reagents.	54
22. Regeneration of UiO-66(Zr) for adsorption of Malathion and 2, 4-D.	55

LIST OF TABLE IN THE APPENDIX

Appendix table	Page
1. Effect of pH on adsorption capacity Malathion, 2, 4-D and mixture on UiO-66(Zr)	76
2. Effect of Contact time on adsorption capacity Malathion, 2, 4-D and mixture on UiO-66(Zr)	77
3. Effect of Adsorbent dose on adsorption capacity Malathion, 2, 4-D and mixture on UiO-66(Zr)	78
4. Effect of Agitation speed on adsorption capacity Malthion, 2, 4-D and mixture on UiO-66(Zr)	79
5. Effect of Initial concentration on adsorption capacity Malathion, 2, 4-D and mixture on UiO-66(Zr)	80
6. Results for Malathion, 2, 4-D and mixture adsorption isotherms of UiO-66(Zr)	81
7. Results for Malathion kinetic Adsorption of UiO-66(Zr)	82
8. Results for 2,4-D kinetic Adsorption of UiO-66(Zr)	83
9. Results for mixture kinetic Adsorption of UiO-66(Zr)	84
10. Dimensionless equilibrium parameter (R_L)	85
11. Recovery (%) values of UiO-66(Zr) based analysis in real water samples (n = 3 mean \pm SD)	86

LIST OF FIGURE IN THE APPENDIX

Appendix figure	Page
1. Calibration curve of Malathion (a^1, a^{11}), 2,4-D (b^1, b^{11}) and mixture(c^1, c^{11}) for pH and contact time optimization, respectively.	87
2. Calibration curve of Malathion (a^1, a^{11}), 2, 4-D (b^1, b^{11}) and mixture (c^1, c^{11}) for Agitation speed and Adsorbent dose optimization, respectively.	88
3. Calibration curve of Malathion (a^1, a^{11}), 2, 4-D (b^1, b^{11}) and mixture (c^1, c^{11}) for initial concentration optimization and Adsorption isotherm, respectively.	89
4. Calibration curve of Malathion (a), 2,4-Dm(b) and mixture (c) for kinetic studies.	90

Synthesis and Characterization of UiO-66 (Zr-MOF) for the adsorptive removal of Malathion and 2, 4-D from Aqueous Solution

ABSTRACT

UiO-66(Zr) metal organic frame work was successfully synthesized by solvothermal method. The as synthesized UiO-66(Zr) was characterized using FTIR, XRD, TGA and SEM techniques to investigate the functional group, structural crystallinity, thermal stability and morphology of the material, respectively. Adsorptive removal of Malathion and 2, 4-D with UiO-66(Zr) were studied to understand its applicability in the removal of pesticides from contaminated water. According to the outcome of this study, UiO-66(Zr) exhibited fast adsorption capacity (t, one hour) and importantly the adsorption of both pesticides over UiO-66(Zr) were favorable at low concentrations. The high adsorption capacity of UiO-66(Zr) may be attributed to its high porosity, smaller particle sizes and high crystalline nature. The effects of different experimental parameters, namely, pH, adsorbent dose, contact time, speed of agitation and initial pesticides concentration were studied by using batch experiment. The adsorption isotherm experiment showed that the equilibrium data were fitted to the Freundlich model. The kinetic study demonstrated that pseudo-second-order model gave a best fitting to the adsorption of Malathion and 2, 4-D on the (UiO-66) adsorbent. The thermodynamic parameters were calculated and the results show that the adsorption of Malathion and 2,4-D on the adsorbent is a spontaneous and exothermic process. To evaluate the matrix effect on adsorption performance of UiO-66(Zr), real sample, (tap water) were spiked and its recovery were evaluated. The results revealed that the recovery values were satisfactory (found to be in the range of (70-120%), and it can be said that the matrix effect from the water samples on the adsorption of Malathion and 2, 4-D on to UiO-66(Zr) was not affect their adsorption. Therefore, UiO-66(Zr) is the promising adsorbent for the removal of pesticides in waste water.

Keywords: 2, 4-D, Adsorbent, Adsorption, Malathion, UiO-66(Zr) metal organic frame work and Real sample

1. INTRODUCTION

Pesticides are chemicals which can be used to facilitate the growth of the plants, to prevent agricultural harvests from a variety of damages and to increase the production of crops. The rapid and indiscriminate use of pesticides in modern agriculture practices for social betterment such as to chop crop losses, enhance yield and meet rising food need has become a matter of social accountability (Bai *et al.*, 2006). On the other hand, extensive consumption of a variety of pesticides has raised concerns at local, regional, national and global scales because of the fact that pesticide residues may be ingested by human *via* foodstuff, drinking water and/or air, and are being bio accumulated in blood, mother milk, and tissues. Hence, pesticides contribute to symbolic human symptomatic illnesses, both acute and chronic (FAO, 2014).

In spite of their numerous merits, pesticides are among the most dangerous pollutants on humans and other animals, as well as on the equilibrium of ecosystems because of their stability, mobility, capable of bioaccumulation and long-term effects on the biota. When pesticides are introduced into the environment through spraying on crops, some parts of these chemicals reside in the area where applied and/or transported to various environmental compartments (Deng *et al.*, 2017; Endale *et al.*, 2017). They may reach streams or groundwater through spillage, leaching and adsorbed by plants and eatable vegetables which are the main sources of pesticides exposure in living organisms. Therefore, effluents discharged without treatment into surface water such as rivers, lakes can cause environmental damage such as polluting ground, surface and drinking water (Kumar *et al.*, 2014).

Among different pesticides, Malathion and 2, 4-Dichlorophenoxyacetic acid (2, 4-D) are among the abundantly used pesticides in agriculture, industrial and public health field (Beomet *et al.*, 2013; Kumar *et al.*, 2014).

Malathion (Diethyl dimethoxythiophosphorylthio succinate) which is a broad spectrum, highly toxic organophosphorous insecticide (contribute 73% poisoning), registered in 1956, is abundantly used in agriculture, industrial and public health field to kill insects, ants, aphids, bagworm, beetle, cotton leaf worm, mosquito, lice and the like by inhibiting Cholinesterase enzyme (Venugopal *et al.*, 2011). Malathion is rapidly and effectively absorbed by all routes including the gastrointestinal tract, skin, mucous membrane and lungs and causes blurred vision,

excessive salivation, headache, giddiness, nausea and vomiting due to its active metabolite malaoxon which is about 61 times more toxic than malathion. It can also cause child leukemia, anemia, kidney failure, and human birth defects. It is believed that malathion is an agent in causing DNA abnormalities at all doses. Besides, there are also reports of malathion causing “deletions” in one section of the chromosome thereby inducing mutations in human beings (Nair and Pradeep, 2007). It should be also noted that malathion can persist in the human body for at least two generations (Kumar *et al.*, 2014).

2, 4-dichlorophenoxyacetic acid (2, 4-D) is a chlorinated phenoxy herbicide, which have been also widely used for post emergence control of annual and perennial broad-leaved weeds in cereal cropland, pastures, forests and many other crops because of its low cost and good selectivity. However, 2, 4-D exhibits serious ecological effects (Mansooreh *et al.*, 2014). In addition to its toxic effects on birds, beneficial insects, soil annelids and non-target plants, it also negatively impacts aquatic life, affecting algae, small invertebrates, amphibians, and fishes, especially in their juvenile stages. Since this compound exhibit high water-solubility, lifetime and mobility, its continuous use may cause soil percolation and groundwater contamination growth (Carlos *et al.*, 2013; Mansooreh *et al.*, 2014).

The wide range of pesticides used makes it extremely difficult to produce a single method for pesticide disposal that applies universally. As a result, chemical oxidation with ozone, precipitation, flotation, ion exchange, biological degradation and adsorption are among the most commonly used strategies. Several authors have been successfully studied a variety of cost effective and locally available adsorbents such as: bagasse fly ash (Gupta *et al.*, 2002) oil shale (Qodah *et al.*, 2007), date palm stones (Hameed *et al.*, 2009), and clays (Pal and Vanjara, 2001; Salman *et al.*, 2011) for the removal of different types of pesticides. Nevertheless, there are some disadvantages associated with these types of adsorbents such as incompatible for column operation because of non-granulometric nature which results in choking of industrial columns, adsorption of pesticides at low levels, and high regeneration cost. Other techniques such as reverse osmosis, nanofiltration and advanced oxidation processes are vulnerable due to the formation of undesirable oxidation byproducts and membrane fouling (Naushadn *et al.*, 2013).

Ion exchange is one of the most eco-friendly and economical technologies, because most of the materials can be reused, has high sensitivity and selectivity, and the operation process is simple. Even the existing organic materials that can be used in ion exchange are sol-gel adsorbents and polymer resins or membranes, which show rapid exchange kinetics and high ion-exchange capacity, but their low thermal and chemical stability limit their application. Although inorganic ion exchangers, such as zeolites and layered double hydroxides (Moya, 2015) have high thermal and chemical stability, their exchange kinetics and ion exchange capacity are low (Zhang *et al.*, 2014; Chen *et al.*, 2017).

Among the aforementioned approaches for the removal of pesticides, adsorption was frequently used because of its unique advantages, such as low cost, simplicity in operation and fewer harmful by products (Chatterjee *et al.*, 2010). Numerous reports have been issued in the pool of literature for the removal of 2, 4-D and malathion using various adsorbents such as activated carbon, chitosan, resin and bentonite (Salman and Hameed, 2010; Mansooreh, *et al.*, 2014). However, these adsorbents suffered the problem of low adsorption capacity. For instance, adsorption of 2, 4-D with chitosan reported (El Harmoudi *et al.*, 2014) have low adsorption capacity and sorption by coal and bio-based activated carbon adsorbents have used high equilibrium sorbate concentrations (10-200 mg/L) that are not environmentally relevant (Kearns *et al.*, 2014). Consequently, the searching for adsorbents with high specific surface areas and high selectivity for specific contaminants is evident (WHO, 1993; Bazrafshan *et al.*, 2013).

Recently, progress on Nano porous materials has been remarkable for both syntheses and applications. Porous MOFs have attracted considerable attention because of their high and regular porosity (Naushadn *et al.*, 2013). MOFs are a new kind of adsorbent that can be applied for the adsorption of pesticides due to the reason that MOFs composed of organic linkers and inorganic nodes, mainly to their unusual and exceptional features such as accessible cages, tunnels, high porosity, and modifiable pores, have shown great potential in various applications including adsorption (Rostami *et al.*, 2018), separation (Zhang and Chen, 2017), catalysis (Zhang *et al.*, 2018), sensing (Li *et al.*, 2017), among others. One advantage of crystalline MOFs is the regular array of well-defined pores, which can achieve ultrahigh porosity and surface area (Farha *et al.*, 2010; Furukawa *et al.*, 2010).

UiO-66 (UiO stands for University of Oslo), one kind of Zr-MOF, has gained a lot of attention recently since it exhibit exceptionally high chemical and thermal stability due to Zr- carboxylate strong bond (Yingran *et al.*, 2017). This has opened a new direction in application of UiO-66 (Zr-MOF), for adsorption of 2, 4-D and Malathion in aqueous solution. Even though only scarce effort has been reported for the synthesis of this MOF, there is no report on utilization of the UiO-66 (Zr-MOF) in the adsorptive removal of pesticides including 2, 4-D and Malathion from contaminated water. However, it should be noted that the MOFs have been used in the removal of several other organic contaminants. Chen and coworkers studied the adsorptive removal of various anionic and cationic dyes using UiO-66 and NH₂-UiO-66 MOF (Chen *et al.*, 2015). Hitherto, there are no reports on the use of Zr- MOF for the adsorptive removal of 2, 4-D and Malathion to the best of our knowledge. Therefore the main purpose of this study was focused on to synthesize and investigate the sorption properties of UiO-66 (Zr- MOF) on the 2, 4-D and Malathion from aqueous solution.

Objectives

General Objective

- ☞ Synthesis and study the sorption behavior of the UiO-66 (Zr-MOF) for 2, 4-D and Malathion from aqueous solution.

Specific objectives

- To synthesize UiO-66 (Zr-MOF) using solvothermal method.
- To characterize the synthesized MOF with FT-IR, TGA, XRD, UV and SEM.
- To examine the sorption behavior of the synthesized UiO-66 (Zr- MOF) sorbent on (2, 4-D) and Malathion.
- Evaluate the parameters influencing adsorption efficiencies such as: pH, adsorbent dose, initial concentration and contact time.
- To study adsorption isotherm and adsorption kinetics.
- To examine reusability of the adsorbent.

2. LITERATURE REVIEW

2.1. Pesticides

Pesticides can be defined as substances or mixture of substances, natural or synthetic, intended for preventing, destroying, repelling or mitigating any pest. (The term pest includes harmful, destructive or troublesome to animals, plants or microorganisms). They are considered a vital component of modern farming, playing a major role in maintaining high agricultural productivity. Although pesticides are widely used in agriculture, their use may create environmental hazards. Consequently, high-input intensive agricultural production systems in which greater and widespread use of pesticides to manage pests have emerged as a dominant feature (Mustapha *et al.*, 2017). Because of their widespread uses; they leach into surface and ground water and are therefore present in drinking water as well. They persist in the environment and pose a significant health threat and among the possible effects related to this exposure include; genetic damage has significant health implications for the induction of lung cancer, lymphoma, pancreatic cancer, bladder cancer and leukemia (FAO, 2014).

Different classes of pesticides are there based on their application. Among these the main groups are as follows;

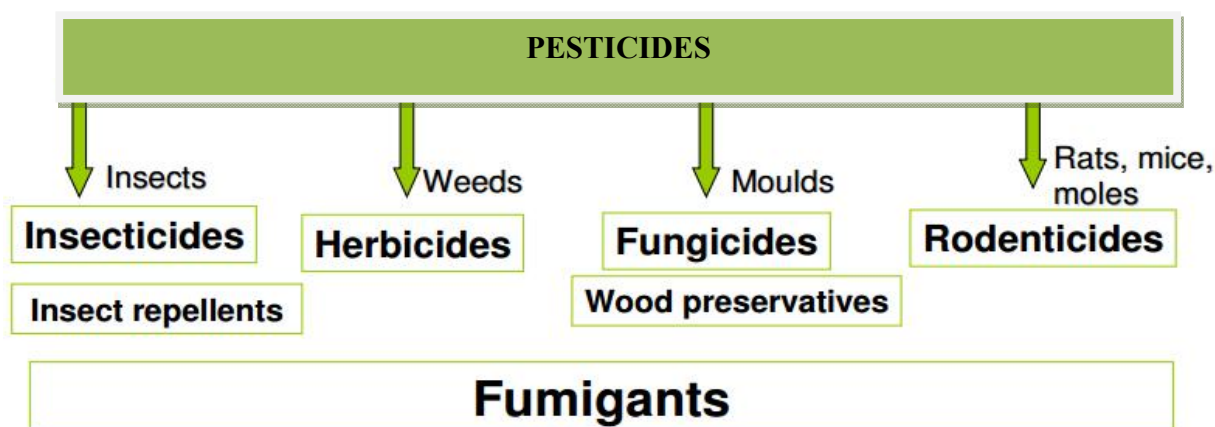


Figure 1. Classes of Pesticides.

Fumigants are pesticides that exist as a gas or a vapour at room temperature and may be used as insecticides, fungicides or rodenticides, especially in closed storage places as they kill every

living organism. They are extremely toxic, due to their physical properties, rapid environmental dissemination and human or animal absorption (Guangcai *et al.*, 2016).

Based on their chemical structure, pesticides are divided into four general categories: (1) organophosphorus, (2) organochlorine, (3) carbamate, and (4) pyrethroid. Due to their long-term stability and fear of their long-term effects, organochlorinated compounds have been replaced by organophosphorus pesticides (OP) (Dehghania *et al.*, 2017). Moreover, each of these organophosphorus pesticide compounds shows special characteristics, since phosphate esters (organophosphates or esters of phosphoric acid) contain different ratios of oxygen, sulfur, carbon and nitrogen atoms in their structure and these atoms are connected to a central phosphorus atom. These compounds have also the highest consumption among the pesticide compounds, so that in some areas of countries, the amount of organophosphate pesticides in water is far more than the standard proposed by the Environmental Protection Agency (EPA) (Costa *et al.*, 2008; Lozowicka *et al.*, 2014).

2.2.1. Malathion

Malathion, an organophosphorus pesticide with a molecular formula of $C_{10}H_{19}O_6PS_2$, used for a large variety of pests, has been most widely used in agriculture, industrial and public health field to kill insects, ants, aphids, bagworm, beetle, cotton leaf worm, mosquito, lice etc. (Naushadn *et al.*, 2013). It is a broad spectrum, highly toxic organophosphorus insecticide, registered in 1956. Malathion is one of the most common organophosphate toxicants in the world and the highest consumption among the pesticide compounds. This pesticide has low thermal stability, decompose rapidly with increasing temperature and form toxic substances (Dehghania *et al.*, 2017). Exposure to high amounts of malathion in the air, water and food may cause difficulty in breathing, vomiting, chest tightness, diarrhea, blurred vision, salivation, watery eyes, dizziness, sweating, headaches, loss of consciousness and even death. According to (Vasimalai and John, 2013) report Malathion can persist in the human body for at least two generations. It is suspected to cause kidney problems, human birth defects and child leukemia. It affects nervous system, immune system, adrenal glands, liver and also carcinogenic in nature. Apart from this it is toxic to birds, fishes other aquatic invertebrates and honey bees (Pal and Vanjara, 2001; Bonner *et al.*, 2006).

Table 1. The physico chemical properties of Malathion

Physical properties	Value	Chemical properties	
			Values
Nature	Amber liquid	Molecular formula	C ₁₀ H ₁₉ PS ₂
		Structure	
Melting point	2.85 °C	Molecular weight	330.36 g /mol
Boiling point	156-157 °C	Solubility Water	145 ppm (20 °C)
Specific Gravity	1.23°C	Solubility in organic solvent	Miscible
Acute toxicity	High		

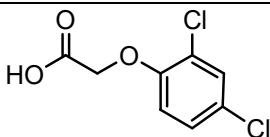
2.2.2. 2, 4-D (2, 4-Dichlorophenoxyacetic acid)

Dichlorophenoxyacetic acid (2,4-D) is a conventional herbicide that has been widely used in agricultural farms to control the weeds. Initially it was first developed during World War II and became famous as a component of the controversial Agent Orange used during the Vietnam War (Salman and AL-Saad, 2012). Recently it is being commonly used for controlling in a wide range of broad leaf weeds, cereal crops, pastures and gardens because of low cost and good selectivity. The 2,4-D residues are often reported in surface and groundwater due to low soil sorption and high rate for leaching. 2,4-D is classified as a possible carcinogen and mutagen by the International Agency for Research on Cancer (Ding *et al.*, 2012) and is one of the widely-known endocrine disrupting chemicals. 2, 4-D is of relatively low toxicity to animals but some formulations can cause severe eye damage. Certain crops, such as grapes, are highly sensitive to 2, 4-D and application of this herbicide should be avoided if they are nearby. Due to water solubility of 2, 4-D and low soil adsorption coefficient, it can be detected in surface and

groundwater and also in the finished drinking water of many countries. The maximum contaminant level (MCL) for 2, 4-D is 0.07 mg/L for drinking water (Wen *et al.*, 2015).

Extensive use and poor biodegradability of 2, 4-D has resulted in its ubiquitous presence in the environment, and has led to contamination of surface and ground waters. 2, 4-D is a selective herbicide that kills dicots (but not grasses) by mimicking the growth hormone auxin, which causes uncontrolled growth and eventually death in susceptible plants (Barr *et al.*, 2007).

Table 2. Structural and some properties of 2, 4-D

Name	2,4-Dichlorophenoxy acetic acid
Pesticide class	Phenoxy herbicide
Molecular formula	C ₈ HCl ₂ O ₃
Structure	
Molecular weight	221 g/mol
Appearance	White powder
Solubility in water	890 mg/l (25)
Dissociation constant(pK _a)	2.73

2.3. Environmental Impacts of Pesticides (Malathion and 2, 4-D)

The residual pesticides present in the environment pose serious health risks to consumers worldwide. As a result, they are considered one of the most important classes of chemical pollutants due to their toxicity and high persistence (Endale *et al.*, 2017). The extensive use and poor biodegradability of Malathion and 2, 4-D resulted their ubiquitous presence in the environment, and have led to contamination of surface and ground waters. This causes drastic affects for both agricultural and wildlife animals including, the deaths of cattle and horses

grazing of treated plants, and the destruction of plant food sources (Hayes *et al.*, 2010; Alisa and Zvi, 2017).

The widespread use of 2, 4-D has created potential health and ecological risks, owing to its high toxicity and recalcitrant nature. It is also a potential carcinogen, an endocrine disruptor and mutagen (Quan *et al.*, 2015) with negative effects on the aquatic life viz. amphibians, small invertebrates, fishes and algae, in their juvenile stages (Tomlin, 2006). The impact of the residual 2, 4-D on aquatic life is mainly due to its mobility, high water solubility and persistence (Abigail and Chidambaram, 2016).

2, 4-D can be absorbed through the skin or through the lungs if inhaled. Applicators of 2, 4-D, particularly those using back-pack sprayers, are at greatest risk of exposure. Absorption through the skin accounts for 90% of the 2, 4-D absorbed by applicators. Once in the body, 2, 4-D is distributed rapidly with the greatest concentrations appearing in the kidneys and liver (Ibrahim *et al.*, 1991). Accidental inhalation resulted in one reported case of acute poisoning. Symptoms included brief loss of consciousness, urinary incontinence, vomiting, muscular hypertonia (an abnormal increase in skeletal or smooth muscle tone), fever, headache, and constipation. Workers that entered an area shortly after treatment with 2,4-D experienced weakness, headache, dizziness, stomach pains, nausea, brief loss of consciousness, and moderate leukopenia (an abnormal reduction in the number of white blood cells, often reducing immune system function) (Stevens and Sumner, 1991).

In birds, 2, 4-D exposure reduced hatching success and caused birth defects. It is also indirectly affects birds by destroying their habitat and food source. The toxicity of 2, 4- D to fish is variable, with the ester form of 2, 4- D expressing greater toxicity than other forms. A product of the breakdown process of 2, 4-D is 2, 4-dichlorophenol. Which is extremely toxic to earth-worms, 15 times more toxic than 2,4-D. Beneficial insects have reduced fecundity when exposed to 2, 4- D (Barr *et al.*, 2007). As reported by (Hayes *et al.*, 2010) a significant increase in the occurrence of malignant lymphoma among dogs is due to 2, 4-D.

Toxic symptoms resulting from human exposure to malathion, include breathing problems, headache, nausea and dizziness, while high exposure can produce fetal poisoning. As reported

by (Vasimalai and John, 2013), malathion can persist in the human body for at least two generations. It is suspected to cause kidney problems, human birth defects and child leukemia.

2.4. Removal of Pesticides (Malathion and 2, 4-D)

Various methods such as photocatalytic and radiolytic degradation, advanced oxidation (including ozonation, hydrogen peroxide, electrochemical oxidation, and UV radiation) and adsorption are employed for Malathion and 2, 4-D removal from water. However, these technologies have some limitations; for example, ozonation is cost and produces toxic byproducts. Moreover, major drawbacks of advanced/electrochemical oxidation and UV radiation are high operational cost, limited reactor configuration and storage of oxidizing agent such as H₂O₂.

Several authors have been successfully studied a variety of cost-effective and locally available adsorbents for the removal of different types of pesticides. Nevertheless, there are some disadvantages associated with these types of adsorbents such as incompatible for column operation, adsorption of pesticides at low levels, high regeneration cost. Reverse osmosis, nanofiltration and advanced oxidation processes are vulnerable due to the formation of undesirable oxidation by products and membrane fouling (Naushadn *et al.*, 2013).

Ion exchange suffered low thermal and chemical stability limit their application in water purification even it is one of the most eco-friendly and economical technologies, because most of the materials can be reused, this method has high sensitivity and selectivity, and the operation process is simple. Although inorganic ion exchangers, such as zeolites and double layered hydroxides (Moya, 2015) have high thermal and chemical stability, their exchange kinetics and ion exchange capacity are low (Zhang *et al.*, 2014; Chen *et al.*, 2017). Other adsorbents suffered the problem of low adsorption capacity (WHO, 1993; Bazrafshan *et al.*, 2013).

Recently, water treatment with porous materials has been considered to have good treatment potential, since effective porous materials production with little resources and less waste to reduce pollution are becoming more and more available in the world. Today, the use of porous materials is considered an effective method to reduce the potential risks of various emerging

contaminants on the environment. To overcome the abovementioned obstacles, adsorption is the most promising technique; among this Metal Organic frameworks (MOFs) may be a group of promising porous materials due to their porous nature and the versatility in building blocks and functionality. Therefore recently Metal Organic Frameworks (MOFs), get attention as a new kind of adsorbent, have been applied for the adsorption of Pesticides (Yingran *et al.*, 2017).

2.5. Metal Organic Frameworks

Metal organic frameworks (MOFs); also known as porous coordination polymers (PCP) are one of the most interesting class of porous materials. It is an emerging class of highly ordered crystalline porous materials with various potential applications and become a new research hotspot in chemistry and materials science during the last few decades, which is mainly attributed to their exceptionally high surface area, tunable pores, as well as intriguing functionalities. Metal organic Frameworks (MOFs) are captivating crystalline nano materials made up of organic linkers (bridging ligands) and inorganic nodes (metal cations) that extend infinitely into different dimensions through metal-ligand bonding organic linkers which possess has high surface area and control features such as the binding strength, the directionality of propagation and size of the pores formed in such materials, but their pores are not uniform and regular and the inorganic connector (have; regular pore size, high thermal and mechanical resistance but their surface is less than that of the organic porous) is metal nodes control the extension geometry(Augustus *et al.*, 2017).

Different metal cations in the periodic table have been used as metal nodes for the construction of MOFs. Generally, the inorganic nodes of MOFs can be constructed from monovalent (Cu^+ , Ag^+ , etc.), divalent (Mg^{2+} , Mn^{2+} , Fe^{2+} , Co^{2+} , Ni^{2+} , Cu^{2+} , Zn^{2+} , Cd^{2+} , etc.), trivalent (Al^{3+} , Sc^{3+} , V^{3+} , Cr^{3+} , Ga^{3+} , In^{3+} , lanthanides $3+$, etc.), or tetravalent (Ti^{4+} , Zr^{4+} , Hf^{4+} , Ce^{4+} , etc.) metal cations (Yuan *et al.*, 2018). Divalent metals such as Zn^{2+} and Cu^{2+} were widely used in MOF synthesis. Despite their numerous advantages, applications of these divalent metal-based MOFs are ultimately limited by their instability under harsh conditions. So in order to enhance the stability of MOFs as reported (Yuan *et al.*, 2018) is to use high-valent metal cations with organic carboxylate linkers. With the same ligands and coordination environment, high-valent metal

cations with high charge densities can form stronger coordination bonds and a more stable framework (Burtch *et al.*, 2014; Yuan *et al.*, 2018).

Group 4 metal cations generally exist in the oxidation state of +4, which is expected to form stable MOFs when combined with carboxylate-based linkers. In addition to the stronger metal-ligand bonds, these 4⁺ metal cations require more ligands to balance their charge. Therefore, their inorganic nodes tend to have high connectivity, which to some extent enhances the stability of the framework by preventing the attack by guests such as water molecules (Devic and Serre, 2014; Bai *et al.*, 2016).

MOFs are distinguished by the diversity of their structure, different symmetry and pore sizes and, hence, by their characteristics. The pore size is determined by the carbon chain length of the linker or the number of benzene rings in it, whereas the introduction of different substituent and functional groups into the linker is responsible for the additional selectivity and unique chemical properties of the pores. In particular, the substitutions of secondary building units, while the linker is the same terephthalic acid, can lead to quite different MOFs Figure 2 (Butova *et al.*, 2016).

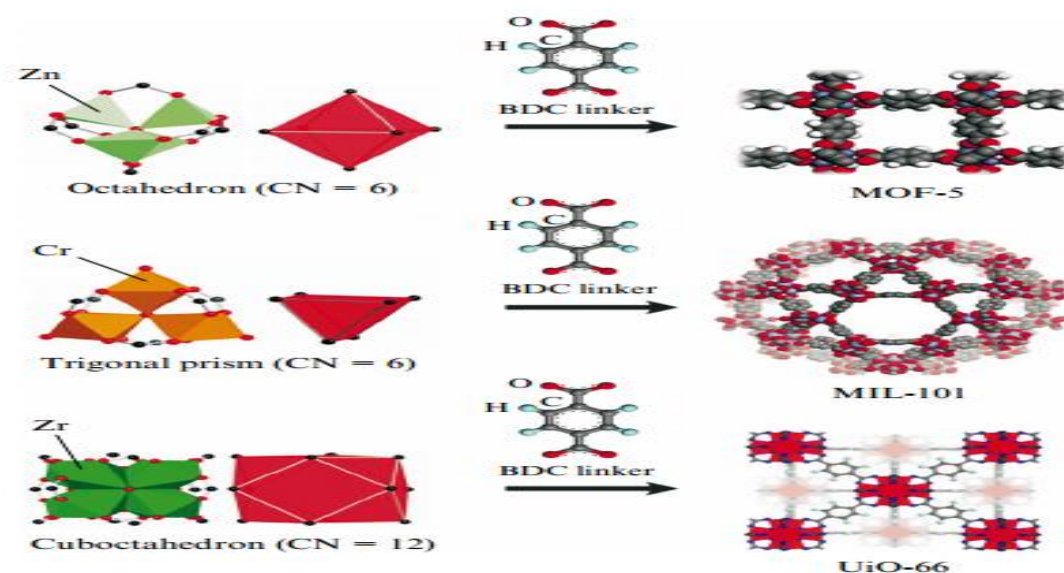


Figure 2. Structures of different MOFs with the terephthalate (BDC) as a linker.

2.6. Synthesis Methods of MOFs

Depending on the final structures and properties, MOFs may be prepared using several distinct synthetic methods such as: hydro or solvothermal synthesis under conventional oven, microwave irradiation and ultrasonic irradiation, electrochemical synthesis, ionothermal synthesis, Sonochemical Synthesis, mechanochemical synthesis (Carson *et al.*, 2011; Min *et al.*, 2017).

2.6.1. Hydro or Solvothermal Synthesis

Hydro or solvothermal synthesis is the most common methods used for making MOFs. They are synthesized by means of solvothermal or hydrothermal methods, in which the reactions are carried out in an organic solvent or in water at high temperature in closed vessels Hydrothermal synthesis, where water is used as the solvent and solvothermal synthesis, where other solvents except water are used as solvents are accompanied. Solvothermal syntheses are a powerful tool to accelerate the discovery of new MOF structures and to optimize synthesis protocols (Rilee *et al.*, 2013). This technique usually produces fine particle powders (high crystal) that are not achieved by most conventional procedures (Augustus *et al.*, 2017). The choice of solvent is based on its ability to dissolve the organic linker. In both cases, the reactions take place inside a Teflon-lined stainless steel autoclave (Vakiti, 2012).

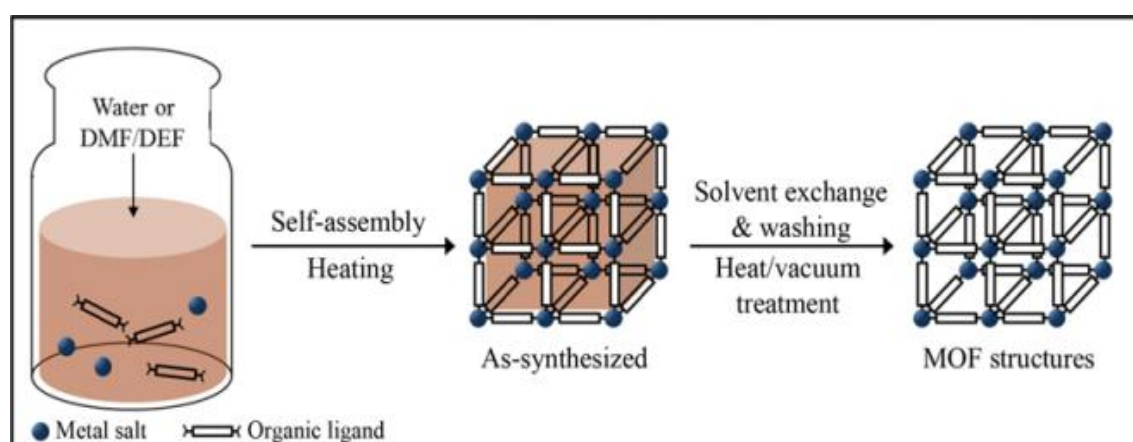


Figure 3. Hydro/solvothermal synthesis of MOFs.

The reaction mixture is normally heated at temperatures ranging from 80 to 220 °C, over a time of several hours to several days. Even though it is the most common methods used for making MOFs, it typically require long reaction times, from several hours up to several months, depending upon the MOF of interest and the reaction solvent, reaction temperature, reagent concentrations, and other factors(Vakiti, 2012).

2.6.2. Microwave Assisted Synthesis

The microwave-assisted synthesis has been termed ‘microwave-assisted solvothermal syntheses for the preparation of MOFs. Such processes involve heating a solution with microwaves for a period of about an hour to produce nanosized crystals. The qualities of the crystals obtained by microwave-assisted processes are generally the same as that produced by the regular solvothermal processes, but provides a very rapid method for the synthesis of MOFs which reduce the qualities of the synthesized powder (Rilee *et al.*, 2013).

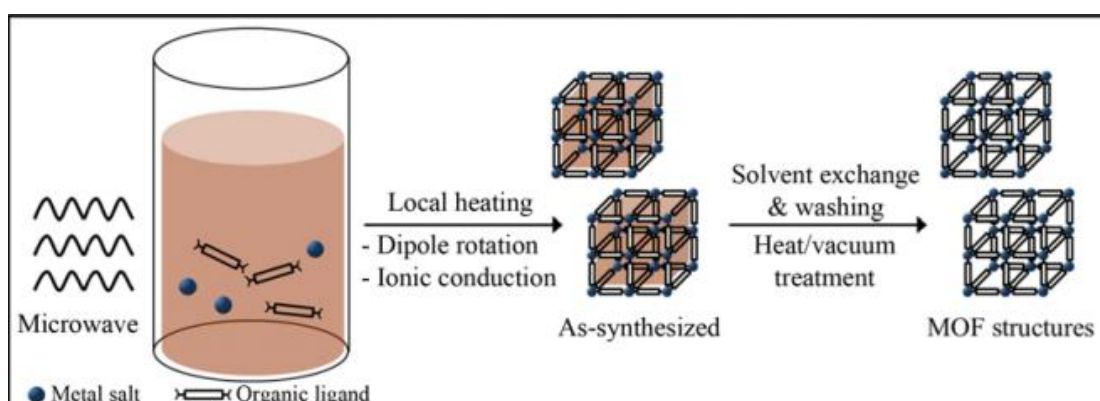


Figure 4. Microwave-assisted solvothermal synthesis of MOFs.

A serious limitation of this approach is the general lack of formation of crystals large enough to obtain good structural data (Liang and D’Alessandro, 2013; Augustus *et al.*, 2017).

2.6.3. Ionothermal Synthesis

In ionothermal synthesis, ionic liquids or eutectic mixtures (mixture of two or more compounds which has a lower melting point than either of its constituents) are used as solvents. Usually high

vapour pressures are generated in solvothermal methods but the most fascinating feature of ionic liquids is that they possess a very low vapour pressure which in turn is safer than the solvothermal methods. Ionic liquids have many attractive properties (high polarity and pre-organized structure) that give them excellent solvating abilities and have been used for producing many new structures. The other important feature of these ionic liquids is that they are not only acting as solvent but can also act as structure directing agents as well (Infas *et al.*, 2011).

2.6.4. Solvent-Free/ Mechanochemical Synthesis

This method adopted for fabrication of MOFs, which is, grinding of two or more solids with a mechanical ball mill in the absence of the solvent. The mechanochemical synthesis method involves the use of mechanical forces to drive the solventless reactions of metal oxides with organic ligands at room temperature. One advantage of this method is that it excludes unneeded anions during the syntheses, which contribute to the waste stream and can complicate the synthesis and purification. Quantitative yields of small MOF particles can be obtained in short reaction times, normally in the range of 10-60 min. In many occasions, metal oxides were found to be preferred than metal salts as a starting material, which results in water as the only side product (Rilee *et al.*, 2013; Augustus *et al.*, 2017).

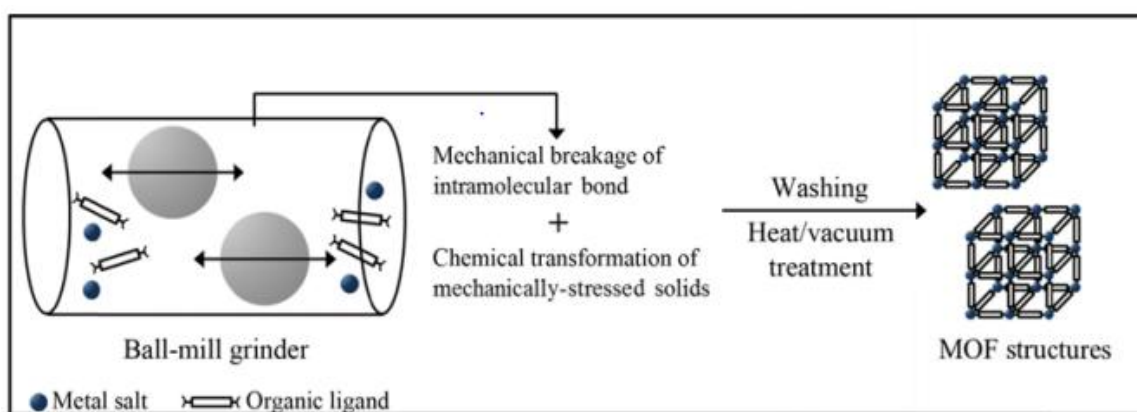


Figure 5. Mechanochemical synthesis of MOFs.

Recently, mechanochemical syntheses have been efficiently employed for the rapid synthesis of MOFs using liquid-assisted grinding (LAG), where a small amount of solvent is added into a

solid reaction mixture that can lead to acceleration of mechanochemical reactions due to an increase of mobility of the reactants on the molecular level (Beldon *et al.*, 2010; Rilee *et al.*, 2013). However the greatest disadvantage encountered in the implementation of mechano synthesis is the difficulty of structural characterization of products. Indeed, the product obtained by grinding is inherently not suitable for characterization via conventional methods of single crystal X-ray diffraction (Beldon *et al.*, 2010).

2.6.5. Electrochemical Synthesis

The electrochemical synthesis of MOFs uses metal ions continuously supplied through anodic dissolution as a metal source instead of metal salts, which react with the dissolved linker molecules and a conducting salt in the reaction medium. The metal deposition on the cathode is avoided by employing protic solvents, but in the process H_2 is generated. The electrochemical route is also possible to run a continuous process to obtain a higher solids content compared to normal batch reactions. Electrochemical MOF synthesis enhances faster synthesis at lower temperatures than conventional synthesis, metal salts are not needed and therefore separation of anions such as NO_3^- or Cl^- from the synthesis solution is not needed prior to solvent recycle, and virtual total utilization of the linker can be achieved in combination with high Faraday efficiencies (Martinea *et al.*, 2012; Rilee *et al.*, 2013).

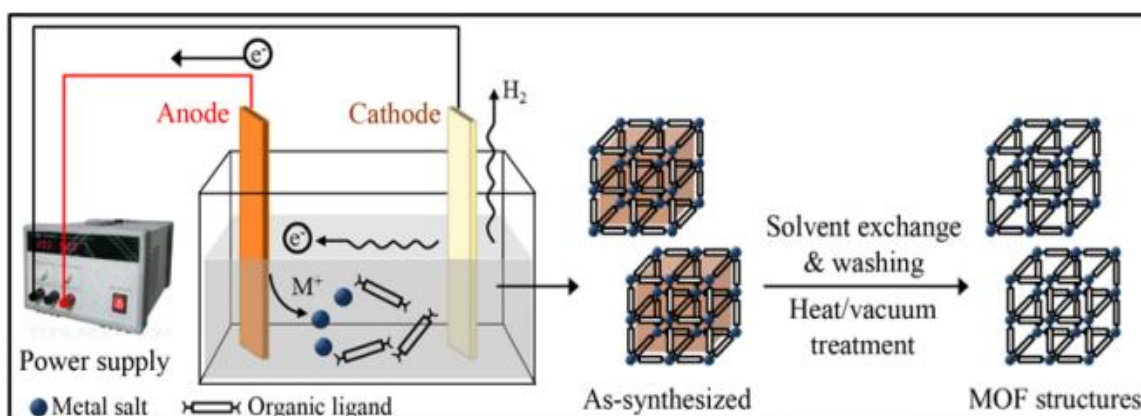


Figure 6. Electrochemical synthesis of MOFs.

The general comparisons between different methods for synthesis of MOFs are given in the Figure 7 summarizes the percentage of crystal MOFs prepared by different methods as reported by (Dey *et al.*,

2014; Augustus *et al.*, 2017). Solvothermal methods are mostly used as (Polyzoidis *et al.*, 2016) reported. According to their reports, the prepared MOFs are in complete manner and crystals prepared have intergrown cubic shapes and are about $1\mu\text{m}$ in size, while those prepared in a continuous manner such as electrochemical, the morphology of the synthesized were not fully crystal, smaller in size and retain spherical shapes (Polyzoidis *et al.*, 2016).

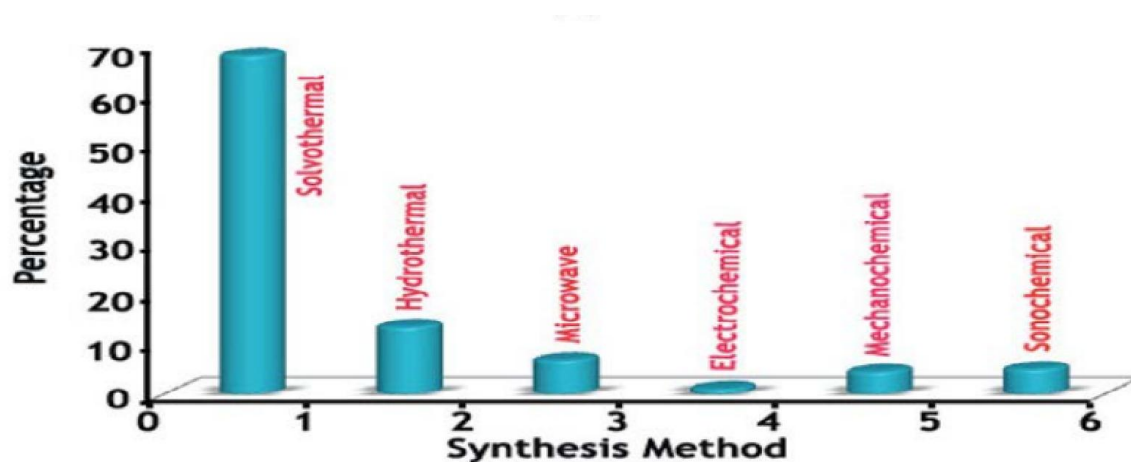


Figure 7. Summary of the various methods employed for the synthesis of crystal MOFs.

2.7. Applications of MOFs

MOFs' structural assets gave much attention recently on more possible applications on environmental applications especially their extraordinary gas capturing ability has been earmarked for the separation of various unwanted and environmentally harmful chemical species (Augustus *et al.*, 2017). MOFs enable flexible structure design of which well-defined pore sizes, surfaces areas and functionalities can be tailored by selecting different building blocks. Hence, its wide range of potential applications ranging from energy storage, gas (e.g. hydrogen) storage and separation, sensing, catalysis, to drug delivery (Min *et al.*, 2017).

2.7.1. Hydrogen Storage

The principal mechanisms based on which selective gas adsorption is achieved in MOFs are adsorbate surface interactions and size-exclusion (molecular sieving effect). Current hydrogen storage techniques involve the use of high pressure tanks, cryogenic tanks, chemisorption, and

physisorption. Pure tank-based hydrogen storage suffers from safety and economic issues. Therefore the most promising hydrogen gas storage obtained by using MOFs. This is due to increasing the surface area enhances the contact between hydrogen and the adsorbent resulting in an increased hydrogen uptake. Compared to other porous materials, some MOFs have higher surface areas and subsequently higher hydrogen uptake capacity. One of the benchmarks is provided by the study on MOF-177 which has a BET surface area of 4500 m²/g and an excess gravimetric hydrogen uptake of 7.5 wt% at 70 bar, 77 K (Ryan *et al.*, 2009).

2.7.2. Catalysis

As porous materials, MOFs may prove to be very useful in catalysis. MOFs with exotic topologies and chemical activities have shown outstanding catalytic performance in various organic transformation reaction such as; oxidation, acetylation, epoxidation, hydrogenation, coupling, condensation, alkylation, hydroxylation and cyclization. Catalytic properties of MOFs can be implemented by active metal centers, which simultaneously serve as nodes for the coordination framework and as reaction centers for the catalyzed reaction itself (Ryan *et al.*, 2009). Among a large number of MOFs, zirconium-based MOFs of the UiO family have attracted considerable attention due to their high thermal, chemical and mechanical stability. Zr-containing UiO-66 type MOFs usually display well Lewis acid character and have exhibited excellent catalytic performances in various acid-catalyzed reactions (Fan Zhou *et al.*, 2016; Sabale *et al.*, 2016).

2.7.3. Energy Storage

The use of nanomaterials for electrochemical energy storage has emerged as a promising approach. Given their unique electrical, mechanical properties, and high surface area, nanosized active materials are expected to bridge the gap towards the realization of the next generation of energy storage device. The direct pyrolysis/carbonization of MOFs is a new method for synthesis of porous materials for energy storage. The uses of pristine MOF and MOF-derived structures for electrochemical energy storage and conversion have been reported (Min *et al.*, 2017).

2.7.4. Sensors

Nanoparticle metal oxides and porous materials with large specific surface areas, and high sensitivity to slight changes in environments (temperature, atmosphere, humidity, and light) are being developed and applied as detectors of combustible gases, humidity, ethanol, and hydrocarbons. Recent studies revealed that metal organic frameworks have the potential for sensor application (Ryan *et al.*, 2009; Wang *et al.*, 2018).

2.7.5. Drug Delivery

As hybrid organic-inorganic compounds, MOFs present themselves as optimal drug-delivery materials due to the adjustability of the framework's functional groups and the tunable pore size. With MOFs, the benefits of using organic materials (biocompatibility and the ability to uptake large amounts of drugs) and inorganic materials (controlled release) may both be utilized. The regular porosity and the presence of organic groups within the framework of MOFs, combined with the low toxicity of carboxylic acids and some transition metals (Fe, Zn, Ti, ...), makes them attractive candidates for the controlled release of drugs. Taking into account it is a non-toxic material; MOFs can be altered for limitless applications in biomedicine in the future (Ryan *et al.*, 2009).

2.8. Adsorption

Adsorption is the phenomenon of accumulation of large number of molecular species at the surface of liquid or solid phase in comparison to the bulk. Process of adsorption arises due to presence of unbalanced or residual forces at the surface of liquid or solid phase. These unbalanced residual forces have tendency to attract and retain the molecular species with which it comes in contact with the surface (Yong *et al.*, 2009).

Or when a solution containing absorbable solute comes into contact with a solid with a highly porous surface structure, liquid-solid intermolecular forces of attraction cause some of the solute molecules from the solution to be deposited at the solid surface. The solute retained (on the solid surface) in adsorption processes is called adsorbate, whereas, the solid on which it is retained is called as an adsorbent. This surface accumulation of adsorbate on adsorbent is called adsorption.

Adsorption is essentially a surface phenomenon. It is completely different from Absorption. While absorption means uniform distribution of the substance throughout the bulk, adsorption essentially happens at the surface of the substance. When both Adsorption and Absorption processes take place simultaneously, the process is called sorption (Adamson, 1990).

The adsorption technology is developed by batch process. As the adsorption progress, an equilibrium of adsorption of the solute between the solution and adsorbent is attained (where the adsorption of solute is from the bulk onto the adsorbent is minimum). Parameters such as temperature, nature of the adsorbate and adsorbent, and the presence of other pollutants along with the experimental conditions (pH, concentration of pollutants, contact time, particle size, and temperature) are among the factors that control the adsorption. The result of adsorption studies can be explained by different models such as: Langmuir, Freundlich, Halsey, Henderson, Smith, Elovich liquid film diffusion which have similar principle but different approaches (Masel, 1996).

2.9. Fundamentals of Adsorption

Depending on the type of interaction between adsorbate and adsorbent surfaces, adsorption may be chemisorption and physisorption. Chemisorption is a type adsorption whereby a molecule adheres to a surface through the formation of a chemical bond. The adsorbate reacts with the surface to form a covalent or an ionic bond. Chemical adsorption results from the chemical link between adsorbent and adsorbate molecule, therefore it is specific as well as irreversible and chemical as well as electronic properties of adsorbent are changed. Binding between adsorbent and adsorbate by covalent bond is called weak chemical adsorption, and that by ionic bonds is called strong chemical adsorption. It typically show bonding energies above 200 KJ/mol. Physisorption is a rapid process caused by nonspecific binding mechanisms such as van der Waal's forces and results in bonding energies up to 4-40 KJ/mol. It is less specific for which compounds adsorb to surface sites, has weaker forces and energies of bonding, operates over longer distances (multiple layers) and is more reversible (John *et al.*, 2005)

The affinity of the adsorbate for an adsorbent is quantified using adsorption isotherms, which are used to describe the amount of adsorbate that can be adsorbed onto an adsorbent at equilibrium

and are usually a function of the liquid phase concentration. To develop isotherms, a known quantity of adsorbate in a fixed volume of liquid is exposed to various dosages of adsorbent. After sufficient time, the adsorption equilibrium is reached and the adsorption equilibrium capacity can be calculated from the mass balance:

$$q_e = \frac{v}{m} (C_o - C_e) \quad (2.1)$$

Where, v is the volume of liquid in (L), m is the mass of adsorbent used (g), C_o is the initial and C_e is the adsorbate residual concentration in solution. In order to describe the adsorption equilibrium mathematically, different models exist, differing in complexity and in the number of parameters necessary. Out of different models mainly two parametric isotherms, formulated by Langmuir and Freundlich (Freundlich, 1906; Langmuir, 1918) are used mostly.

2.9.1. Langmuir Isotherm Model

Langmuir isotherm model assumes uniform energies of adsorption onto the surface without interaction of adsorbate in the plane of the surface where adsorbate molecules can be chemically bound. It is assumed that the reaction has a constant free-energy change for all sites and a maximum of one adsorbate molecule can be bound to each site (monolayer coverage). The Langmuir equation assumes that homogeneous structure of the adsorbent surface, i.e. all adsorption sites are energetically equal. That is why the Langmuir equation is in most cases only applicable for small concentration ranges. The Langmuir nonlinear equation is commonly expressed as follows (Langmuir, 1918; Hameed *et al.*, 2009):

$$q_e = Q_0 \frac{bC_e}{1+bC_e} \quad (2.2)$$

To derive the model parameters Q_0 and b , can be linearized. The linear Langmuir isotherm allows the calculation of adsorption capacities and is equated by the following equation

$$\frac{C_e}{q_e} = \frac{1}{bQ_0} + \frac{C_e}{Q_0} \quad (2.3)$$

Where, C_o is the initial adsorbate concentration in solution (mg/L), C_e is the adsorbate residual concentration in solution, Q_0 is the initial amount of adsorbate per unit mass of adsorbent (mg/g),

m is mass of adsorbent (g) and v is the volume of liquid, q_e is milligrams of adsorbate accumulated per gram of the adsorbent material, Q_o is the maximum uptake corresponding to the site saturation. The plot shown as (C_e/q_e) vs C_e should yield a straight line if the Langmuir equation is obeyed by the adsorption equilibrium with slope $\frac{1}{Q_o}$ and $\frac{1}{Q_o b}$ intercept. The Langmuir equation assumes a homogeneous structure of the adsorbent surface, i.e., all adsorption sites are energetically equal.

The essential characteristics of a Langmuir isotherm can be expressed in terms of a dimensionless constant separation factor or equilibrium parameter R_L (indicates the isotherm shape and whether the adsorption is favorable or not) which is defined by:

$$R_L = \frac{1}{1 + bC_o} \quad (2.4)$$

Where, C_o is the initial adsorbate concentration (mg/L) and b is Langmuir constant (L/mg). R_L indicates the isotherm shape and whether the adsorption is favorable or not, as per the criteria given below (Langmuir, 1918; Hameed *et al.*, 2009).

Table 3. Criteria for Langmuir adsorption isotherm

R_L	Type of isotherm
$R_L > 1$	Unfavorable
$R_L = 1$	Linear
$0 < R_L < 1$	Favorable
$R_L = 0$	Irreversible

2.9.2. Freundlich Isotherm Model

The Freundlich isotherm model is an empirical expression that encompasses the heterogeneity of the surface and the exponential distribution of sites with different adsorption energies. It can be derived assuming a logarithmic decrease in the enthalpy of sorption with the increase in

the fraction of occupied sites. For Freundlich isotherm to be valid, the adsorption must be purely a physical process with no change in the configuration of the molecules in the adsorbent.

The Freundlich model is commonly given by the nonlinear equation (Freundlich, 1906).

$$q_e = K_f C_e^{1/n} \quad (2.5)$$

Where, K_f is a constant for the system related to the bonding energy. Which be defined as the adsorption or distribution coefficient and represents the quantity of adsorbate adsorbed on to adsorbent for unit equilibrium concentration, n is the heterogeneity factor representing the deviation from linearity of adsorption and is also known as Freundlich coefficient. $1/n$ is an empirical constant related to the magnitude of the adsorption driving force on to the sorbent or surface heterogeneity, becoming more heterogeneous as its value gets closer to zero. Both K_f and n have to be determined in batch experiments, using logarithmic regression of the data and the linearized form of the Freundlich equation described below (Sairam *et al.*, 2009).

$$\log q_e = \log K_f + \frac{1}{n} \log C_e \quad (2.6)$$

It has been shown that the Freundlich equation can be derived from the Langmuir equation if a logarithmic decrease of the differential adsorption enthalpy with increasing solid-phase concentration is assumed, corresponding to the behavior of a heterogeneous adsorbent surface. It is important to note that the Freundlich equation can only be used to describe experimental data within a limited concentration range where the constants are valid (Sontheimer *et al.*, 1988).

2.10. Kinetics Studies

Kinetic modeling not only allows estimation of sorption rates but also leads to suitable rate expressions characteristic of possible reaction mechanisms. The two well-known kinetic models, pseudo-first order, pseudo-second order will be investigated to describe the adsorption process for this study.

2.10.1. Pseudo-First-Order

A pseudo-first-order kinetic equation according (Rafiquea and Nasree, 2011) given as:

$$\log(q_e - q_t) = \log q_e - \frac{k_1}{2.303} t \quad (2.7)$$

Where, q_e and q_t (mg/g) are the adsorption capacities of adsorbent at equilibrium and time t (min), respectively and k_1 (min^{-1}) is the pseudo-first order rate constant.

2.10.2. Pseudo-Second Order

This will investigated by plotting $\frac{t}{q_e}$ vs t . The formation of a linear plot shows that the reaction follows second order kinetics (Dariush, 2013) which given as follows;

$$\frac{t}{q_e} = \frac{1}{K_2 q_e^2} + \frac{t}{q_e} \quad (2.8)$$

Where: t (time); q_t amount of adsorbent adsorbed at time t ; q_e amount of target species adsorbed at equilibrium and k_2 = second order rate constant. The rate-limiting step is the surface adsorption that involves chemisorption, where the removal from a solution is due to physicochemical interactions between the two phases (Dariush, 2013).

3. MATERIALS AND METHODS

3.1. Experimental Sites

Synthesis of the MOF and the batch adsorption experiments were carried out at Haramaya University, Central Laboratory and Chemistry Department Research Laboratory. All the characterization techniques were conducted at Addis Ababa University, Adama Science and Technology University, and Addis Ababa science and Technology University.

3.2. Apparatus, Instruments and Chemicals

3.2.1. Apparatus and Instruments

The apparatuses that were used during the study include analytical balance (AFD-720L, Adam) mortar and pestle (Gilson, London) and FTIR Spectrometry (Perkin Elmer), Powder X-ray diffractometer (PXRD, Philips Analytical, PW-3040), Scanning electron microscopy (SEM, UV-Vis spectrophotometer, Deionizer, Orbital shaker (S01, United Kingdom), Thermo gravimetric analyzer (TGA, Shimadzu DTG-60H, South Korea), pH meter (3320, JENWAY, UK), Oven (Gallenkamp, MODEL A050626, London), centrifuge (Hermle, Z 300, Germany) and magnetic stirrer (Hanna instruments,) were among the instruments used in this study.

3.2.2. Chemicals and Reagents

All chemicals and reagents used in this study were all analytical grade. Zirconiumoxychloride octahydrate salt ($ZrOCl_2 \cdot 8H_2O$, 98%, Avra, India). Sodium hydroxide (NaOH, 98%, BDH, England), Hydrochloric acid (HCl, 37%, Blulux, India), 2, 4-Dichlorophenoxyacetic acid (2, 4-D, 97%, Blulux, India), N,N-dimethylformide (DMF, 99.9%, Loba Chemie, India) and Methanol (99.9%, Loba Chemie, India), Benzene-1,4-dicarboxylic (BDC)/Terephthalic acid (98%, Sigma Aldrich, Germany), Malathion (50% EC, China), Acetonitrile (99.9%, Park Scientific, UK) and deionized water was prepared laboratory.

3.3. Experimental Procedure

3.3.1. Synthesis of UiO-66(Zr-MOFs)

Solvothermal method was used for the synthesis of UiO-66 due to its capability of producing high crystal MOFs relative to other techniques. It has advantages such as its simplicity, low pressure it used, cost effectivity and material availability compared with other methods. In brief, 12.7 mmol (3.9 g) of $\text{ZrOCl}_2 \cdot 8\text{H}_2\text{O}$ and 12.1 mmol (2.0 g) of benzene 1, 4-dicarboxylic acid were dissolved in 50 mL of DMF and stirred for 30 min on magnetic stirrer each separately. The metal salt solution was added to the linker solution slowly and stirred for 24 hr. The reaction continued 24 hr in the oven at 120°C and a white precipitate was formed. The white formed precipitate was centrifuged at 2500 rpm for 30 min washed with DMF and methanol several times for solvent exchange and to remove other impurities. The obtained solid material $\text{Zr}_6\text{O}_4(\text{OH})_4[\text{C}_6\text{H}_4(\text{CO}_2)_2]_{12}$ (Silva *et al.*, 2016; Tsegaye G, 2016) was dried in open air at room temperature (Silva *et al.*, 2010) and stored for further characterization and experimental studies.

3.3.2. Characterization of UiO-66 MOFs

The as-synthesized material, UiO-66 MOFs, was characterized for its thermal stability, structure and crystallinity, morphology and composition using the state-of-the-art instruments such as TGA, XRD, SEM and FTIR, respectively.

3.3.3. Preparation of Malathion and 2, 4-D Standard Solutions

The stock solution (1000 mg/L) of Malathion and 2, 4-D were prepared by dissolving 50 mg and 0.1 mL of each Malathion and 2, 4-D standard materials, respectively, in 50 mL acetonitrile. The respective intermediate and working standards were freshly prepared from their respective stock solutions by diluting with deionized water. Mixture standard solution which comprises the two standards, 2, 4-D and Malathion, were prepared by mixing equal ratio (v/v) of an intermediate standard solution (100 mg/L) of each 2, 4-D and Malathion.

3.3.4. Batch Adsorption Studies

Adsorption process were studied by batch experiment in which adsorbent is mixed with the solution to be treated in a suitable reaction vessel for the stipulated period of time, until the concentration of adsorbate in solution reaches an equilibrium value. Agitation generally provided to ensure proper contact of the two phases (Ahmad *et al.*, 2010). Accordingly, 30 mL of standard solutions containing 5 mg/L of each standards and mixture were mixed with 0.15 g of the prepared adsorbent (UiO-66) under continuous mixing condition with magnetic stirrer at room temperature. These solutions were agitated until complete adsorption assumed to occur. After it filtered, the concentration of non-adsorbent analyte in the filtrate was determined using UV-Vis spectroscopy at 294.5, 291.5 and 296 for Malathion 2, 4-D and their mixture respectively. The effects of various experimental parameters like pH, contact time, initial adsorbate concentration, adsorbent dose and agitation rate were systematically evaluated.

3.4. Optimization of Experimental Parameters

3.4.1. The Effect of pH

The effect of pH on the adsorption of Malathion, 2, 4-D and mixture were carried out by adding 0.1 g of the adsorbent (UiO-66) into Erlenmeyer flasks containing 30 mL of each Malathion 2, 4-D and mixture standard solutions, separately. The pH was adjusted by adding 0.01 M HCl or 0.01 M NaOH solutions from 2 to 9 by one factors while keeping other parameters (initial adsorbent concentration, 5 mg/L; adsorbent dose, 0.1 g; contact time, 60 min and agitation speed, 150 rpm constant. Then, equilibrium concentrations of the pesticides were measured with the UV-Vis spectroscopy after agitation and filtration.

3.4.2. Effect of Adsorbent Dose

To investigate the effect of adsorbent dose on the Malathion, 2, 4-D and mixture removal, the amount of adsorbent dose was varied as; 0.04, 0.06, 0.08, 0.1, 0.2, 0.3 and 0.4 g while keeping other parameters at (pH, 4, 3 and 4, optimum values; initial concentration, 5 mg/L; contact time, 60 min and agitation speed, 150 rpm values).

3.4.3. Effect of Contact Time

In order to determine the effect of contact time on the adsorption of Malathion, 2, 4-D and mixture solutions, the amount of adsorbed pesticides were determined by varying the contact time as 30, 60, 90, 120, 150, and 180 minutes while keeping pH and adsorbent dose at the optimum values. The other parameter, initial concentration and agitation speed were kept at 5 mg/L.

3.4.4. Effect of Agitation Speed

The effect of agitation speed on the adsorption of pesticides (from separate and mixed solutions) were studied by varying the agitation speed as, 50, 75, 100, 120, 150, 180, 200, 225 and 250 rpm while keeping other parameters constant such as pH (4, 3 and 4), adsorbent dose (0.1 g), contact time (60 min) and initial concentration (5 mg/L) constant, respectively.

3.4.5. Effect of Initial Concentration

To study the effect of initial adsorbent concentration, the experiments were carried out using different initial concentrations. The initial concentration varied from 1 to 50 mg/L while keeping others constant at their optimum values; pH (4, 3, and 4), adsorbent dose (0.1 g), contact time (60 min) and agitation speed (125, 100 and 150 rpm).

3.5. Kinetics Studies

The effect of adsorption kinetics for Malathion, 2, 4-D and the mixture solutions were determined by varying contact time as, 30, 60, 90, 120, 150, and 180 min and by keeping all parameters; pH, adsorbent dose, agitation speed and initial pesticides concentrations at the optimized values. It was obtained by using 0.1 g adsorbent placed in Erlenmeyer flasks each containing 25 mL of 5 mg/L Malathion, 2, 4-D and mixture solutions, separately. The flasks were continuously shaken at optimized speed. After filtration, the percent of adsorption (%) were calculated using the following equation (Gupta and Nayak, 2012).

$$\text{Percent of adsorption (\%)} = \frac{C_0 - C_e}{C_0} \times 100 \quad (3.1)$$

Where, C_o and C_e are initial and equilibrium concentration of the adsorbate, respectively.

3.6. Adsorption Isotherms

Freundlich and Langmuir models were employed to describe the experimental results of effect of pesticides (Malathion, 2, 4-D and their mixture) adsorption. These were determined by keeping all parameters at optimum condition and initial concentrations of Malathion, 2, 4-D and mixture were varied from 1 to 50 mg/L. To each separate flask each initial concentration (25 mL) of 2, 4-D, Malathion and mixture 0.1 g of UiO-66(Zr) were added. After the end of the adsorption process, all samples were filtered and analyzed using UV-Vis spectrophotometer.

3.7. Thermodynamic Studies

In order to get the thermodynamic parameters such as ΔG (free energy change), ΔH (enthalpy change) and ΔS (entropy change), the adsorption were further carried out at various temperatures. In order to investigate the effect of temperature on sorption phenomenon, all predetermined and optimized values of other parameters (pH, dosage, contact time, speed of agitation and initial concentration) were used and the temperature were varied from, 298, 308, 318, 328 and 338 °C (Beom *et al.*, 2013; Kumar *et al.*, 2014).

3.8. Determination of pH of Zero Charge (pH_{PZC})

The pH_{PZC} of UiO-66 (Zr-MOF) was determined by adding 0.5 g of UiO-66 (Zr-MOF) that has 50 mL of NaCl (0.01 M). About 5 flasks each having 0.5 g UiO-66 and 50 mL of 0.01 M NaCl were prepared by adjusting the pH. After shaking for 48 h the pH of each flask were measured and the graph was plotted that used to determine pH_{PZC} from the graph of pH_i vs pH_f .

3.9. Desorption Studies

To evaluate desorption study, 0.1 g of UiO-66 adsorbent was added to 50 mL optimized concentration (5 mg/L) of Malathion and 2, 4-D. The agitation rate and pH were kept constant throughout the desorption experiment. Then, the saturated solutions were centrifuged at 3500

rpm for 20 min (*Bakhtiary et al.*, 2013) and the supernatant were carefully removed. The residual solution were washed with 10 mL Methanol, Acetonitrile, distilled water, 0.1 M NaOH and 0.1 M HCl four times each to obtain good desorption yields (*Sahin and Emik*, 2018). The solutions were shaken for 60 min, filtered and were analyzed with Uv–Vis spectrophotometer.

3.10. Recyclability

About 0.1 g the adsorbent, of UiO-66(Zr), was added to 50 mL of Malathion and 2, 4-D (initial concentration= 5 mg/L). After completion of adsorption process, the used UiO-66 was separated by filtration. For the regeneration of the used UiO-66(Zr), the adsorbent was washed 4 times with 10 mL Acetonitrile, and then air dried and again tested for adsorption process. Regeneration process was performed with 3 cycles (*Azhara et al.*, 2017; *Mohammadi et al.*, 2017).

3.11. Real Sample Analysis

To investigate the practical applicability of the synthesized MOF, tap water samples collected from two sampling locations, Bate and Haramaya University main Campus, were considered. The real samples were treated with UiO-66(Zr) at optimum condition and the adsorption process was conducted by taking 50 mL of the sample and 0.1 g of UiO-66(Zr). Then shaken at 150 rpm and at the end of the process, the samples were filtered and analyzed with Uv–Vis spectrophotometer.

4. RESULT AND DISCUSSION

4.1. Characterization of UiO-66(Zr) Adsorbent

4.1.1. FTIR Spectra Analysis

The FTIR spectrum of UiO-66 was acquired (Figure 8) to study the available functional groups on the surface of the adsorbing material. The broad peaks around 3419 cm^{-1} show the presence of OH group at the external surface of the adsorbent. The carboxylate group of ligand BDC has two strongly coupled C–O bonds, which give rise to two sharp peaks, a symmetric C–O stretching band at 1398 cm^{-1} and an asymmetric C–O stretching band at 1586 cm^{-1} . In addition to the peak existing at 1586 cm^{-1} , the small bands at 1504 cm^{-1} could be assigned to the C=C of the benzene ring of the ligand, BDC, in the structure.

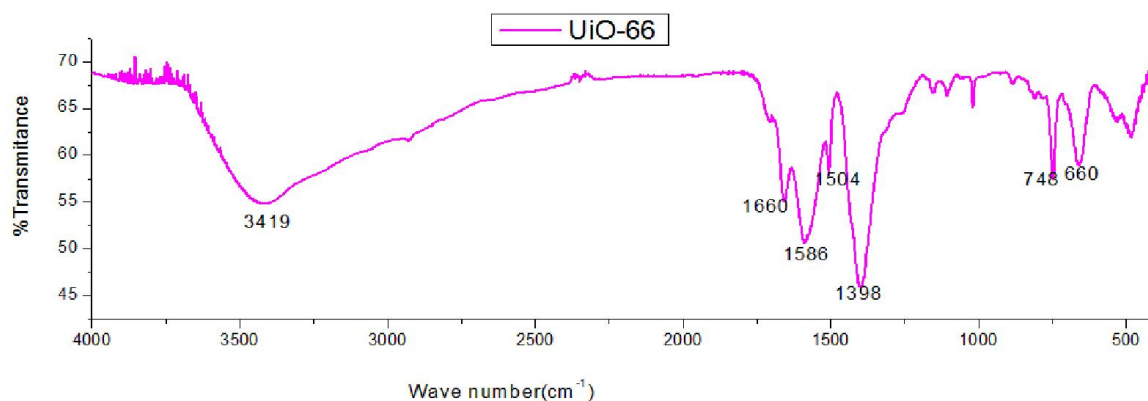


Figure 8. FTIR spectra of as synthesized UiO-66(Zr).

The characteristic peak at 1660 cm^{-1} (Figure 8) can be assigned to the stretching vibrations of C=O in the carboxylic acid present in BDC and this may also indicate coordinate bonding of the metal with the organic fraction of terephthalic acid. The peak at 660 and 748 cm^{-1} are attributed $\mu_3\text{-O}$ stretching with Zr-(OC). The result from the spectrum is in line with some reports (Valenzano *et al.*, 2011; Azhara *et al.*, 2017; Ma *et al.*, 2017).

As can be seen below (Figure 9), there is slight peak shift around 3400 cm^{-1} and the increment of the peak intensities is observed after the adsorption of Malathion and 2, 4-D on the surface of the

adsorbent. However, clear peak spectra change was not observed on the spectrum of UiO-66(Zr) before and after adsorption of both pesticides (Figure 9). This may justify that surface adsorption is the main adsorption mechanism for both pesticides on the UiO-66(Zr). If strong electrostatic attraction between adsorbent and the adsorbate (Malathion and 2, 4-D)) was there, change in spectra could be expected due to the formation of new bond or bond breakage that occur in the original UiO-66(Zr). Therefore, the removal mechanism of both pollutants was assumed to be physical adsorption.

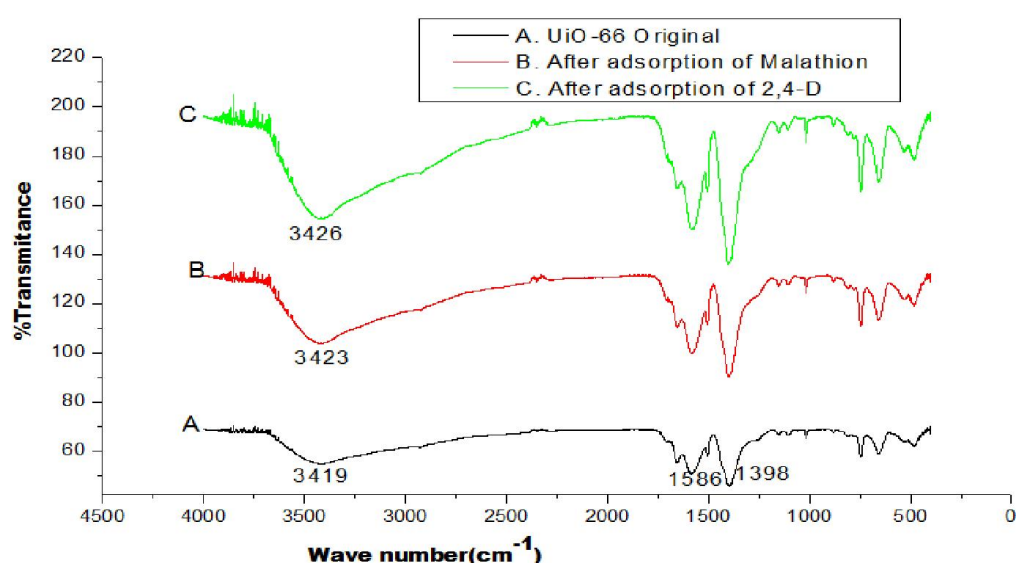


Figure 9. FTIR spectra of UiO-66 before and after adsorption of Malathion and 2, 4-D.

4.1.2. PXRD Analysis

Powder X-ray diffraction (XRD) is a non-destructive analytical technique that can be applied for the phase identification and for the determination of materials properties. It is the most important and beneficial technique in solid state chemistry and it has been applied for the fingerprint characterization of crystals and for the determination of their structures (Bunaciu *et al.*, 2015). The diffraction spectra (Figure 10) of the synthesized material was acquired with Powder X-ray diffraction (XRD, Philips Analytical, PW-3040) equipped with the graphite monochromatized (Ni-filtered) Cu K α radiation ($\lambda = 1.5406 \text{ \AA}$) in 2θ angles ranging from 5° to 90° with a step

size of 0.05 °C and scanning rate of 2 °C per min. The spectrum was used to figure out structural information, crystallinity and phase identification of the material.

As showed in Figure 10, the most probable diffraction peaks for MOFs were found below scattering angle (2θ) of 10 degree confirms that UiO-66(Zr) as MOF's character and good agreement with (Kim *et al.*, 2015; Deng Zhang *et al.*, 2017). The intensive peaks appearing at small 2θ angles in the XRD pattern (Figure 10) are characteristics of porous materials, which possess abundant pores or cavities. This may be due to the inverse relation of 2θ and porosity of the adsorbent (Lin *et al.*, 2012). The major peaks was observed at 7.46 and 8.12 degree indicate the MOF character and additional peaks from the most probable 2θ values which account for the presence of UiO-66(Zr) corresponding oxides or may un reacted acid linker molecules.

The well-defined major diffraction peaks observed of the as synthesized UiO-66(Zr) powder in good agreement with the reported literature (Katz *et al.*, 2013; Zhang *et al.*, 2017), indicating the symmetric cubic structure and high crystallinity.

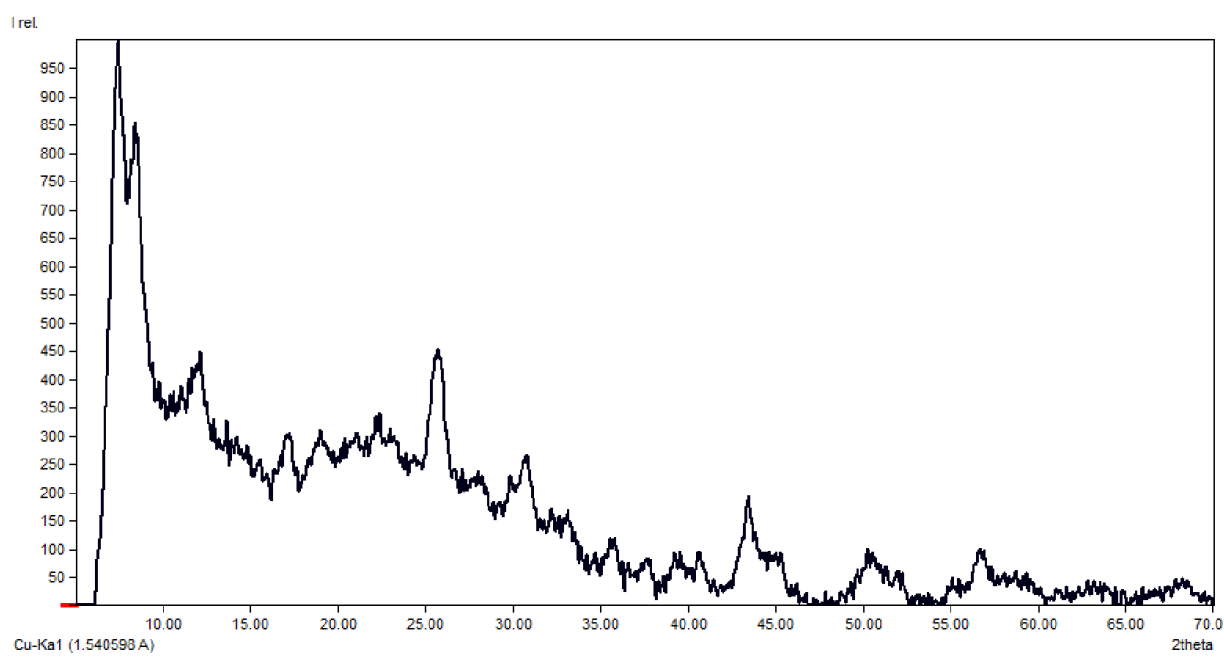
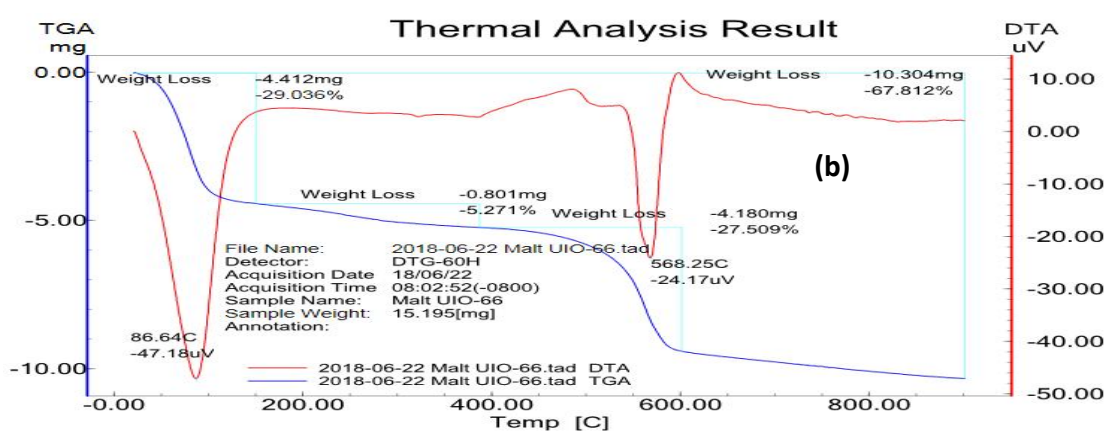
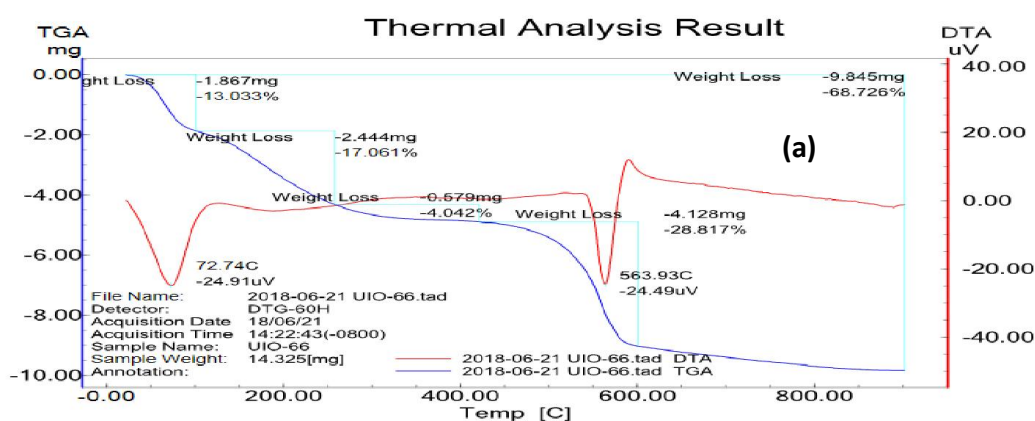


Figure 10. PXRD pattern of as synthesized UiO-66(Zr).

4.1.3. TGA Analysis

The thermal stability and structural integrity of UiO-66(Zr) before and after adsorption of Malathion and 2,4-D were further studied by thermogravimetric analysis. For the pristine UiO-66(Zr), thermogravimetric analysis curve (Figure 11a) showed two weight loss steps between 25 and 600 °C. The first weight loss of 26.5% below 300 °C may be attributed to the release of guest H₂O, methanol and surface adsorbed DMF molecules. On further heating, a weight loss of 43% between 450 and 600 °C may corresponds to the thermal decomposition of organic linker. The residual weight after heating of UiO-66(Zr) was 30% at 800 °C which is in good agreement with theoretical value (25.7%). The final product after 600 °C obtained was ZrO₂ as can be confirmed from the PXRD above which indicate that there was cubic ZrO₂ (JCPDS: 96-152-1754).



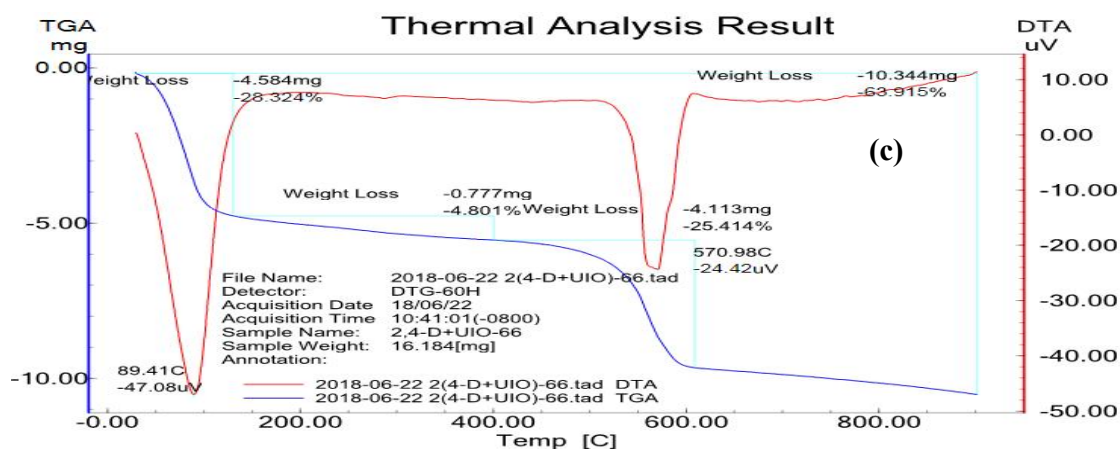


Figure 11. TGA of UiO-66(Zr) before (a), after adsorption of Malathion (b) and 2, 4-D (c).

After adsorption of Malathion and 2, 4-D, the weight loss below 200 °C increased 29 % for Malathion (Figure 11b) and 28 % for 2, 4-D (Figure 11c). This confirms that the adsorptions of these pesticides were occurred on the surface of UiO-66(Zr). The stability of UiO-66(Zr) before and after adsorption of Malathion and 2, 4-D is not changed. After adsorption, from 500 to 600 °C there was the thermal decomposition of the organic linker in all cases.

4.1.4. Determination of pH point Zero Charge

The pH_{PZC} of an adsorbent is a very important characteristic that indicates the pH at which the adsorbent do have a neutral, positive or negative surface charge. The adsorbent surface has a zero surface charge (neutral) when $pH = pH_{PZC}$, net positive surface charge at $pH < pH_{PZC}$, whereas the surface exhibits net negative surface charge at $pH > pH_{PZC}$. It was observed that pH_{PZC} of UiO-66 for this study was found to be ≈ 5 as shown in Figure 12 which is in good agreement with the previous reports (Tsegaye, 2016; Azhara *et al.*, 2017). Accordingly, UiO-66 has a positively charged surface below its pH_{PZC} , ($pH = 5$), and in this medium anions are probably adsorbed on the surface. On the other hand, adsorptions of cations are favored above pH_{PZC} of UiO-66.

This indicates that both 2, 4-D and Malathion are adsorbed below pH_{PZC} of UiO-66. This is due to weak electrostatic attraction between the positive surface the adsorbent (UiO-66) and anions

of 2, 4-D and Malathion, that favors the accumulation of these pesticide on the surface of adsorbate.

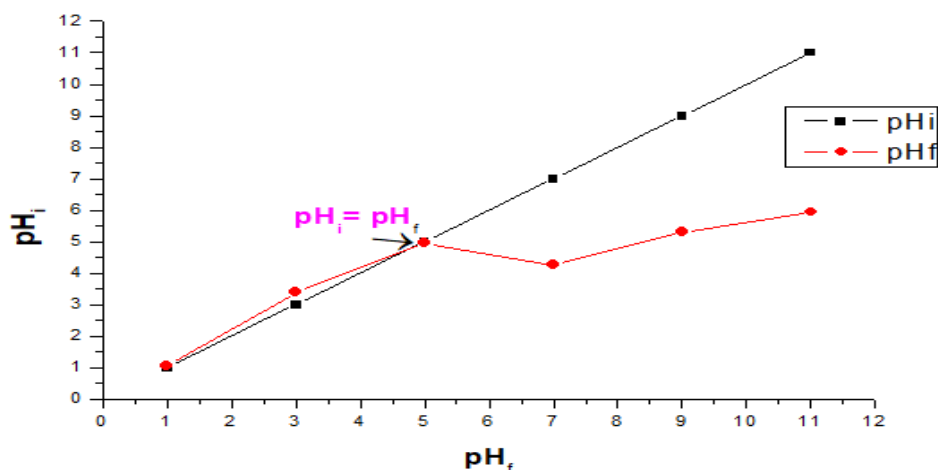


Figure 12. pH point zero charge (pH_{PZC}) of UiO-66.

4.2. Optimization of Experimental Conditions

4.2.1. The Effect of pH

The pH is an important parameter to be optimized for maximum removal of pesticides; because it determines the surface charge of the adsorbent and degree of ionization of the adsorbate (Nejati *et al.*, 2013). Change in pH lead to variation in the surface properties of the adsorbent and the degree of ionization (Naushadn *et al.*, 2014). In this study, the effect of pH on the adsorption of Malathion, 2, 4-D and mixture on to UiO-66 was carried out in pH range from 2 to 9 by keeping other parameters constant.

High percentage removal of Malathion, 2, 4-D and mixture were favored in acidic conditions (Figure 13). The sorption of Malathion and mixture were increased from 76.7 and 70.3% to 99.3 and 88.9% as the pH increased from 2 to 4 and readily decreased to 17.0 and 40.0% from pH 4 to 9. The maximum sorption for both adsorbate were observed at pH 4 which may be due to the electrostatic attraction between anions of the pesticides and the surface of adsorbent (UiO-66). Since pH_{PZC} of UiO-66 was nearly at 5, surface of the adsorbent is positively charged below

pH_{PZ} , and hence, adsorbates (pesticides in this case) with negatively charged are attracted to ward the surface of UiO-66. Kumar and his coauthors reported that (Kumar *et al.*, 2014) the adsorption of Malathion was also favored under acidic condition.

For the case of adsorption of 2, 4-D, removal efficiency was found to decrease from 99.1 to 31.9% as the pH increases from 3 to 9. At low pH value, the adsorption removal increased to its highest value, whereas at high pH value, the removal percentage was intensely decreased (Figure 13). A decrease in adsorption capacity at high pH is explained by the electrostatic repulsion between the surface of adsorbents and the 2, 4-D anions because the pKa value of 2,4-D is around 2.7-2.8. Therefore, the favorable adsorption of 2, 4-D over UiO-66, especially at a pH of 3 is explained by the electrostatic interaction between the anions of 2, 4-D and the positive charged surface of UiO-66. Similar results have been also obtained in various reports in the literature (Beom *et al.*, 2013).

As the initial pH of the solution increased, the positive charge on the surface decreased and the number of negatively charged sites increased. The negatively charged surface site on the UiO-66 (Zr-MOF) was not favorable for the adsorption of the anionic pesticides due to electrostatic repulsion. However, slight constant adsorption of 2, 4-D was observed at pH 5-6 as can be seen from Figure 14 which might be explained with $\pi - \pi$ stacking (between the benzene rings of 2, 4-D and UiO-66) on the porous UiO-66, because both the adsorbate and the adsorbent have benzene rings (Beom *et al.*, 2013). Therefore, pH values of 3, for 2, 4-D, and 4 for Malathion and the mixture solution were considered as an optimum values and was used in the subsequent experiments.

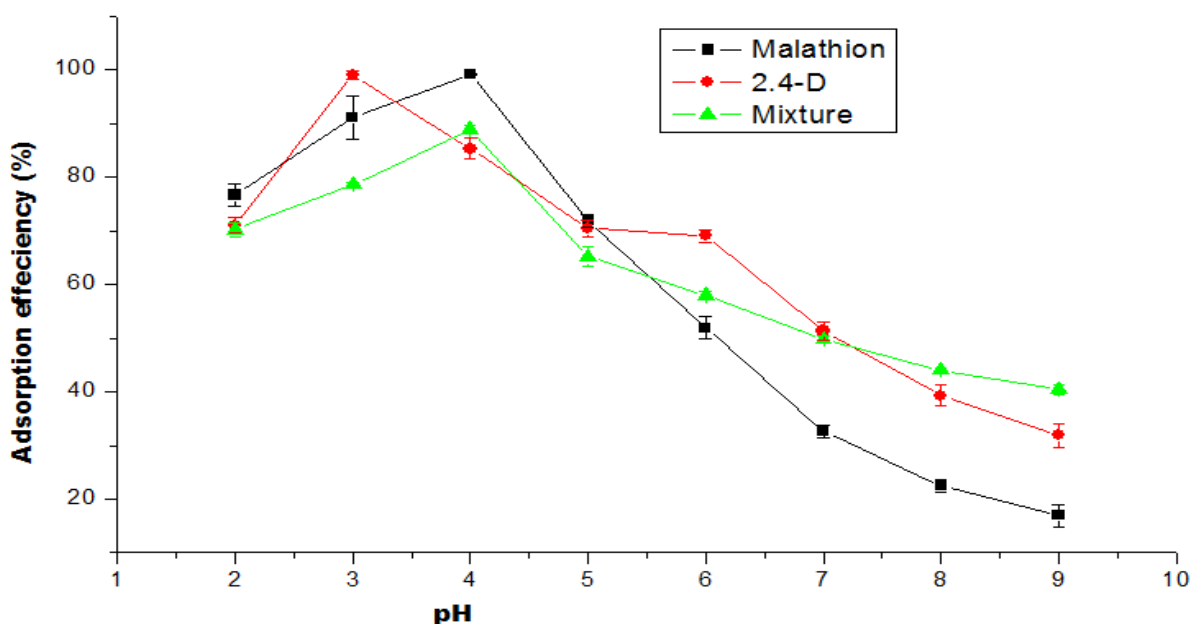


Figure 13. Effect of pH on the removal of Malathion, 2, 4-D and mixture (at $C_0 = 5$ mg/L; adsorbent dose = 0.1 g; contact time = 60 min; agitation speed = 150 rpm).

4.2.2. Effect of Adsorbent Dose

The effect of adsorbent dose on the removal of Malathion, 2, 4-D and mixture on to UiO-66(Zr) were studied by varying the adsorbent amount in the range of 0.04 to 0.4 g by 0.02 factor at optimum pH of, 4, 3 and 4 respectively, and by keeping other parameters (initial concentration, 5 mg/L; contact time, 60 min and agitation speed, 150 rpm) constant. The results shown in Figure 14 suggest that increase in the dose of adsorbents results in increase in adsorption efficiency due to the fact that the sorption sites remain unsaturated during the sorption as well as number of sites available for sorption site increases by increasing the adsorbent dose. However, further increase after 0.1 g did not increase the adsorption which might be due to the interference between binding sites of adsorbent doses. The maximum adsorption efficiency of Malathion, 2, 4-D and Mixture on the UiO-66(Zr) were 98.0, 97.1 and 95.1%, respectively at 0.1 g dose. Hence, the optimal adsorbent dose was considered to be 0.1 g and this value was used in further experiments.

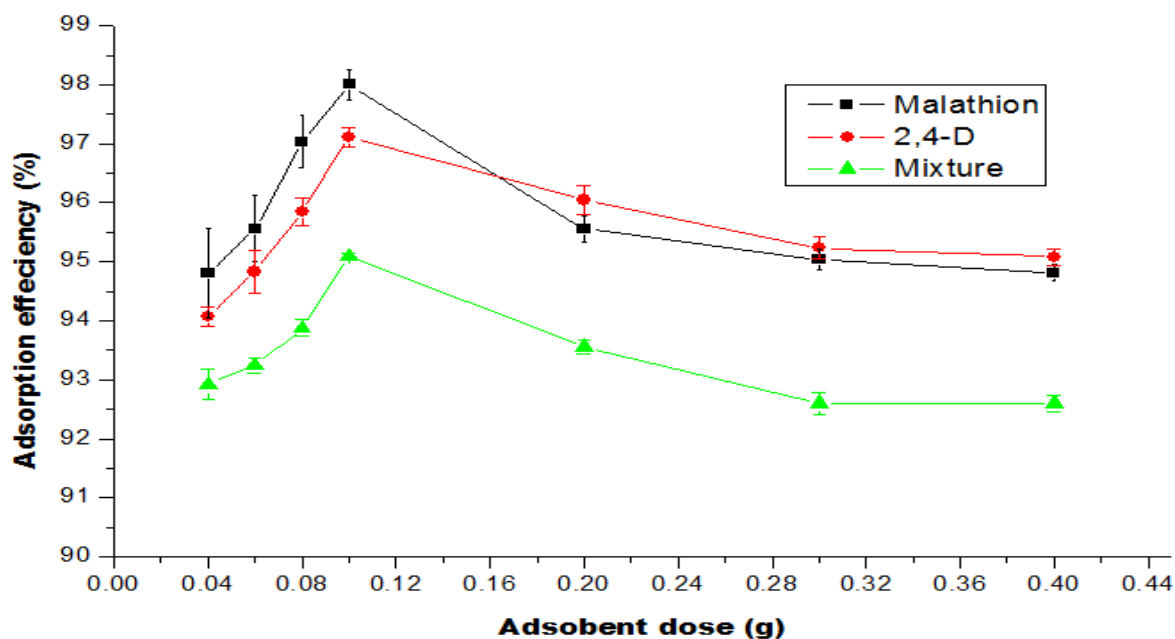


Figure 14. Effect of Adsorbent dose on the removal of Malathion, 2, 4-D and Mixture onto UiO-66 (at $C_0 = 5$ ppm; Contact time = 1h; Agitation speed = 150 rpm and optimized pH = 4, 3, 4 respectively).

4.2.3. Effect of Contact Time

Contact time is a key factor in designing a treatment process with minimum time and maximum efficiency. The effect of contact time on the removal of Malathion, 2, 4-D and mixture by UiO-66(Zr) were carried out by varying contact time from 30 min to 180 min (Figure 15). The removals of these pesticides were rapid in the first 30 to 60 minutes and decreased after 60 minutes. It was observed that instant adsorption of Malathion, 2, 4-D and mixture was achieved within 60 min and the adsorption efficiency of 99.6, 98.2 and 96.3%, respectively. It was noted that the adsorption increased rapidly in the initial stages and then became slow at later stages till the equilibrium was attained. The fact is that initially all adsorbent sites were vacant and hence, the adsorption was high. Later, due to the decrease in the available adsorption sites on the adsorbent surface as well as decrease in the adsorbate concentration, the adsorption became slow. Similar results were reports in the literature on the removal of 2, 4-D (69%) on Cu-Fe-layered double hydroxide nanoparticles (Nejati *et al.*, 2013) and Malathion (91%) on Cross

linked polystyrene based strongly basic anion exchange resin De-Acidite FF-IP (Dehghania, *et al.*, 2017). Consequently, the optimum contact time for this study was at 60 minutes and was used in the subsequent experiments.

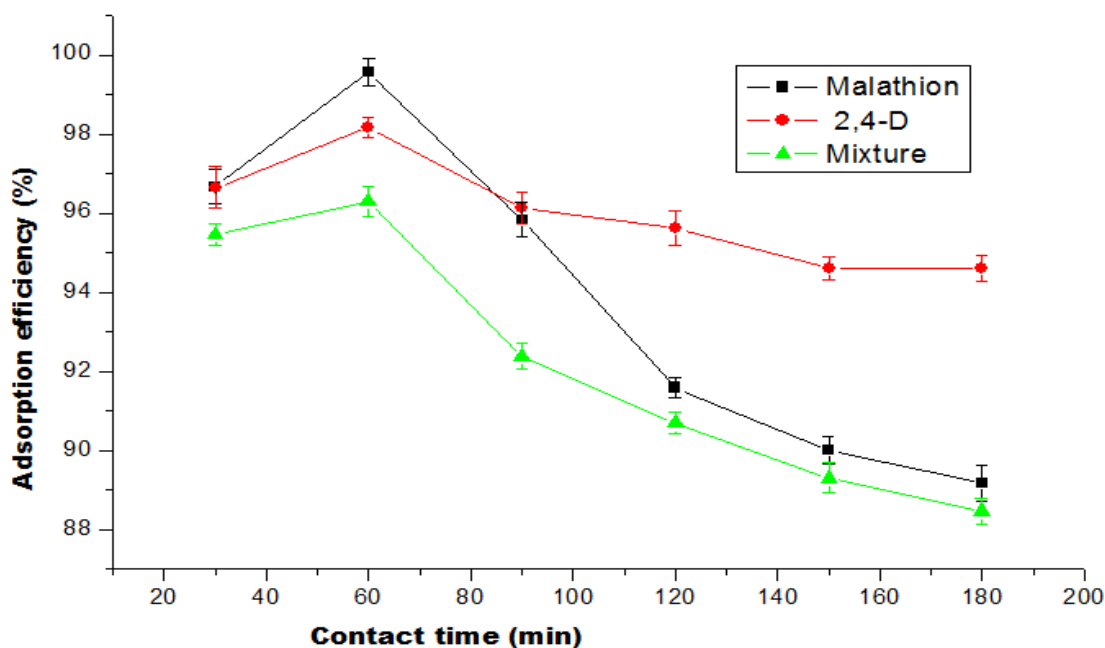


Figure 15. Effect of Contact time on the removal of Malathion, 2, 4-D and mixture (at $C_0 = 5$ mg/L; Agitation speed = 150 rpm and optimized pH = 4, 3 and 4; Adsorbent dose = 0.1 g respectively).

4.2.4. Effect of Agitation Speed

The influence of the agitation speed on the adsorption of Malathion, 2, 4-D and mixture on UiO-66(Zr) from the aqueous solution were studied by varying agitation speed from 50 to 250 rpm by keeping other parameters at optimum conditions (pH, 4, 3 and 4; adsorbent amount, 0.1 g and contact time, 60 min) and keeping the initial concentration constant (5 mg/L). It can be acquired from Figure 16 that the adsorption efficiency increases as the agitation speed increases to some extent. The adsorption efficiency increased as agitation speed increases from 50 to 100 rpm for Malathion, 50 to 125 rpm for 2, 4-D and 50 to 150 rpm for mixture with maximum adsorption of 97.6%, 98.1% and 96.7%, respectively. This effect can be attributed to the increased turbulence (which insures an intimate contact between the phases) and as a consequence, the decrease

boundary layer thickness around the adsorbent particles as a result of increasing the degree of mixing.

The agitation speed required for adsorption of Malathion was relatively lower (100 rpm) than for 2, 4-D and the Mixture. With the increasing of the agitation speed, the rate of diffusion of the Malathion molecules from the bulk liquid to the liquid boundary layer surrounding UiO-66(Zr) particle become higher because of an enhancement of the turbulence and a decrease of the thickness of the liquid boundary layer (Kus'mierek and S'wiajtkowski, 2015). Therefore, the agitation speed for Malthion, 2, 4-D and mixture were attained at 100, 125, 150 rpm, respectively.

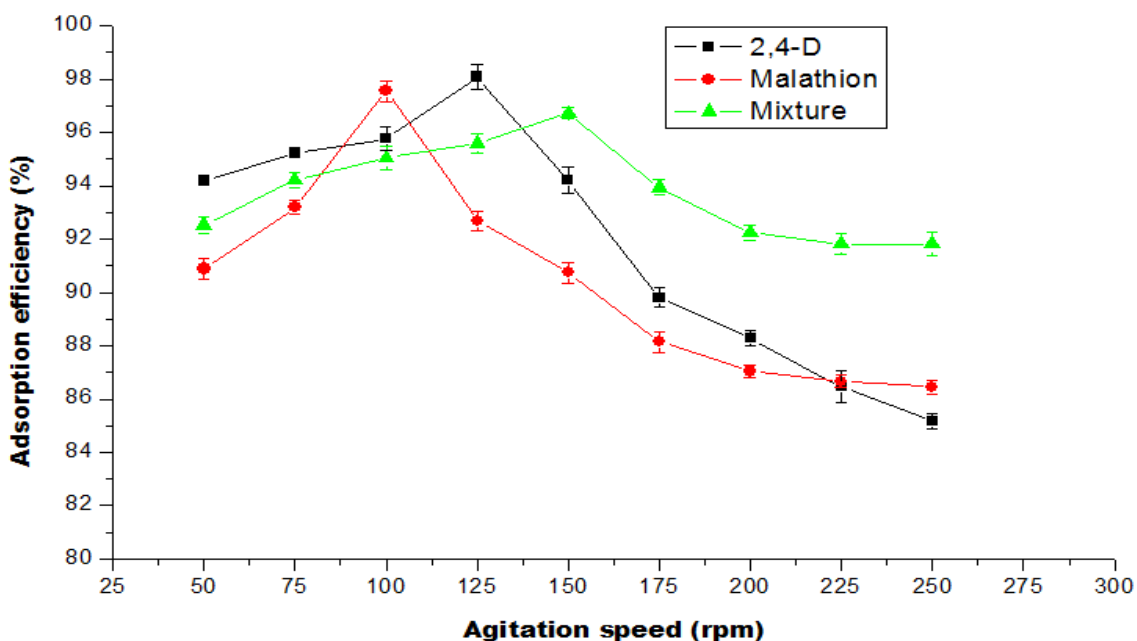


Figure 16. Effect of Agitation speed on the removal of Malathion, 2, 4-D and mixture onto UiO-66 (at $C_0 = 5$ ppm and optimized pH = 4, 3 and 4; Adsorbent dose = 0.1 g; Contact time = 1 hr respectively).

4.2.5. Effect of Initial Concentration

The effect of initial Malathion, 2, 4-D and mixture concentrations on the adsorption phenomena onto the UiO-66(Zr) adsorbent were performed by varying the initial concentrations from 1 to 50

mg/L while other parameters were kept constant at their optimum value and the results were presented in Figure 17.

Percentage removal of the pesticides was found to decrease with increase in sorbate concentrations up to a certain concentration and remained constant with further increase in concentration, which may be attributed to the increase in concentration gradient and thus, indicating the saturation of sorption sites (Alka and Anita, 2014). It is also evident from Figure 17 that the percentage removal of Malathion, 2, 4-D and mixture decreased from 98.5% to 93.1%, 97.6% to 92.2% and 92.4 to 87.9%, and then constant as their concentration increased from 20 mg/L to 50 mg/L, respectively.

This can be explained by the fact that in case of low concentrations, the ratio of the initial number of moles of solutes to the available surface area of adsorbent is large enough and the fractional adsorption becomes independent of initial concentration and consequently, higher adsorption yields were obtained. Besides, high adsorption rate at low initial concentration of pesticides were due to the abundance of free binding sites of the adsorbent (UiO-66(Zr)). However, at higher concentration most of the adsorption sites of UiO-66(Zr) could be occupied by the ions and the available sites for adsorption would become fewer, hence, the adsorption percentage depends up on the initial concentrations could decrease. Therefore, 5 mg/L was considered as an optimum initial concentration of the analytes.

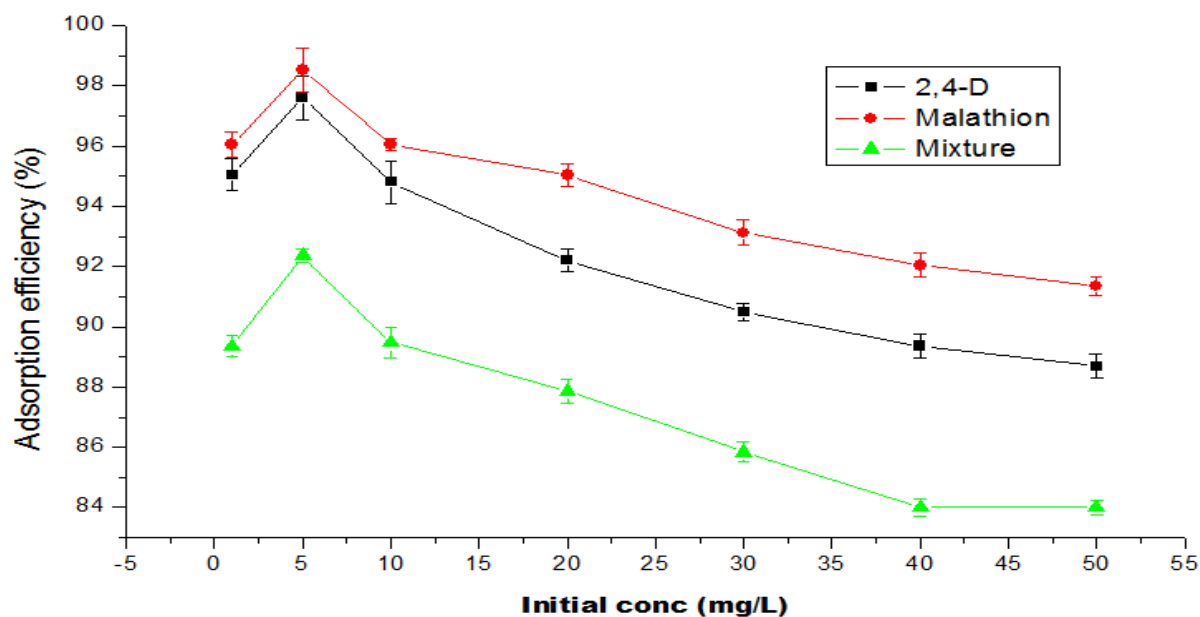


Figure17. Effect of Initial concentration on the removal of Malathion, 2, 4-D and mixture onto UIO-66 (at optimized pH = 4, 3 and 4; Adsorbent dose = 0.1 g; Contact time = 1 hr; Agitation speed = 125,100,150 rpm respectively).

4.3. Adsorption Isotherms Study

The study of adsorption isotherms is very important in ascertaining how solutes interact with adsorbents and to understand the feasibility of different adsorption processes on adsorbing a particular adsorbate. Such study is also useful in investigating the distribution of adsorption molecules between liquid and solid phase when the state of equilibrium is achieved (Wanjer *et al.*, 2018). The adsorption isotherms correlate the equilibrium adsorption data with different mathematical models to describe how adsorbate interact with adsorbents and, is critical in optimizing the use of adsorbent (Bharathi and Ramesh, 2012). Shortly it gives an idea about the feasibility of an adsorbate-adsorbent system. In the current study, the adsorption isotherms were conducted by varying initial concentration of Malathion, 2, 4-D and mixture at room temperature by keeping other parameters at optimum condition. The two commonly used sorption models, Langmuir and Freundlich, were employed in this study.

Langmuir isotherm assumes that adsorption takes place at specific homogeneous sites within the adsorbent and there is no significant interaction among the adsorbed species. Also, the adsorption rate is proportional to the number of free sites on the adsorbent and fluid concentration (Chen *et al.*, 2012). It can be expressed as follows:

$$\frac{C_e}{q_e} = \frac{1}{bQ_0} + \frac{C_e}{Q_0} \quad \text{Linear form} \quad (4.1)$$

Where, C_e is the equilibrium concentration of solution (mg/L), q_e is the amount of pesticide adsorbed; Q_0 the maximum adsorption capacity (mg/g) and b is the sorption equilibrium constant (L/mg), indicating the sorbent affinity and energy of adsorption. The linear plots of C_e/q_e vs. C_e suggest the applicability of the Langmuir isotherms as well as the value of Q_0 and b is calculated from slope and intercepts of the graph respectively as shown table below (Table 4).

The Freundlich isotherm used for isothermal adsorption is a special case for heterogeneous surface energy in which the energy term in the Langmuir equation varies as a function of surface coverage strictly due to variation of the sorption. The equation is given as (Chen *et al.*, 2012):

$$\log q_e = \log K_f + 1/n \log C_e \quad (4.2)$$

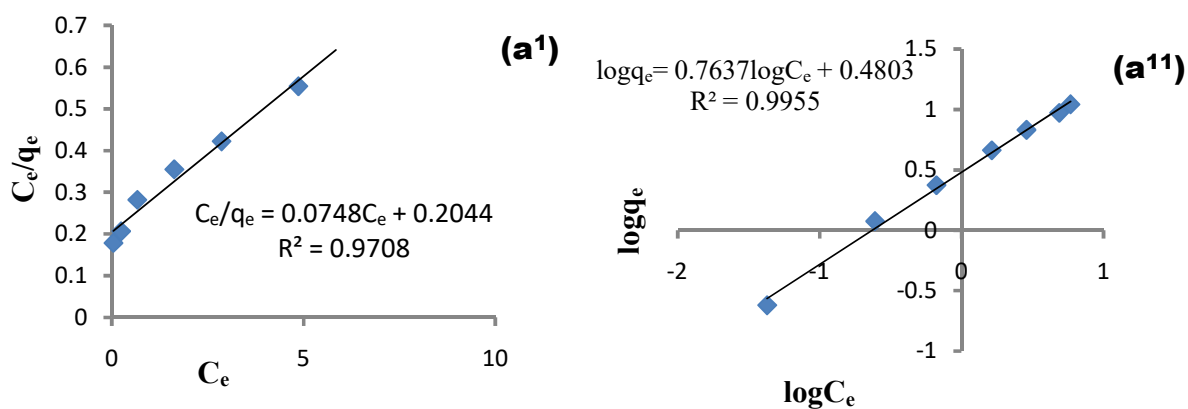
Where, K_f and n are Freundlich constants representing adsorption capacity and the energy of adsorption effectiveness respectively. The values of K_f and n obtained from experimental results are tabulated in Table 4. The values of $1/n$ give an indication of the favorability of adsorption. As value of n is greater than unity for all adsorbents, it demonstrates a favorable adsorption condition (Kumar *et al.*, 2014).

The Langmuir and Freundlich isotherm constants for adsorption of Malathion, 2, 4-D and Mixture on UiO-66 (Zr) were calculated from this isotherm and their values are given in Table 4.

Table 4. Langmuir and Freundlich isotherm constants for adsorption of Malathion, 2, 4-D and Mixture on UiO-66 (Zr)

Adsorbent	Adsorbate	Langmuir				Freundlich		
		Q ₀ (mg/g)	b	R _L	R ²	K _f	1/n	R ²
UiO-66(Zr)	Malathion	13.37	0.37	0.23	0.971	3.02	0.764	0.996
	2,4-D	21.98	0.11	0.42	0.968	1.95	0.852	0.997
	Mixture	19.12	0.204	0.313	0.966	2.813	0.820	0.995

The linearized Langmuir and Freundlich graphs for the adsorption of Malathion, 2, 4-D and mixture on UiO-66(Zr) are given in Figure 18.



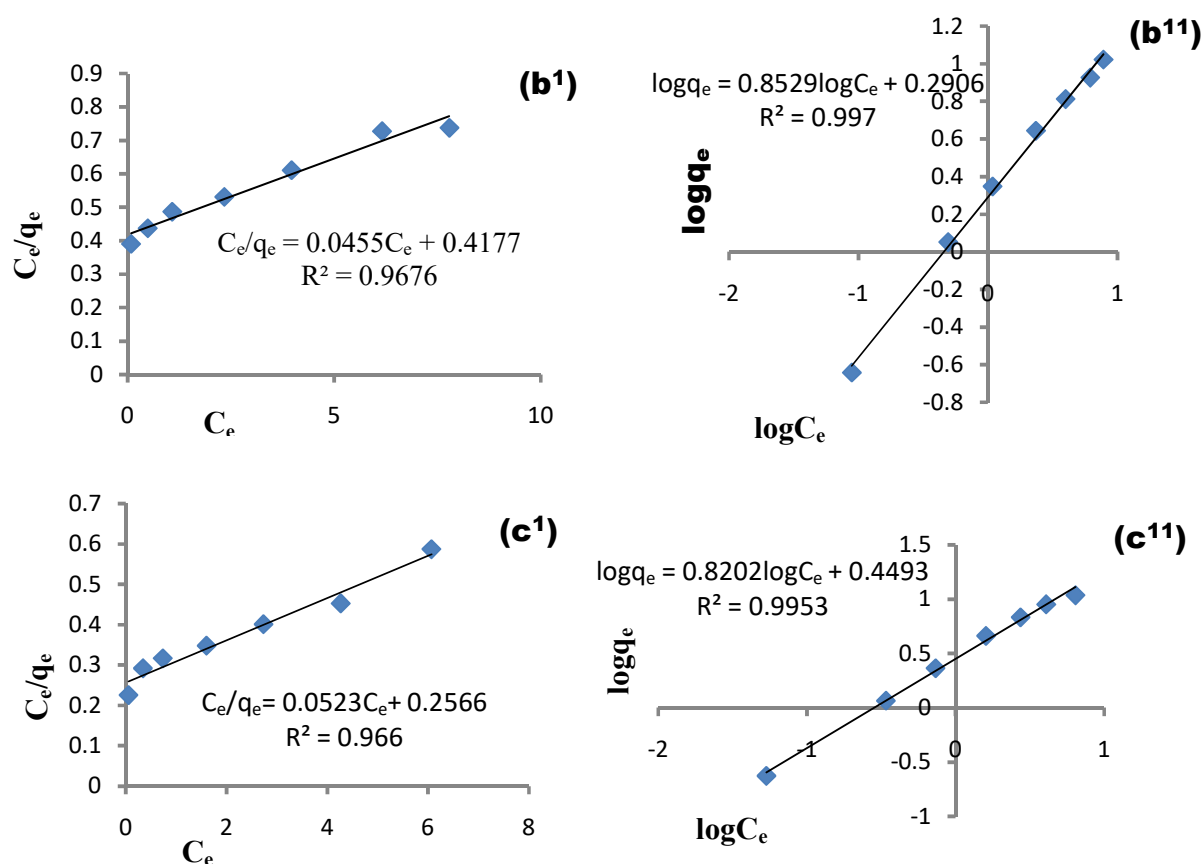


Figure 18. Langmuir (a¹, b¹ and c¹) and Fredlich (a¹¹, b¹¹ and c¹¹) isotherm for Adsorption of Malathion, 2, 4-D and mixture on UiO-66(Zr), respectively.

The graph of C_e/q_e vs q_e yields a straight line with a value of Q_0 (13.37, 21.98 and 19.12 mg/g) and b (0.37, 0.11 and 0.204) for the adsorption of Malathion, 2, 4-D and mixture on UiO-66(Zr), respectively. To confirm the favorability of the adsorption process, the separation factor (R_L) was determined as provided in Table 4. The values were found to be between 0 and 1 and confirm that the ongoing adsorption process is favorable.

Also the plot of $\log q_e$ vs $\log C_e$ gave straight line K_f (3.32, 1.95 and 2.81) and $1/n$ (0.764, 0.852 and 0.820) for the adsorption of Malathion, 2, 4-D and mixture on UiO-66(Zr), respectively (Table 5). K_f gives the adsorption capacity of the adsorbent and n a constant related to energy and intensity of adsorption. The values of $1/n$ indicate the type of isotherm to be irreversible ($1/n = 0$), with favorable ($0 < 1/n < 1$) and unfavorable ($1/n > 1$). The value of n less than one indicate

chemical adsorption process while the n value greater than one tells about the physical process and in this study, since the calculated n value was greater than one (Table 4), the adsorption process may go through physical process (Nejati *et al.*, 2013).

The coefficient of determination (R^2) obtained for Langmuir and Freundlich isotherms were (0.971, 0.968 and 0.966) and (0.996, 0.997 and 0.995), respectively, for the adsorption of Malathion, 2, 4-D and mixture on UiO-66(Zr). The R^2 values of Freundlich model was found to be greater than that of Langmuir model, indicating that Freundlich is suitable for describing the adsorption equilibrium of the pesticides (2, 4-D and Malathion) onto UiO-66(Zr) and this suggests that the adsorption taken place at heterogeneous surface within adsorbent. Similar phenomenon was also reported for the removal of Malathion and 2, 4-D (Naushadn *et al.*, 2013; Abigail and Chidambaram, 2016).

4.4. Adsorption Kinetics

The kinetic study is very important in the adsorption study which gives an idea of adsorbate uptake rate and efficiency of adsorption. The mechanism of adsorption depends on the physical and chemical characteristics of the adsorbent as well as the mass transfer process. It provides an understanding of adsorption rate and controlling mechanism of the process (Muthukumarana *et al.*, 2016). Kinetic profiles of Malathion, 2, 4-D and mixture removal were generated for the UiO-66 adsorbent by assessing the equilibrium time in order to test the suitability of the two common kinetic models, pseudo first order and pseudo second order. The pseudo first order kinetics may be expressed as follows (Kumar *et al.*, 2014):

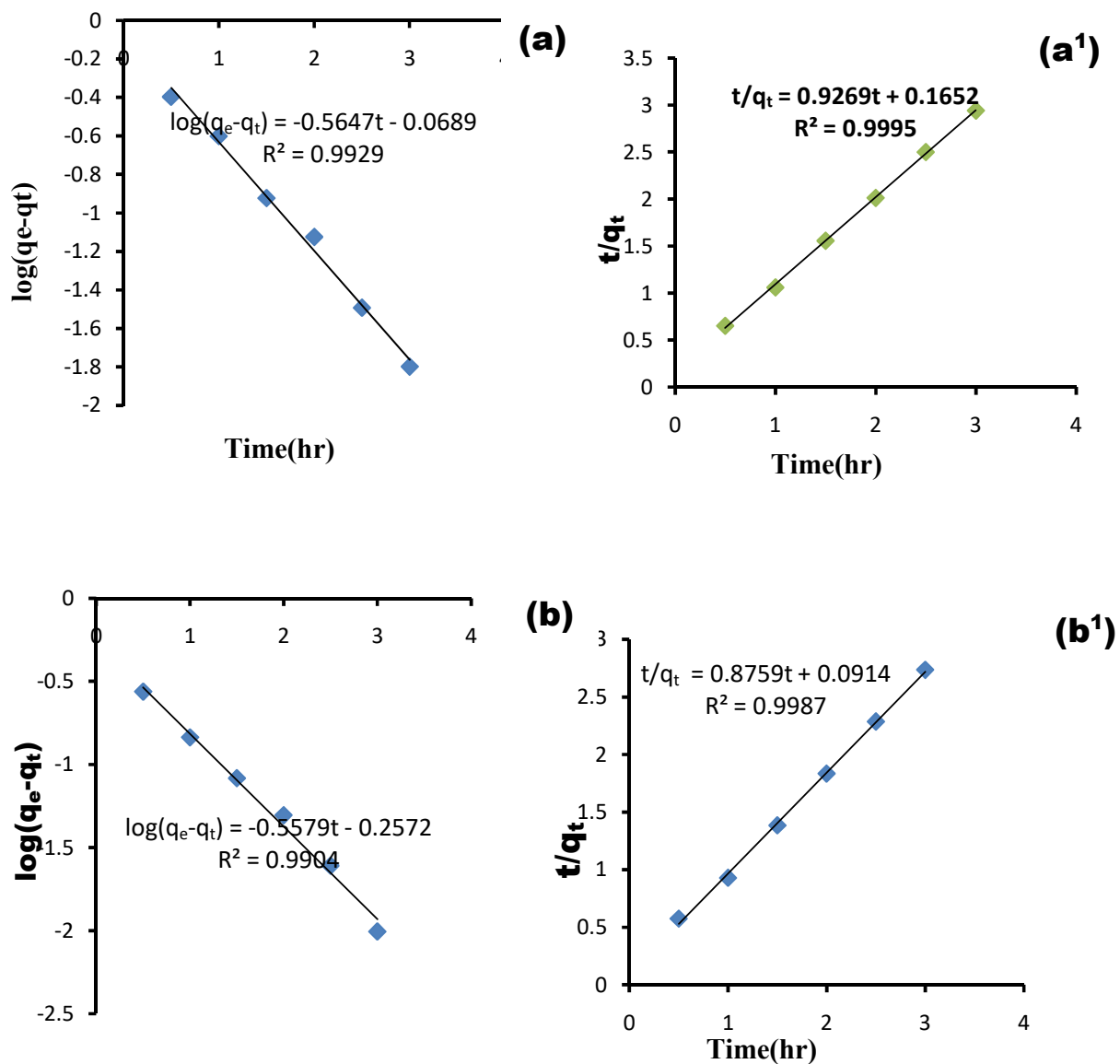
$$\log(q_e - q_t) = \log q_e - \frac{K_1}{2.303} t \quad (4.3)$$

Where q_t are the amount of adsorbate per unit mass of adsorbent at time t . The pseudo-first order rate constant K_1 and q_e can be determined from slope and intercept of the graph by plotting $\log(q_e - q_t)$ vs time t .

The pseudo second order kinetics also expressed as;

$$\frac{t}{q_e} = \frac{1}{K_2 q_e^2} + \frac{t}{q_e} \quad (4.4)$$

Where K_2 is the rate constant for adsorption, q_e (mg/g) the amount of adsorbate adsorbed at equilibrium and q_t (mg/g) is the amount of adsorbent adsorbed at time t . The values of above model parameters such as K_1 , K_2 and correlation coefficients (R^2) are obtained from the graph (Figure 19) and their respective values are presented in Table 5.



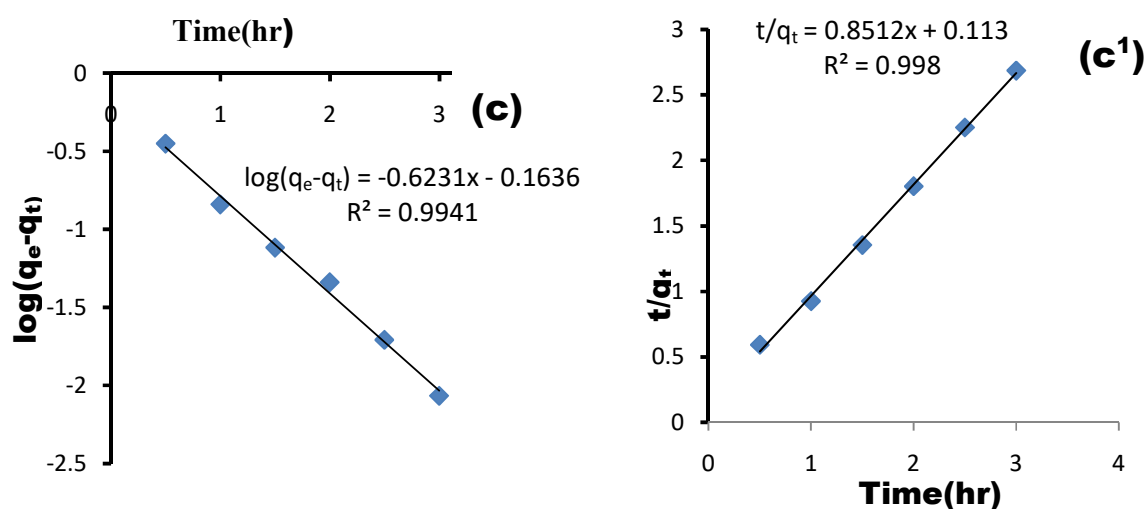


Figure 19. Graph for the pseudo-first order (a, b and c) and pseudo-second order (a¹, b¹ and c¹) of the adsorption of Malathion, 2,4-D and mixture on to UiO-66(Zr) respectively.

Table 5. The values of parameters and correlation coefficients of kinetic models

Adsorbent	Adsorbate	Pseudo-first order				Pseudo-second order		
		qe(mg/g) experimental	K ₁	qe(mg/g) (calculated)	R ²	K ₂	qe(mg/g) (calculated)	R ²
UIO-66	Malathion	1.19	1.30	0.85	0.993	5.5	1.08	0.999
	2,4-D	1.22	1.28	0.55	0.990	8.40	1.142	0.998
	Mixture	1.23	1.44	0.69	0.994	6.41	1.17	0.998

It was evident that pseudo-second order kinetic model fitted better than pseudo-first one in all three cases (Figure 19). This phenomenon was confirmed by correlation coefficient (R²) summarized in Table 5. The coefficient of determination (R²) for pseudo second-order model were (0.999, 0.999 and 0.998) which is slight greater than pseudo-first order (0.993, 0.990 and

0.994) for Malathion, 2, 4-D and mixture respectively. Moreover, the calculated q_e values for pseudo second-order (1.021, 1.108 and 1.109) agreed with the experimental (1.25, 1.225 and 1.24) than pseudo-first order model (0.983, 0.967 and 0.365) for Malathion, 2, 4-D and mixture respectively. This suggests that the adsorption of Malathion, 2, 4-D and mixture on to UiO-66(Zr) follows second-order kinetics indicates that the adsorption rate should be more relying on the availability of adsorption sites rather than the concentration of adsorbate in the medium (Liu *et al.*, 2016). Similar results were reported in recent for the adsorption of 2, 4-D and Malathion by MIL-53 (Cr-BDC) and agricultural and commercial adsorbents from aqueous solutions (Beom *et al.*, 2013; Kumar *et al.*, 2014).

4.5. Adsorption Thermodynamics

Temperature has an impact on the adsorption capacity to some extent. It is well known that a temperature change alters the adsorption equilibrium in a specific way determined by the exothermic or endothermic nature of a process. In the present study, the effect of temperature was studied in the range 298 to 338 K to determine the thermodynamic feasibility of the adsorption process of Malathion and 2, 4-D and their mixture solutions on to UiO-66(Zr). Thermodynamic parameters related to the adsorption process; standard free energy change (ΔG°), standard enthalpy change (ΔH°) and standard entropy change (ΔS°) were determined (Salman *et al.*, 2011). The values of ΔH° and ΔS° were determined from the slope and intercept of the van't Hoff plot of $\ln K_c$ versus $1/T$ for optimized initial concentration of pesticide using the expression given in equation (4.5).

$$\ln K_c = \frac{\Delta S^\circ}{R} - \frac{\Delta H^\circ}{RT}, \quad \text{Where: } K_c = \frac{q_e}{C_e} \quad (4.5)$$

$$\Delta G^\circ = \Delta H^\circ - T\Delta S^\circ \quad (4.6)$$

Also ΔG° verified with the following equation:

$$\Delta G^\circ = -RT \ln K_c \quad (4.7)$$

Where, K_c is the thermodynamic equilibrium constant, q_e is the equilibrium adsorption capacity of adsorbate on adsorbent at different temperature, C_e is equilibrium concentration of adsorbate

in the solution, T (K) is the absolute temperature, R ($8.314 \text{ J mol}^{-1}\text{K}^{-1}$) is universal gas constant. The plot of $\ln K_c$ versus $1/T$ and the calculated thermodynamic parameters are shown Figure 20 and Table 6.

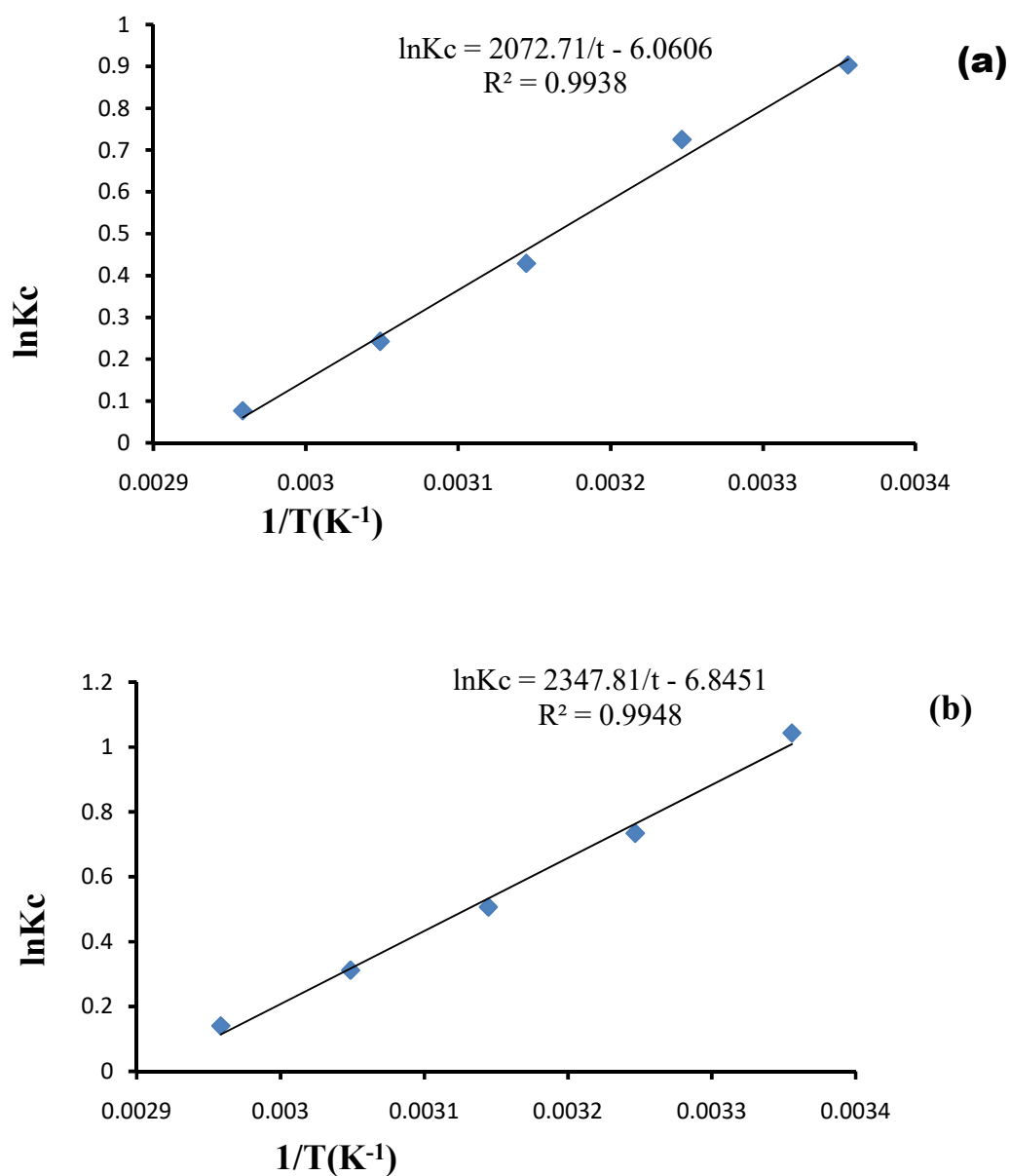


Figure 20. Thermodynamic graph of the $\ln K$ against $1/T$ of 2, 4-D (a) and Malathion (b).

Table 6. Thermodynamic parameters for 2, 4-D and Malathion adsorption onto UiO-66(Zr)

Adsorbent	Adsorbate	T (K)	ΔG (KJ/mol)	ΔH (KJ/mol)	ΔS (J/mol K)
UiO-66(Zr)	2,4-D	298	-2.210		
		308	-1.710		
		318	-1.203	-17.23	-50.4
		328	-0.699		
		338	-0.195		
	Malathion	298	-2.554		
		308	-1.98		
		318	-1.416	-19.513	-56.91
		328	-0.866		
		338	-0.277		

Thermodynamically, spontaneous and non-spontaneous processes are indicated by negative and positive ΔG° changes, respectively. Therefore, as summarized in Table 6, the negative values of ΔG° at all temperatures studied indicated that the adsorption processes were spontaneous and feasible. For both 2,4-D and Malathion the values of ΔH° are negative, indicating the exothermic nature of the process, which further explain the fact that the adsorption efficiency decreased with the increase of temperature. For 2, 4-D the exothermic adsorption may be due to a weaker interaction between the pre-adsorbed water and the adsorbent than the interaction between 2, 4-D (actually the anionic or deprotonated form) and the adsorbent. This may show a relatively strong electrostatic interaction between the 2, 4-D anions and the positive surface of

UiO-66(Zr) adsorbent relatively at low temperature. Similar results were reported for adsorption of 2, 4-D on MIL-53 (MIL stands for Material of Institute Lavoisier Similar reports (Cr-BDC) and banana stalk activated carbon (Salman *et al.*, 2011; Beom *et al.*, 2013).

The thermodynamic calculation for Malathion was also negative which reveal that the mechanism of Malathion adsorption from the aqueous solution was feasible and spontaneous. The negative value of ΔH° indicates exothermally along with strong adsorbate-adsorbent electrostatic attraction (Kumar *et al.*, 2014).

The magnitude of ΔH° may also give an idea about the type of sorption. Two main types of adsorption are physical and chemical. Generally, the magnitude of ΔH° value ranges from 0-40 KJ/mol for physisorption and 40-120 KJ/mol for chemisorption mechanisms (Fairouz *et al.*, 2015). In the present investigation, the ΔH° values were found to be -17.23 and -19.51 KJ/mol for 2, 4-D and Malathion, respectively, and this indicate that physisorption is the major adsorption mechanism. The physisorption mechanism inferred is supported by the findings from the isotherm study which indicated multilayer adsorption. Additionally, the negative value of ΔS implies less randomness at the solid/solution interfaces during the adsorption process.

4.6. Desorption and Reusability

To keep the processing cost as low as possible, it is very important to carry out desorption and regeneration studies. Desorption study of Malathion and 2, 4-D were carried out by the batch processes using different desorbing reagents (Methanol, Acetonitrile, distilled water, 0.1 M NaOH and 0.1 M HCl) in order to check their desorption performances.

The comparative results of desorption yields obtained by Methanol, Acetonitrile distilled water, 0.1 M NaOH and 0.1 M HCl solutions is shown in Figure 22. Relatively the best result was achieved by Acetonitrile with 75 and 85% of Malathion and 2, 4-D desorption respectively. This outcome indicates that the adsorbed Malathion and 2, 4-D on the surface of UiO-66(Zr) released in Acetonitrile than other solvents due to high solubility of both adsorbates in the reagent. Desorption efficiency of the analytes in other solvents was found to be (69 and 78%) in Methanol, (65 and 71%) in deionized water, (53 and 56%) in 0.1 M NaOH and (46 and 45%) in 0.1 M HCl for

Malathion and 2, 4-D, respectively (Figure 21). Even though desorption of adsorbate from the surface of adsorbent (UiO-66) were possible, high desorption efficiency were not possible in these solvents compared to Acetonitrile. This might due to strong electrostatic attraction between the surface of adsorbent and adsorbates.

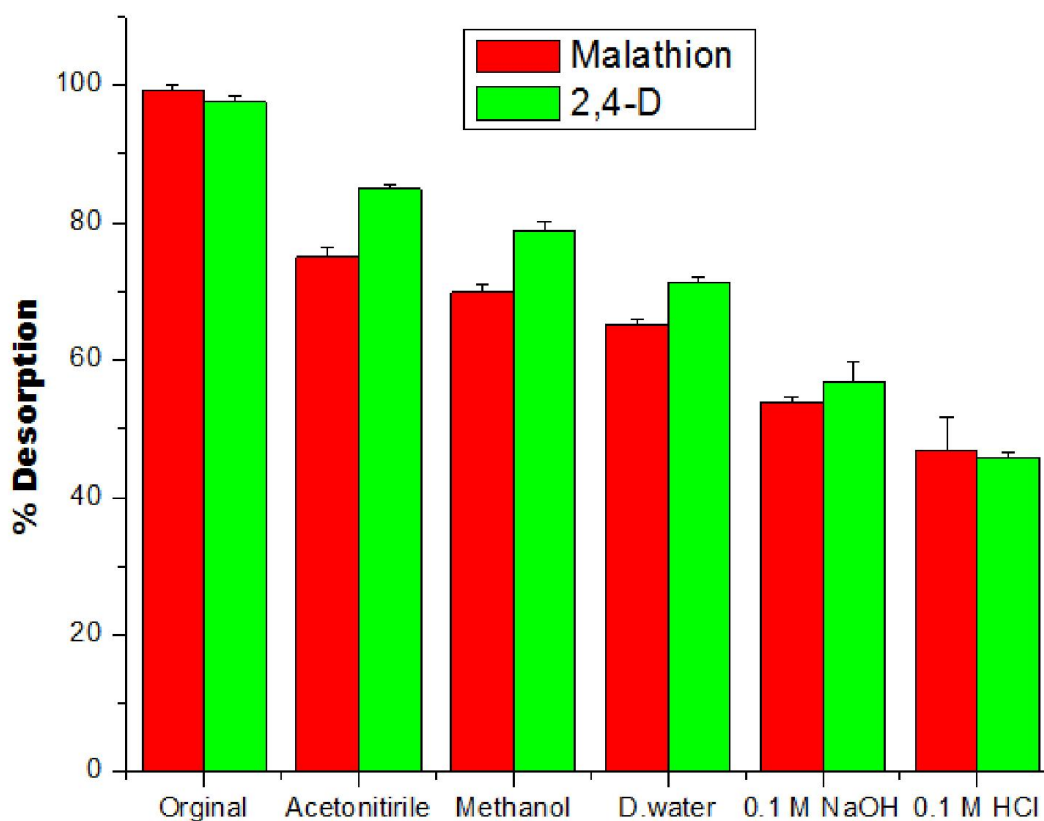


Figure 21. Desorption of Malathion and 2, 4-D using different reagents.

To keep the process of adsorption more economical, it is very important to regenerate the adsorbent. Since commercial applications of an adsorptive removal rely on the reusability of an adsorbent, an adsorption will surely be improved greatly if the reusability of the adsorbents is confirmed (Beom *et al.*, 2013). In this study the reusability of the UiO-66(Zr) was estimated after solvent washing of the used MOF. Among desorption reagents (Methanol, Acetonitrile distilled water, 0.1 M NaOH and 0.1 M HCl) used for desorption of both Malathion and 2, 4-D, Acetonitrile is used for regeneration, due to its slight highest desorption efficiency.

The results of Malathion and 2, 4-D sorption through original and regenerated UiO-66 (Zr-MOF) are shown on the figure 22. Accordingly UiO-66 retains about 70% adsorption capacity after three runs. This implies that the spent adsorbent (UiO-66) can be regenerated and re-used. The percent desorption decrease from 80 to 68 % and 85 to 72 % for Malathion and 2, 4-D, respectively, after three cycles. There is no such significant variation within regeneration cycles. This reveals that UiO-66 can be regenerated and reused multiple times as it was also suggested by Lin *et al.*, 2015.

The variations in adsorption between the original and regenerated adsorbent may due to the nature of the adsorbate and the surface of adsorbent. Since no complete desorption is possible, the adsorbates that are weakly attached on the surface of UiO-66(Zr) can be easily removed while those adsorbed strongly may be difficult to desorb easily.

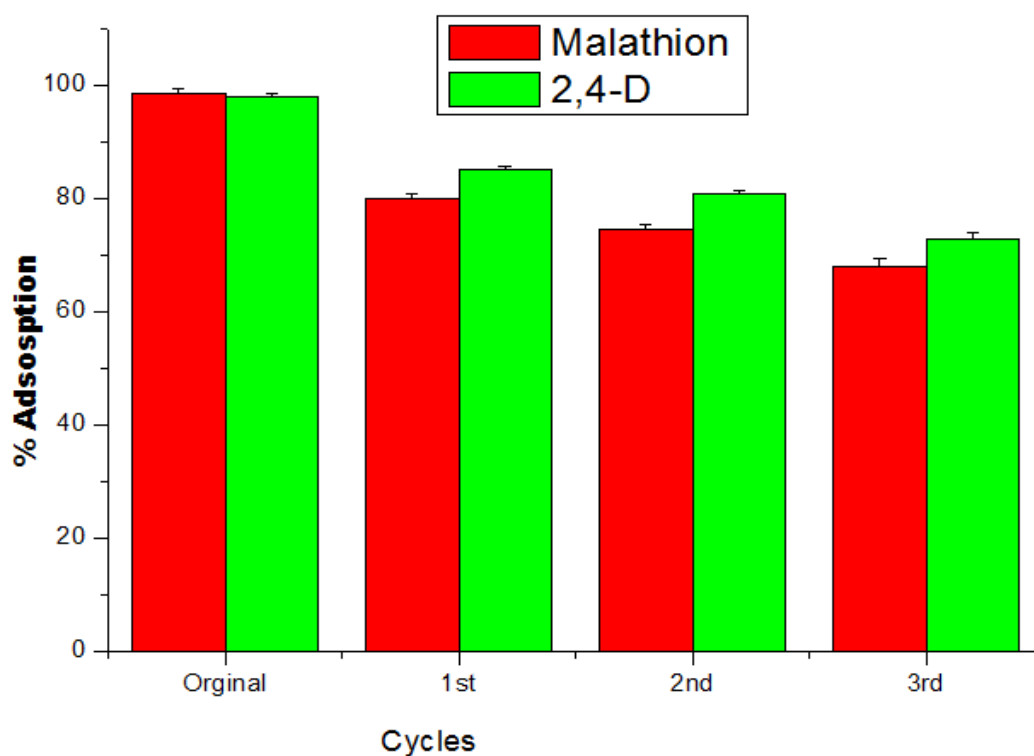


Figure 22. Regeneration of UiO-66(Zr) for adsorption of Malathion and 2, 4-D.

4.7. Real Sample Analysis

To assure the practical applicability of the developed strategy for the removal of pesticides from real samples, tap water samples from Bate and Haramaya University main campus were treated with UiO-66(Zr) at the optimized conditions. In the assayed samples, the target analytes (Malathion and 2, 4-D) were not detected. Therefore, the samples were spiked with known standard solution to evaluate the adsorption performance of UiO-66(Zr) in the matrix effect. The results listed in Table 7 shows the recovery values for the adsorption of Malathion and 2, 4-D in the two samples. The obtained recovery values of the analyte in both tap water samples were in the ranges of 78-107% and 90-111% at 5 and 10 mg/L spiking levels for Malathion and 2, 4-D, respectively. Since the result met the criteria for matrix effect (70–120%) according to the guidance document on analytical quality control and validation procedures for pesticide analysis in water (Pizzutti *et al.*, 2016). The recovery values were satisfactory, and it can be said that the matrix effect from the water samples on the adsorption of Malathion and 2, 4-D on to UiO-66(Zr) was not significant.

Table 7. Recovery (%) values of UiO-66(Zr) based analysis of real sample

Sample	Pesticide	% Recovery \pm SD		
		Unspiked	5 mg/L spiked	10 mg/L spiked
Haramaya University	Malathion	ND*	104 \pm 3.7	78.9 \pm 3.6
	2,4-D	ND*	98.7 \pm 3.4	90.8 \pm 0.9
Bate	Malathion	ND*	108 \pm 1.9	79 \pm 3.6
	2,4-D	ND*	111 \pm 5.0	97.4 \pm 2.0

*Not detected

5. CONCLUSION AND RECOMMENDATION

5.1. Conclusion

Zirconium based metal organic frame work; UiO-66 was successfully prepared by solvothermal method using DMF as organic linker at 120 °C. It was characterized by FTIR, PXRD, TGA and SEM for confirming functional groups, phase identification, thermal stability and its morphology respectively.

FTIR revealed that peaks at 3419 cm^{-1} show the presence of OH group at the external surface, a band at 1396 cm^{-1} and 1586 cm^{-1} due to the presence of carboxylate group of BDC in MOF structure and peak at 660 and 748 cm^{-1} are attributed $\mu_3\text{-O}$ stretching with Zr-(OC). A PXRD result confirms that the as-synthesized material was MOFs. The most probable diffraction peaks for MOFs were found below scattering angle (2θ) of 10. TGA analysis of the UiO-66 (Zr) shows two steps weight loss prior to the formation of final ZrO_2 product. Thermal stability study tells us, the synthesized MOF has a good thermal stability.

The performance of UiO-66(Zr) for the adsorptive removal of pesticides namely Malathion and 2, 4-D was studied batch process. The amounts of pesticide (Malathion and 2, 4-D) adsorbed on the UiO-66(Zr) were found to vary with pH, contact time, Adsorbent dose, Agitation speed and initial concentration. The maximum removal efficiency of Malathion, 2, 4-D and Mixture by UiO-66(Zr) occurred at pH (4, 3 and 4), dose and contact time (0.1 g and 60 min), agitation speed (100, 125 and 150 rpm) and initial concentration (5 mg/L) for each respectively.

The sorption data was analyzed by using Freundlich and Langmuir models. It was found that the coefficient of determination for Freundlich models were close to unity indicating that the best fit model were Freundlich. Values of the equilibrium parameter (R_L) from Langmuir isotherm and n values from the Freundlich isotherm have indicated that the adsorption process is favorable.

Controlling mechanism of pesticide adsorption from aqueous solution were examined by kinetics model namely pseudo first order and second order kinetics. The coefficient of determination (R^2) pseudo-second order tends to unity a well as the calculated q_e values for pseudo second-order relatively agreed with the experimental q_e values for both Malathion and 2,4-D. Due to these, it

concluded that pseudo-second order kinetic model described the data better than pseudo-first order kinetic models.

Important thermodynamic parameters such as standard free energy change (ΔG°), standard enthalpy change (ΔH°) and standard entropy change (ΔS°) of adsorption that can confirm the feasibility, spontaneity, and heat change for the adsorption process were determined. Accordingly, the negative values of ΔG° and ΔH° implying that the adsorption process of Malathion and 2,4-D are spontaneous, feasible, exothermic and physical in nature from the negative values of ΔG and ΔH respectively.

Reusability of UiO-66(Zr) after desorption of the adsorbed Malathion and 2, 4-D indicates that multiple adsorption of the used adsorbent was possible after washing with Acetonitrile. The applicability of UiO-66(Zr) for the adsorption for Malathion and 2, 4-D in the real sample were confirmed by checking the percent of recoveries since the expected analyte were not detected in the real sample taken. Recovery values were satisfactory, and it can be said that the matrix effect from the water samples on the adsorption of Malathion and 2, 4-D on to UiO-66(Zr) was not significant.

5.2. Recommendation

The following recommendations can be made as a result of the outcome of this study:

- Further research should be under taken for removal other very toxic pollutants such as Parathion, Mercury and 2, 4-dicholorophenol (oxide of 2, 4-D) using UiO-66(Zr) adsorbent.
- To improve the removal efficiency of the adsorbent through continuous optimization of additional parameters like effect of ionic strength and selection of solvents, synthesis method, post treatment method further studies could be undertaken.
- To obtain ultra-high porosity and large pore opening of UiO-66(Zr), further study such as post synthetic modification and Multivariating (in which multiple organic functionalities are incorporated within a single framework, have provided many

opportunities for designing complexity within the pores of UiO-66 in a controlled manner) should be required.

- Further research should be carried out under optimized condition deeply to explore the efficiency of UiO-66 for the removal of pesticides from soil to confirm its use for farmers.
- The impact of the synthesized metal frame work (UiO-66) should also needs serious studies for the future.

6. REFERENCES

- Abigail, M.E and Chidambaram, R. 2016. Rice husk as a low cost nanosorbent for 2, 4-dichlorophenoxyacetic acid removal from aqueous solutions. *Ecological Engineering*, 92: 97-105.
- Adamson, A. 1990. Physical Chemistry of Surfaces, 5th Edition. John Wiley & Sons, New York.
- Alam, J.B., Dikshit, A.K. Bandyopadhyay, M. 2005. Evaluation of thermodynamic properties of sorption of 2, 4-D and atrazine by tire rubber granules. *Separation and Purification Technology*, 42: 85-90.
- Alka, T. and Anita, B. 2014. Effective Removal of Pesticide (Dichlorvos) by Adsorption onto Super Paramagnetic Poly (styrene-co-acrylic acid) Hydrogel from Water. *International Research Journal of Environment Sciences*, 3(11): 41-46.
- Al-Qodah, Z., Shawaqfeh, A.T., Lafi W.K. 2007. Adsorption of pesticides from aqueous solutions using oil shale ash. *Desalination* 208: 294–305.
- Augustus, E.N., Nimibofa, A., Kesiye, I.A., Donbebe, W. 2017. Metal organic Frameworks as novel adsorbents. *American Journal of Environmental Protection*, 5(2): 61-67.
- Azhara, M., Abid, H., Periasamy, V., Sun, H., Tade, M., Wang Sh. 2017. Adsorptive removal of antibiotic sulfonamide by UiO-66 and ZIF-67 for wastewater treatment. *Journal of Colloid and Interface Science*, 500: 88-95.
- Azhara, M.R., Abid, H. R., Sun, H., Periasamy, V., Tade, M. O., Wang, Sh. 2017. One-pot synthesis of binary metal organic frameworks (HKUST-1 and UiO-66) for enhanced adsorptive removal of water contaminants. *Journal of Colloid and Interface Science*, 490: 685-694.
- Bai, Y.H., Zhou, L., Wang, J. 2006. Organophosphorous pesticides residues in market foods in Shaanxi area. *Food Chemistry*, 98; 240-242.
- Bakhtiary, S., Shirvani, M., Shariatmadari H. 2013. Adsorption-desorption behavior of 2, 4-D on NCP-modified bentonite and zeolite: Implications for slow-release herbicide formulations. *Chemosphere*, 90: 699-705.
- Barr, D., Panuwet, P., Nguyen, J., Udunka, S., Needham, L. 2007. Assessing exposure to atrazine and its metabolites using biomonitoring. *Environmental Health Perspective*, 115: 1474-1478.

- Basini, G., Bianchi, F., Bussolati, S., Baioni, L., Ramoni, R., Grolli, S., Conti, V., Grasselli, F. 2012. Atrazine disrupts steroidogenesis, VEGF and NO production in swine granulosa cells. *Ecotoxicology and Environmental Safety*, 85: 59-63.
- Bazrafshan, E., Mahvi, A., Nasser, S., Shaieghi, M. 2007. Performance evaluation of electrocoagulation process for diazinon removal from aqueous environments by using iron electrodes. *Iran Journal of Environmental Health Science Engineering*, 4(2): 127-132.
- Bazrafshan, E., Mostafapour, F., Faridi, H., Farzadkia, M., Sargazi, S., Sohrabi, A. 2013. Removal of 2, 4-Dichlorophenoxyacetic Acid (2, 4-D) from aqueous environments using single Walled Carbon Nanotubes. *Health Scope*, 2(1): 39-46.
- Beldon, P.J., Fa'bia'n, L., Stein, R.S., Thirumurugan, A., Cheetham, A.K. 2010. Rapid room-temperature synthesis of zeoliticimidazolate frameworks by using mechanochemistry *Angewandte Chemie International Edition*, 49: 9640-9643.
- Beom, K., Jung, Zubair, H., Sung, H. 2013. Adsorptive removal of 2, 4-dichlorophenoxyacetic acid (2, 4-D) from water with a metal organic framework. *Chemical Engineering Journal*, 234: 99-105.
- Bonner, M.R., Coble, J., Blair, A. 2007. Malathion exposure and the incidence of cancer in the agricultural health study. *American Journal of Epidemiology*, 166: 1023-1034.
- Bunaciu, A. A., Udriștioiu, E., Aboul-Enein, H.Y. 2015. X-Ray Diffraction: Instrumentation and Applications, *Critical Reviews in Analytical Chemistry*, 45(4): 289-299.
- Carboneras, B., Villaseñor, J., Francisco, M. 2017. Modelling aerobic biodegradation of atrazine and 2, 4-dichlorophenoxy acetic acid by mixed cultures. *Bioresource Technology*, 243: 1044-1050.
- Carlos, A., Sandoval, C., Deifilia A., Juvencio, G., Nora, R., Cleotilde J., Fernando, M. 2013. Biodegradation of a mixture of the herbicides ametryn, and 2, 4-dichlorophenoxyacetic acid (2, 4-D) in a compartmentalized biofilm reactor. *Bioresource Technology*, 145: 33-36.
- Carson, C., Brown, A., Sholl, D. Nair, S. 2011. Sonochemical synthesis and characterization of sub micrometer crystals of the metal-organic framework Cu. *Crystal Growth Design*, 11: 4505-4510.

- Chavan, S.M., Shearer, G.C., Svelle, S., Olsbye, U., Bonino, F., Ethiraj, J., Lillerud, K.P., and Bordiga, S. 2014. Synthesis and Characterization of Amine-Functionalized Mixed Ligand Metal Organic Frameworks of UiO-66 Topology. *Inorganic Chemistry journal*, 53: 9509-9515.
- Chavan, S. M., Shearer, G.C., Svelle, S., Olsbye, U., Bonino, F., Ethiraj, J., Lillerud, K. P., Bordiga, S. 2014. Synthesis and Characterization of Amine-Functionalized Mixed Ligand Metal Organic Frameworks of UiO-66 Topology. *Journal of Inorganic Chemistry*, 53 (18): 9509-9515.
- Chen, C., Zhang, M., Guan, Q., Li, W. 2012. Kinetics and thermodynamic studies on the adsorption of xylenol orange onto MIL-101(Cr). *Journal of Chemical Engineering*, 183: 60-67.
- Chen, Q., He, Q. Lv, M., Xu, Y., Yang, H., Liu, X., Wei, F. 2015. Selective adsorption of cationic dyes by UiO-66-NH₂. *Journal of Applied Surface Science*, 327: 77-85.
- Chen, T., Zhang, C., Qin, Y., Yang, H., Peng, Z., Ye, F. 2017. Preparation of Cationic MOFs with Mobile Anions by Anion Stripping to Remove 2, 4-D from Water. *Materials*, 10: 879-782.
- Costa, L.G., Giordano, G., Guizzetti, M. A. 2008. Neurotoxicity of pesticides: a brief review, *Front. Journal of Biosciences*, 13: 1240-1249.
- Curran, W. 1998. Persistence of Herbicides in Soil. *Journal of Agronomy of Facts and Agricultural science*, 1: 1-4.
- Dariush Robati. 2013. Pseudo-second-order kinetic equations for modeling adsorption systems for removal of lead ions using multi-walled carbon nanotube. *Journal of Nanostructure in Chemistry*, 3(55): 1-6.
- Dehghania, M. H., Niasar, Z. Sh., Mehrnia M.R., Shayeghi, M., Al-Ghoutif, M.A., Heibati, B., Gordon M.K. and Yetilmezsoy, K. 2017. Optimizing the removal of Organophosphorus pesticide malathion from water using multi-walled carbon nanotubes. *Chemical Engineering Journal*, 310: 22-32.
- Deng, K., Tsai, F., Ma, N., Xia, Y., Liu, H., Zhan, X., Yu, X., Zeng, X., Jiang, T., Shi, D., Chang, Ch. 2017. Adsorption Behavior of High Stable Zr-Based MOFs for the Removal of Acid Organic Dye from Water. *Materials*, 10(205): 1-11.

- Deng, H., Feng, D., He, J., Fang-ze L., Hua-mei Y., Cheng-jun G. 2017. Influence of biochar amendments to soil on the mobility of atrazine using sorption-desorption and soil thin-layer chromatography. *Ecological Engineering*, 99: 381-390.
- Dey, C., Kundu, T., Bishnu, P., Mallick, A. and Banerjee, R. 2014. Crystalline Meta-Organic Frameworks (MOFs): Synthesis, Structure and Function. *Acta Crystallographica Section B: Structural Science journal*, 70: 7-10.
- El Harmoudi, H., El Gaini, L., Daoudi, E., Rhazi, M., Boughaleb, Y., El Mhammedi, M.A., Migalska-Zalas, A., Bakasse, M. 2014. Removal of 2, 4-D from aqueous solutions by adsorption processes using two biopolymers: chitin and chitosan and their optical properties. *Journal of optical Materials*, 36: 1471-1477.
- Endale Teju, Bezuayehu Tadesse and Negussie Megersa. 2017. Salting out-assisted liquid-liquid extraction for the pre-concentration and quantitative determination of eight herbicide residues simultaneously in different water samples with high-performance liquid chromatography. *Separation Science and Technology*, 1-11. <http://dx.doi.org/10.1080/01-496395.2016.1276596>.
- Endale Tesfaye, Negussie Megersa, Abi Taddese, Endale Teju. 2016. Adsorption of herbicides by Fe-Al-Mn nano composite in aqueous solution. *International Journal in Physical & Applied Sciences*, 3(7): 1-13.
- Fairooz, N.E., Jwad, Z.A., Zahra, M.A. 2015. Adsorption isotherms and thermodynamic data for removal pesticides from aqueous solution on pomegranate peel surface. *American Journal of Applied Chemistry*, 3(4): 147-152.
- FAO (Food and Agricultural Organization) of the United Nations [Online], 2014. Pesticides: Balancing Crop Protection and Responsible Use. Plant Production and Protection Division. FAO, Rome, Italy.
- Farha, O., Yazaydin, A., Eryazici, I., Malliakas, C., Hauser, B., Kanatzidis, M., Nguyen, S., Snurr, R., Hupp, J. 2010. De novo synthesis of a metal organic framework material featuring ultrahigh surface area and gas storage capacities. *Nature Chemistry*, 2: 944-948.
- Freundlich, H. 1906. Über die Adsorption in Lösungen. *Zeitschrift für physikalische Chemie*, 57: 385-470.

- Furukawa, H., Ko, N., Aratani, S., Choi, E., Choi, A., Yazaydin, R., Snurr, M., O’Keeffe, J. 2010. Ultra high porosity in metal organic frameworks. *Science*, 329: 424-428.
- Guangcai, T., Weiling, S., Yaru, X., Hongyuan, W., Nan, X. 2016. Sorption of mercury (II) and atrazine by biochar, modified biochars and biochar based activated carbon in aqueous solution. *Bioresource Technology*, 211: 727-735.
- Gupta, V. K., Jain, C.K., Ali, I., Chandra, S., Agarwal, S. 2002. Removal of lindane and malathion from waste water using bagasse fly ash- a sugar industry waste. *Water Research*, 36: 2483-2490.
- Hameed, B.H., Salman, J.M., Ahmad, A.L. 2009. Adsorption isotherm and kinetic modeling of 2, 4-D pesticide on activated carbon derived from date stones. *Journal of Hazardous Materials* 163: 121-126.
- Han, D., Jia, W and Liang, H. 2010. Selective removal of 2, 4-dichlorophenoxyacetic acid from water by molecularly imprinted amino-functionalized silica gel sorbent. *Journal of Environmental Science China*, 22: 23-30.
- Haque, E., Lee, E., Jang, T., Hwang, K., Chang, J.S., Jegal, J., Jung, S.H. 2010. Adsorptive removal of methyl orange from aqueous solution with metal organic frameworks, porous chromium-benzene dicarboxylates. *Journal of Hazardous Materials*, 181: 535-542.
- Hayes, T., Collins, A., Lee, M., Mendoza, M., Noriega, N., Stuart A., Vonk, A. 2002. Hermaphroditic, demasculinized frogs after exposure to the herbicide atrazine at low ecologically relevant doses. *Proceedings of the National Academy of Sciences*, 99: 5476-5480.
- Infas, M., Mohideen, H., Xiao, B., Paul, S., Wheatley, Alistair, C., Mckinlay, Yang, L., Alexandra, M. 2011. Novel Metal Organic Frameworks: Synthesis, Characterization and Functions. *Nature Chemistry*, 3: 304-310.
- Kamellia, N., Soheila, D., Marziye, S. 2013. Study of 2,4 dichlorophenoxyacetic acid (2,4-D) removal by Cu-Fe-layered double hydroxide from aqueous solution. *Applied Surface Science*, 280: 67-73.
- Katz, M.J., Brown, Z.J., Colón, Y.J., Siu, P.W., Scheidt, K.A., Snurr, R.Q., Hupp, J.T., Farha, O.K. 2013. A facile synthesis of UiO-66, UiO-67 and their derivatives. *Journal of the Chemical Society D: Chemical Communications*, 49: 9449-4951.

- Kearns, J.P., Wellborn, L.S., Summers, R.S., Knappe D.R. 2014. 2, 4-D adsorption to biochars: Effect of preparation conditions on equilibrium adsorption capacity and comparison with commercial activated carbon literature data. *Journal of water research* 62: 20-28.
- Kim, S., Lee, Y., Hong, S., Jang, M., Ahn, W. 2015. Pilot scale synthesis of a zirconium-benzenedicarboxylate UiO-66 for CO₂ adsorption and catalysis. *Catalysis Today*, 245: 54-60.
- Kumar, P., Singh, H., Kapur, M., Mondal, M.K. 2014. Comparative study of malathion removal from aqueous solution by agricultural and commercial adsorbents. *Journal of Water Process Engineering*, 3: 67-73.
- Kus'mierek, K. and S'wiajtkowski, A. 2015. The influence of different agitation techniques on the adsorption kinetics of 4-chlorophenol on granular activated carbon. *Reaction Kinetics, Mechanisms, and Catalysis journal*, 116: 261-271.
- Langmuir, I. 1918. The adsorption of gases on plane surfaces of glass mica and platinum. *Journal of the American Chemical Society*, 40(9): 1361-1403.
- Li, Ch., Huang, J., Zhu, H., Liu, L., Feng, Y., Hu, G., Yu, X. 2017. Dual emitting fluorescence of Eu/Zr-MOF for ratiometric sensing formaldehyde. *Sensors and Actuators B*, 253:275-282.
- Li, J.R., Sculley, J. and Zhou, H.C. 2012. Metal-organic frameworks for separations, *Chemical Review*, 112(2): 869-932.
- Liang, W. and D'Alessandro, D.M. 2013. Microwave-assisted solvothermal synthesis of zirconium oxide based metalorganic frameworks. *Chemical Communication*, 49: 3706-3708.
- Lin, K. A., Chen, Sh. and Jochems A. P. 2015. Zirconium-based metal organic frameworks: Highly selective adsorbents for removal of phosphate from water and urine. *Journal of Materials Chemistry and Physics*, 160: 168-176.
- Long, J., Dinca, M., Yu, A. 2006. Microporous metal organic framework incorporating 1, 4-benzeneditetrazolate: Syntheses, structures, and hydrogen storage properties. *Journal of American Chemical Society*, 128: 8904-8913.
- Lozowicka, B., Kaczynski, P., Paritova, A., Kuzembekova, G., Abzhaliyeva, A., Sarsembayeva, N., Alihan, K. 2014. Pesticide residues in grain from Kazakhstan and potential health risks associated with exposure to detected pesticides. *Journal of Food and Chemical Toxicology*, 64: 238-248.

- Ma, D., Bopeh, Sh., Han, G., Borchon, Sh. 2017. Thin-Film Nanocomposite (TFN) Membranes Incorporated with Super-Hydrophilic Metal–Organic Framework (MOF) UiO-66: Toward Enhancement of Water Flux and Salt Rejection. *ACS Applied Materials & Interfaces*, 9: 7523-7534.
- Mahvi, A. 2009. Application of ultrasonic technology for water and wastewater treatment. *Iran Journal of Public Health*, 38(2): 1-17.
- Mahvi, A., Maleki, A., Rezaee, R., Safari, M. 2009. Reduction of humic substances in water by application of ultra sound waves and ultraviolet irradiation. *Iran Journal of Environmental Health Science Engineering*, 6(4): 233-240.
- Mansooreh, D., Simin, N., Mojtaba, K. 2014. Removal of 2, 4-Dichlorophenolxyaceticacid (2, 4-D) herbicide in the aqueous phase using modified granular activated carbon. *Journal of Environmental Health Science*, 12: 28-35.
- Martinea, A., Juanalcaniz, J., Sera-Crespo, P., Kapteijn, F. and Gascon, J. 2012. Electrochemical synthesis of some Archetypical Zn^{2+} , Cu^{2+} , and Al^{3+} Metal Organic Frameworks. *Crystal Growth & Design journal*, 12(7): 3489-3498.
- Min, H., Kam, L., George Z. 2017. Synthesis and applications of MOF derived porous nano-structures. *Green Energy and Environment*, 5: 1-28.
- Mitiku Abdissa, 2015. Removal of 2, 4-D, Atrazine and major metabolites of atrazine from aqueous solution by Fe-Zr-Mn nanocomposite. Thesis Submitted to The School of Graduate Studies, Department of Chemistry, Haramaya University, Ethiopia.
- Mohammadi, A.A., Alinejad A., Kamarehie, B., Javan, S. Ghaderpoury, A., Ahmadpour, M. and Ghaderpoori, M. 2017. Metal organic framework Uio-66 for adsorption of methylene blue dye from aqueous solutions. *International Journal of Environmental Science and Technology*, 14(9): 1959-1968.
- Moya, A.A. 2015. Theory of the formation of the electric double layer at the ion exchange membrane solution interface. *Journal of Physical Chemistry Chemical Physics*, 17:5207-5218.
- Mudhoo, A. and Garg, V. 2011. Sorption, transport and transformation of atrazine in soils, minerals and composts. *Pedosphere*, 21(1): 11-25.

- Mustapha, F., Dawood, G., Mohammed, S., Albaho, Vimala, Y., Binson, M. 2017. Pesticide risk behaviors and factors influencing pesticide use among farmers in Kuwait. *Science of the Total Environment*, 57: 490-498.
- Muthukumarana, C., Sivakumar, V. M., Thirumarimurugan, M. 2016. Adsorption isotherm and kinetic studies of crystal violet dye removal from aqueous solution using surfactant modified magnetic nano adsorbent. *Journal of the Taiwan Institute of Chemical Engineers*, 63: 354-362.
- Nair, S.A. and Pradeep, T. 2007. Extraction of Chlorpyrifos and Malathion from water by metal Nanoparticles. *Journal of Nanoscience and Nanotechnology*, 7: 1-7.
- Naushadn, M., Alothman, Z.A., Khan M.R. 2013. Removal of malathion from aqueous solution using De-Acidite FF-IP resin and determination by UPLC–MS/MS: Equilibrium, kinetics and thermodynamics studies. *Talanta*, 115: 15-23.
- Nejati, K., Davary, S., Saati, M. 2013. Study of 2, 4-dichlorophenoxyacetic acid (2, 4-D) removal by Cu-Fe-layered double hydroxide from aqueous solution. *Journal of Applied Surface Science*, 280: 67-73.
- Pal, O.R. and Vanjara, A.K. 2001. Removal of Malathion and butacholor from an aqueous solution by clays and organoclay, *Journal of Separation and Purification Technology*, 24: 167-172.
- Pizzutti, I.R., Dias, J.V. Kok, A., Cardoso, C. D., Vela G.E. 2016. Pesticide residues Method Validation by UPLC-MS/MS for Accreditation Purposes. *Journal of the Brazilian Chemical Society*, 27(7): 1165-1176.
- Potential applications of metal organic frameworks (PDF Download Available)*. Available from: https://www.researchgate.net/publication/239217610_Potential_applications_of_metal-organic_frameworks [accessed Sep 4, 2017].
- Pourata, R., Khataee, A., Aber, S., Daneshvar, N. 2009. Removal of the herbicide Bentazon from contaminated water in the presence of synthesized nanocrystalline TiO₂ powders under irradiation of UV-C light. *Desalination*, 249: 301-307.
- Qingxiang, Y., Qianqian, Z., ShuangShuang, R., ZhijunChen, H. 2017. Assembly of Zr-MOF crystals onto magnetic beads as a highly adsorbent for recycling nitrophenol. *Chemical Engineering Journal*, 323: 74-83.

- Rafiquea, U. and Nasreen, S. 2011. Decontamination of 2, 4-D and Atrazine through Adsorption on Soil under Different Modifications and its Kinetic and Equilibrium Studies. *International Journal of Chemical and Environmental Engineering*, 4 (2): 1-7.
- Ri Lee, Y., Kim, J., and Ahn, W. 2013. Synthesis of metal-organic frameworks: A mini review. *Korean Journal of Chemical Engineering*, 30(9): 1667-1680.
- Ross, M., Jones, T., Filipov, N. 2009. Disposition of the Herbicide 2 chloro-4-(ethylamino)-6 (isopropylamino)-s-triazine (Atrazine) and its major metabolites in Mice: A Liquid Chromatography/Mass Spectrometry analysis of Urine, Plasma, and Tissue Levels. *Journal of Drug Metabolism and Disposition*, 37: 776-786.
- Rostami, S., Pour, A.N., Salimi, A., Abolghasempour, A. 2018. Hydrogen adsorption in metal-organic frameworks (MOFs): Effects of adsorbent architecture. *International journal of hydrogen energy*, 43: 7072-7080.
- Ryan, J., Kuppler, Daren, J., Timmons, Qian-Rong, F., Trevor, A., Makal, M., Young, Daqiang, Y., Dan, Z., Wenjuan, Z., Hong, C. 2009. Potential applications of metal organic frameworks. *Coordination Chemistry Reviews*, 253: 3042-3066.
- Sabale, S, Zheng, J, Vemuri, R. 2016. Recent Advances in Metal Organic Frameworks for Heterogeneous Catalyzed Organic Transformations. *Synthesis and Catalysis*. 1(1): 1-8.
- Şahin, S. and Emik, S. 2018. Fast and highly efficient removal of 2, 4-D using amino-functionalized poly (glycidyl methacrylate) adsorbent: Optimization, equilibrium, kinetic and thermodynamic studies. *Journal of Molecular Liquids*, 260: 195-202.
- Salman, J.M. Njoku, V.O., Hameed B.H. 2011. Adsorption of pesticides from aqueous solution onto banana stalk activated carbon. *Chemical Engineering Journal*, 174: 41-48.
- Salman, J.Mand AL-Saad, K. A. 2012. Adsorption of 2, 4-dichlorophenoxyacetic acid onto date seeds activated carbon: equilibrium, kinetic and thermodynamic studies. *International journal of Chemical Sciences*, 10(2): 677-690.
- Silva, G.C., Luz, I., Francesc, X., Corma, A. and Garcia, H. 2010. Water stable zirconium benzenedicarboxylate metal organic frameworks as photocatalysts for hydrogen generation. *Chemistry: A European Journal*, 16: 11133-11138.
- Stevens, J. and Sumner, D. 1991. Herbicides. Handbook of pesticide toxicology, Vol. 3, San Diego, California, Academic Press.

- Tomlin, C, 1994. Pesticide manual, 10th Edition, British Crop Protection Council the Royal Society of Chemistry.
- Toytcheva, 2011. Food and Agriculture Organization of the United Nations. Accessed on 20/08/-017 though: <http://www.fao.org/docrep/014/am719e/am719e00.pdf>
- Tsegaye Girma, 2016. Synthesis and characterization of uio-66 metal organic frameworks for simultaneous sorption of methyl orange and methylene blue from aqueous solution. MSc. Thesis Submitted to The School of Graduate Studies, Department of Chemistry, Haramaya University, Ethiopia.
- Vakiti, R. 2012. Hydro/solvothermal synthesis, structures and properties of metal-organic frameworks based on s-block metals, masters theses & specialist projects. Western Kentucky University, Bowling Green, Kentucky.
- Valenzano, L., Civalleri, B., Chavan, S., Bordiga, S., Nilsen, M.H., Jakobsen, S., Lillerud, K.P., Lamberti, C. 2011. Disclosing the complex structure of UiO-66 metal organic framework: a synergic combination of experiment and theory. *Journal of Chemistry of Materials*, 23: 1700-1718.
- Vasimalai, N. and John, S. A. 2013. Biopolymer capped silver nanoparticles as fluorophore for Ultra-sensitive and selective determination of malathion. *Talanta*, 115: 24-31.
- Venugopal, N., Sumalatha, B., Syedabano. 2011. Spectrophotometric determination of malathion in environmental samples. *European Journal of Chemistry*, 9: 857-862.
- Wang, X., Song, X., Sun, K., Cheng, L., Ma, W. 2018. MOFs derived porous nanomaterials for gas sensing. *Polyhedron*, 152: 155-163.
- Wanjeri, V.W., Sheppard C.J., Prinsloo, A.R., Ngila, J.C., Ndungu P.G. 2018. Isotherm and kinetic investigations on the adsorption of Organophosphorus pesticides on graphene oxide based silica coated magnetic nanoparticles functionalized with 2-phenylethylamine. *Journal of Environmental Chemical Engineering*, 6: 1333-1346.
- Wei L., Yang Q., Zhilin Y., Wang W. 2016. Adsorption of 2, 4- D on magnetic graphene and mechanism study. *Colloids and Surfaces A: Physicochemical and Engineering Aspects*, 509: 367-375.
- World Health Organization (WHO). 1993. Guidelines for drinking-water quality. Recommendations, 2nd edition, Geneva.

- Yaghi, O.M. and Long, J.R. 2009. The pervasive chemistry of metal organic frameworks. *Chemical Society Review*, 38: 1213-1214.
- Yan, B., Yibo, D., LinHua, X., William, R., Jianrong, L. 2016. Zr-based metal organic frameworks: design, synthesis, structure, and applications. *Chemical Society Reviews*, 43: 5415-5418.
- Yingran, H., PanTang, Y., Dangchen, M., TaiShung, Ch. 2017. UiO-66 incorporated thin film nano composite membranes for efficient selenium and arsenic removal. *Journal of Membrane Science*, 541: 262-270.
- Zhang, K.D., Zhan, Z.Q., Tsai, F.C., Yu, X.Y., Zeng, X.Z., Jiang, X.Z., Jiang, T., Shi, D., Chang, C.J. 2017. Adsorption behavior of High Stable Zr-Based MOFs for the Removal of Acid Organic Dye from water. *Materials*, 10 (205): 1-11.
- Zhang, S.; Zeng, M.; Li, J.; Li, J.; Xu, J.; Wang, X. 2014. Porous magnetic carbon sheets from biomass as an adsorbent for the fast removal of organic pollutants from aqueous solution. *Journal of Material Chemistry A*, 2: 4391-4397.
- Zhang, J and Chen, Z. 2017. Metal-organic frame works as stationary phase for application in chromatographic separation. *Journal of Chromatography A*, 1530: 1-18.
- Zhang, Y., Yang, X., Cai Zhou H. 2018. Synthesis of MOFs for heterogeneous catalysis via linker design. *Polyhedron*, 154: 189-201.
- Zhou, F., Lu, N., Fan, B., Wang, H., Ruifeng, L. 2016. Zirconium containing UiO-66 as an efficient and reusable catalyst for transesterification of triglyceride with methanol. *Journal of Energy Chemistry*, 25: 874-879.

7. APPENDICES

7.1. Appendix Table

Appendix table 1. Effect of pH on adsorption capacity Malathion, 2, 4-D and mixture on UiO-66(Zr)

Malathion			2,4-D				Mixture		
pH	C_e (mg/L)	%A	q_e (mg/g)	C_e (mg/L)	%A	q_e (mg/g)	C_e (mg/L)	%A	q_e (mg/g)
2	1.165±0.103	76.7	0.959±0.026	1.45±0.072	71.01	0.888±0.018	1.487±0.064	70.26	0.878±0.016
3	0.443±0.206	91.1	1.139±0.052	0.047±0.036	99.06	1.238±0.009	1.068±0.024	78.63	0.983±0.006
4	0.034±0.006	99.3	1.241±0.001	0.155±0.072	96.91	1.211±0.018	0.552±0.042	88.95	1.112±0.01
5	1.405±0.06	71.9	0.899±0.015	1.474±0.075	70.53	0.882±0.019	1.738±0.087	65.24	0.816±0.022
6	2.402±0.103	52	0.649±0.026	1.546±0.055	69.09	0.864±0.014	2.1±0.042	57.99	0.725±0.01
7	3.364±0.06	32.7	0.409±0.015	2.433±0.091	51.34	0.642±0.023	2.505±0.024	49.9	0.624±0.006
8	3.88±0.06	22.4	0.28±0.015	3.032±0.095	39.35	0.492±0.024	2.798±0.024	44.04	0.551±0.006
9	4.155±0.103	16.9	0.211±0.026	3.404±3.404	31.92	0.399±0.027	2.979±0.042	40.42	0.505±0.01

Appendix table 2. Effect of Contact time on adsorption capacity Malathion, 2, 4-D and mixture on UiO-66(Zr)

Malathion				2,4-D			Mixture		
Con.time(min)	C_e (mg/L)	%A	q_e (mg/L)	C_e (mg/L)	%A	q_e (mg/L)	C_e (mg/L)	%A	q_e (mg/g)
30	0.167±0.072	96.67	1.208±0.018	0.168±0.076	96.64	1.208±0.019	0.227±0.042	95.46	1.193±0.011
60	0.021±0.007	99.58	1.245±0.002	0.092±0.076	98.17	1.227±0.019	0.185±0.042	96.3	1.204±0.011
90	0.208±0.072	95.83	1.198±0.018	0.193±0.044	96.13	1.202±0.011	0.381±0.106	92.38	1.155±0.026
120	0.421±0.007	91.58	1.145±0.002	0.219±0.117	95.62	1.195±0.029	0.465±0.064	90.7	1.134±0.016
150	0.5±0.125	90	1.125±0.031	0.27±0.159	94.61	1.183±0.04	0.535±0.087	89.3	1.116±0.022
180	0.542±0.072	89.17	1.115±0.018	0.27±0.159	94.61	1.183±0.04	0.577±0.064	88.46	1.106±0.016

Appendix table 3. Effect of Adsorbent dose on adsorption capacity Malathion, 2, 4-D and mixture on UiO-66(Zr)

Malathion				2,4-D			Mixture		
Dose(g)	C_e (mg/L)	%A	q_e (mg/g)	C_e (mg/L)	%A	q_e (mg/g)	C_e (mg/L)	%A	q_e (mg/g)
0.04	0.259±0.17	94.81	1.185±0.042	0.297±0.038	94.07	1.176±0.01	0.354±0.096	92.92	1.161±0.02
0.06	0.222±0.111	95.56	1.194±0.028	0.259±0.038	94.83	1.185±0.01	0.338±0.028	93.24	1.165±0.007
0.08	0.148±0.028	97.04	1.213±0.007	0.208±0.022	95.84	1.198±0.005	0.306±0.048	93.88	1.173±0.012
0.1	0.1±0.051	98	1.225±0.013	0.144±0.038	97.11	1.214±0.01	0.246±0.01	95.09	1.189±0.002
0.2	0.222±0.111	95.56	1.194±0.028	0.198±0.046	96.05	1.201±0.012	0.322±0.055	93.56	1.169±0.014
0.3	0.248±0.076	95.04	1.188±0.019	0.238±0.019	95.23	1.19±0.005	0.37±0.073	92.6	1.157±0.018
0.4	0.259±0.17	94.81	1.185±0.042	0.246±0.022	95.08	1.189±0.005	0.37±0.073	92.6	1.157±0.018

Appendix table 4. Effect of Agitation speed on adsorption capacity Malathion, 2, 4-D and mixture on UiO-66(Zr)

Malathion				2,4-D			Mixture		
A.speed	C_e (mg/L)	%A	q_e (mg/g)	C_e (mg/L)	%A	q_e (mg/g)	C_e (mg/L)	%A	q_e (mg/g)
50	0.456±0.019	90.89	1.136±0.005	0.289±0.059	94.21	1.178±0.015	0.373±0.01	92.53	1.157±0.003
75	0.341±0.013	93.19	1.165±0.003	0.238±0.045	95.25	1.191±0.011	0.289±0.041	94.21	1.178±0.01
100	0.122±0.019	97.56	1.219±0.005	0.212±0.022	95.76	1.197±0.006	0.248±0.072	95.04	1.188±0.018
125	0.367±0.068	92.67	1.158±0.017	0.096±0.059	98.09	1.226±0.015	0.22±0.086	95.59	1.195±0.022
150	0.463±0.085	90.74	1.134±0.021	0.289±0.059	94.21	1.178±0.015	0.164±0.01	96.72	1.209±0.003
175	0.593±0.17	88.15	1.102±0.042	0.509±0.059	89.82	1.123±0.015	0.303±0.048	93.94	1.174±0.012
200	0.648±0.162	87.04	1.088±0.04	0.587±0.059	88.27	1.103±0.015	0.388±0.004	92.23	1.153±0.001
225	0.667±0.111	86.67	1.083±0.028	0.677±0.081	86.46	1.081±0.02	0.409±0.004	91.82	1.148±0.001
250	0.678±0.113	86.44	1.081±0.028	0.742±0.045	85.17	1.065±0.011	0.409±0.007	91.82	1.148±0.002

Appendix table 5. Effect of Initial concentration on adsorption capacity Malathion, 2, 4-D and mixture on UiO-66(Zr)

Malathion				2,4-D			Mixture		
In.conc	C_e (mg/L)	%A	q_e (mg/g)	C_e (mg/L)	%A	q_e (mg/g)	C_e (mg/L)	%A	q_e (mg/g)
1	0.04±0.004	96.05	0.24±0.001	0.05±0.04	95.05	0.238±0.009	0.107±0.06	89.35	0.223±0.015
5	0.074±0.037	98.52	1.231±0.009	0.12±0.04	97.6	1.22±0.009	0.381±0.052	92.37	1.155±0.013
10	0.395±0.021	96.05	2.401±0.005	0.52±0.07	94.81	2.37±0.018	1.052±0.052	89.48	2.237±0.013
20	0.988±0.077	95.06	4.753±0.019	1.56±0.07	92.21	4.611±0.018	2.426±0.079	87.87	4.393±0.02
30	2.062±0.247	93.13	6.985±0.062	2.85±0.05	90.49	6.787±0.013	4.247±0.103	85.84	6.438±0.026
40	3.185±0.037	92.04	9.204±0.009	4.25±0.04	89.36	8.936±0.009	6.258±1.546	84.36	8.436±0.387
50	4.321±0.566	91.36	11.42±0.141	5.65±0.05	88.69	11.09±0.013	9.935±0.13	84.13	10.02±0.032

Appendix table 6. Results for Malathion, 2, 4-D and mixture adsorption isotherms of UiO-66(Zr)

Malathion				2,4-D			Mixture		
In.conc	C_e (mg/L)	q_e (mg/g)	C_e/q_e	C_e (mg/L)	q_e (mg/g)	C_e/q_e	C_e (mg/L)	q_e (mg/g)	C_e/q_e
1	0.043±0.021	0.239	0.179	0.089±0.068	0.228	0.39	0.053±0.031	0.237	0.225
5	0.245±0.029	1.189	0.206	0.493±0.17	1.127	0.437	0.34±0.031	1.165	0.292
10	0.665±0.056	2.334	0.285	1.085±0.231	2.229	0.487	0.733±0.503	2.317	0.317
20	1.63±0.073	4.592	0.355	2.344±0.111	4.414	0.531	1.6±0.201	4.6	0.348
30	2.863±0.056	6.784	0.422	3.974±0.17	6.506	0.611	2.733±0.306	6.817	0.401
40	4.866±0.56	8.784	0.554	6.159±0.231	8.46	0.728	4.067±0.115	8.983	0.453
50	5.842±0.366	11.04	0.529	7.789±0.111	10.553	0.738	6.4±0.200	10.9	0.587

Appendix Table 7. Results for Malathion kinetic Adsorption of UiO-66(Zr)

Malathion						
Cont.(hr)	C_e (mg/L)	q_e (mg/g)	q_t (mg/g)	log(q_e-q_t)	t/ q_t	%Adsorption
0.5	0.33±0.23	1.17±0.06	0.77±0.06	-0.398	0.625	93.3
1	0.23±0.03	1.19±0.01	0.94±0.02	-0.602	1.06	95.5
1.5	0.67±0.12	1.08±0.03	0.96±0.01	-0.924	1.56	86.7
2	0.73±0.07	1.07±0.02	0.99±0.02	-1.126	2.01	85.5
2.5	0.8±0.2	1.05±0.04	1±0.02	-1.494	2.5	84
3	0.83±0.06	1.04±0.01	1.02±0.01	-1.799	2.94	83.3

Appendix Table 8. Results for 2,4-D kinetic Adsorption of UiO-66(Zr)

2,4-D						
Cont.(hr)	C_e (mg/L)	q_e (mg/g)	q_t (mg/g)	log(q_e-q_t)	t/ q_t	%Adsorption
0.5	0.422±0.001	1.145±0.0	0.87±0.01	-0.562	0.575	91.6
1	0.105±0.006	1.224±0.002	1.077±0.025	-0.836	0.929	97.9
1.5	0.33±0.017	1.168±0.004	1.083±0.015	-1.083	1.385	93.4
2	0.438±0.017	1.14±0.004	1.09±0.01	-1.305	1.835	91.2
2.5	0.522±0.011	1.12±0.003	1.093±0.012	-1.609	2.287	89.6
3	0.562±0.025	1.11±0.006	1.097±0.006	-2.006	2.736	88.8

Appendix Table 9. Results for mixture kinetic Adsorption of UiO-66(Zr)

Mixture						
Cont.(hr)	C_e (mg/L)	q_e (mg/g)	q_t (mg/g)	log(q_e-q_t)	t/ q_t	%Adsorption
0.5	0.211±0.011	1.197±0.003	0.843±0.006	-0.451	0.593	95.8
1	0.098±0.016	1.225±0.02	1.08±0.02	-0.841	0.926	98
1.5	0.263±0.011	1.184±0.003	1.107±0.011	-1.117	1.355	94.7
2	0.379±0.021	1.155±0.0	1.109±0.0	-1.339	1.803	92.4
2.5	0.481±0.016	1.13±0.004	1.11±0.0	-1.709	2.252	90.4
3	0.495±0.055	1.126±0.014	1.117±0.015	-2.067	2.687	90.1

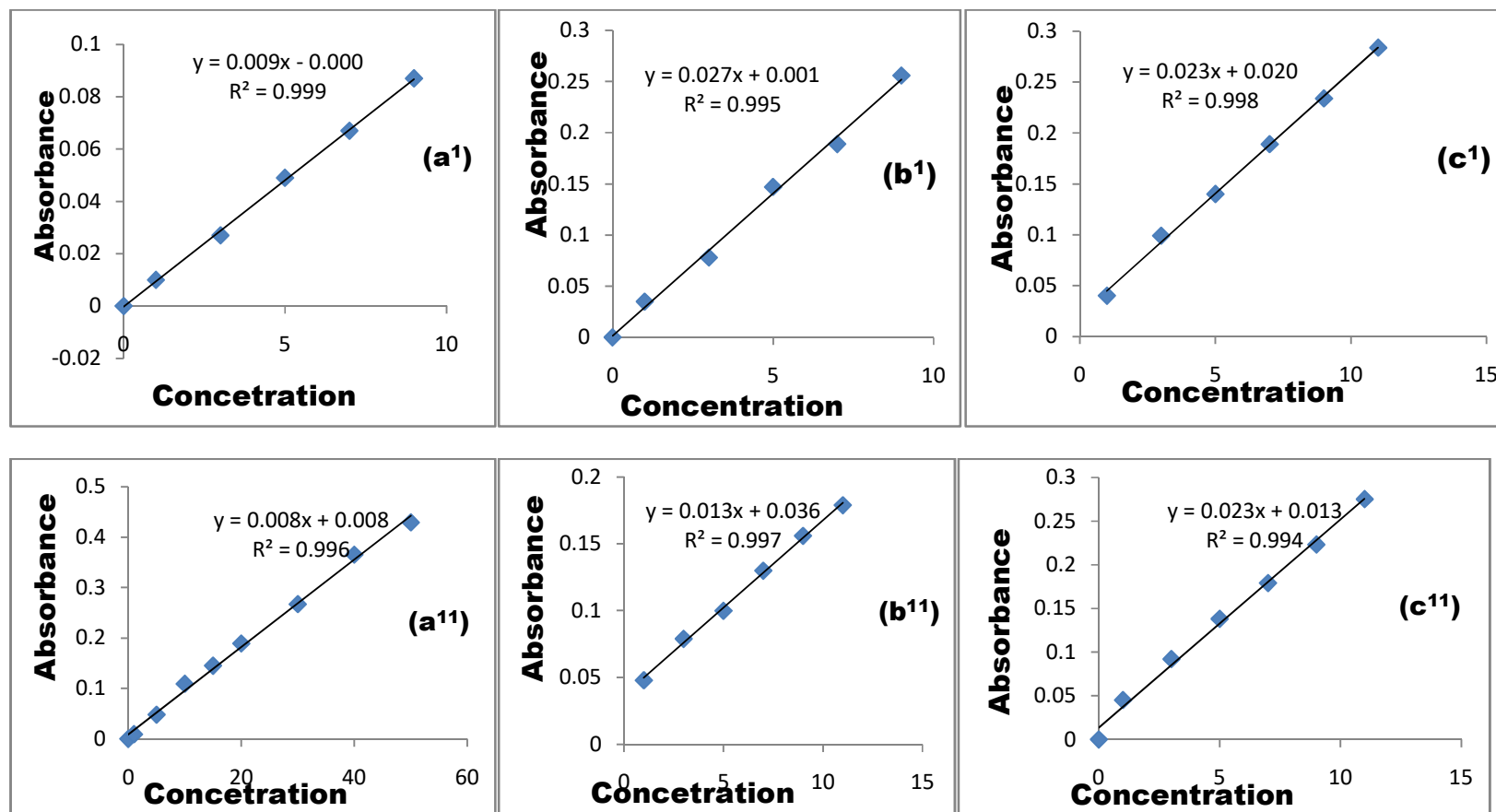
Appendix table 10. Dimensionless equilibrium parameter (R_L)

Dimensionless equilibrium parameter (R_L)			
Intial-concentration	Malathion	2,4-D	Mixture
1	0.73	0.901	0.831
5	0.351	0.645	0.495
10	0.213	0.476	0.329
20	0.119	0.313	0.197
30	0.083	0.233	0.14
40	0.063	0.185	0.109
50	0.051	0.154	0.089

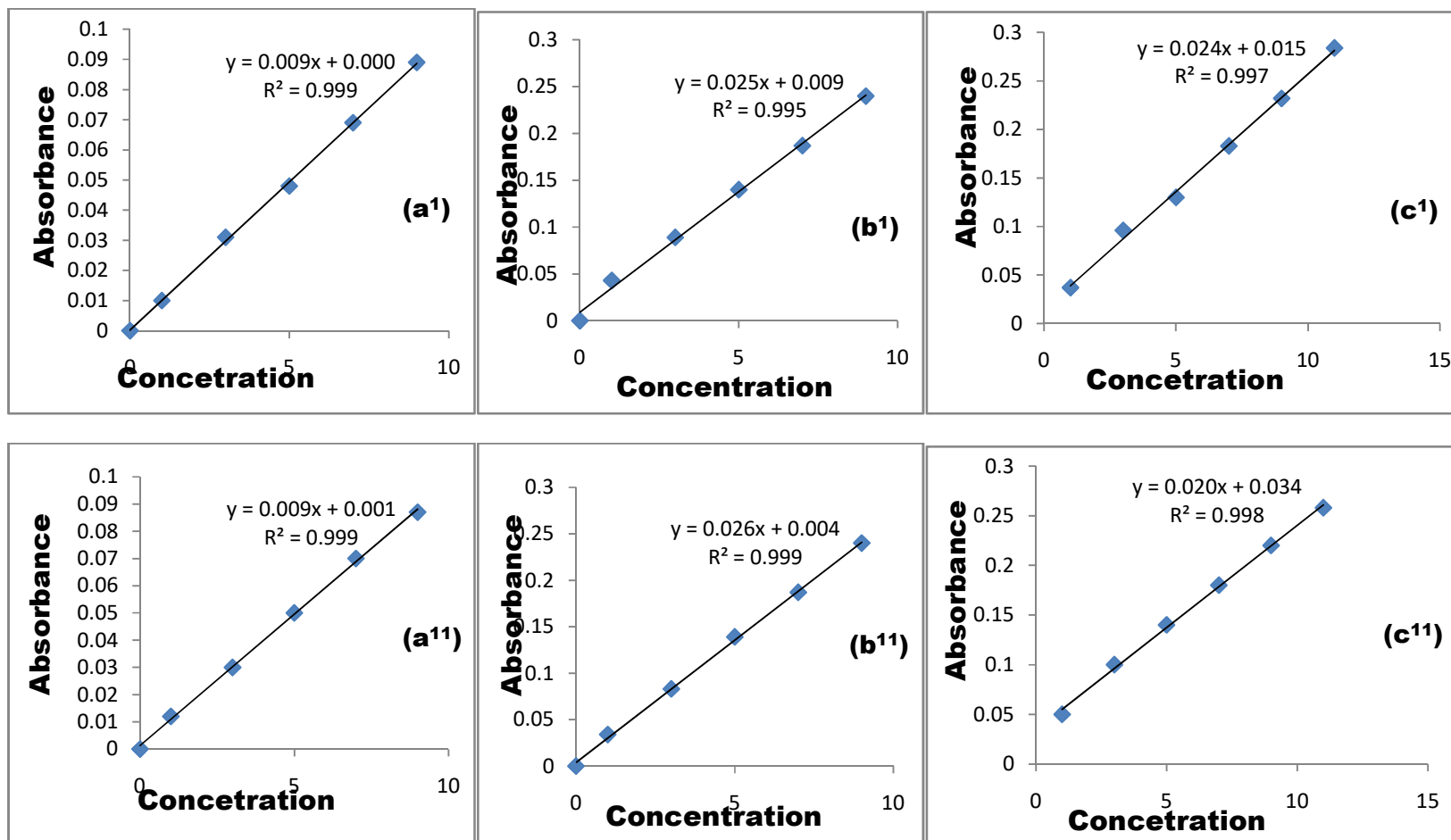
Table 11. Recovery (%) values of UiO-66(Zr) based analysis in real water samples (n = 3 mean \pm SD)

Sample	Pesticide	% Recovery \pm SD		
		Unspiked	5 mg/L spiked	10 mg/L spiked
Tap water (Hu)	Malathion	ND	104 \pm 3.7	78.9 \pm 3.6
	2,4-D	ND	98.7 \pm 3.4	90.8 \pm 0.9
Tap water (bate)	Malathion	ND	108 \pm 1.9	79 \pm 3.6
	2,4-D	ND	111 \pm 5.0	97.4 \pm 2.0

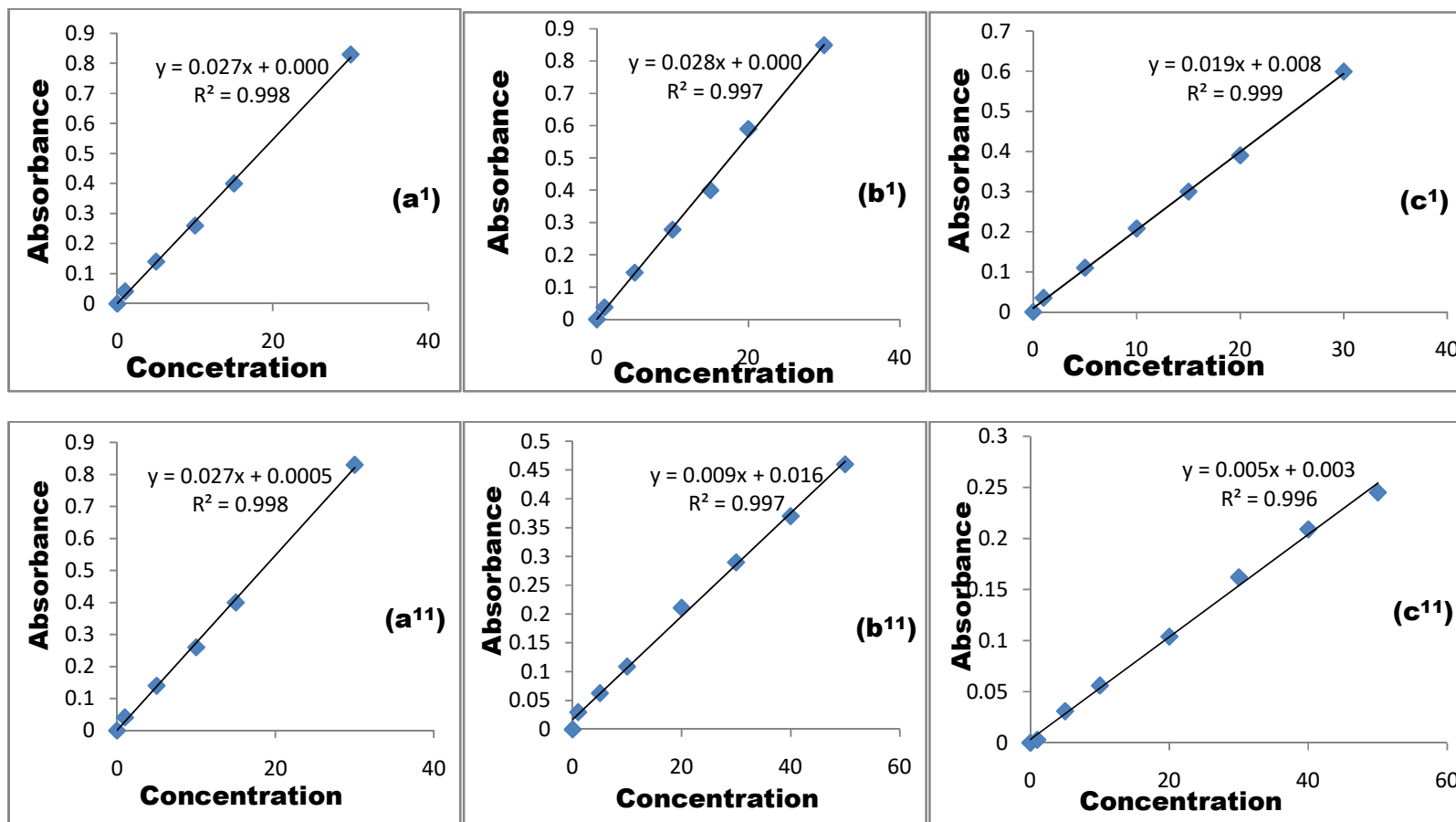
7.2. Appendix Figures



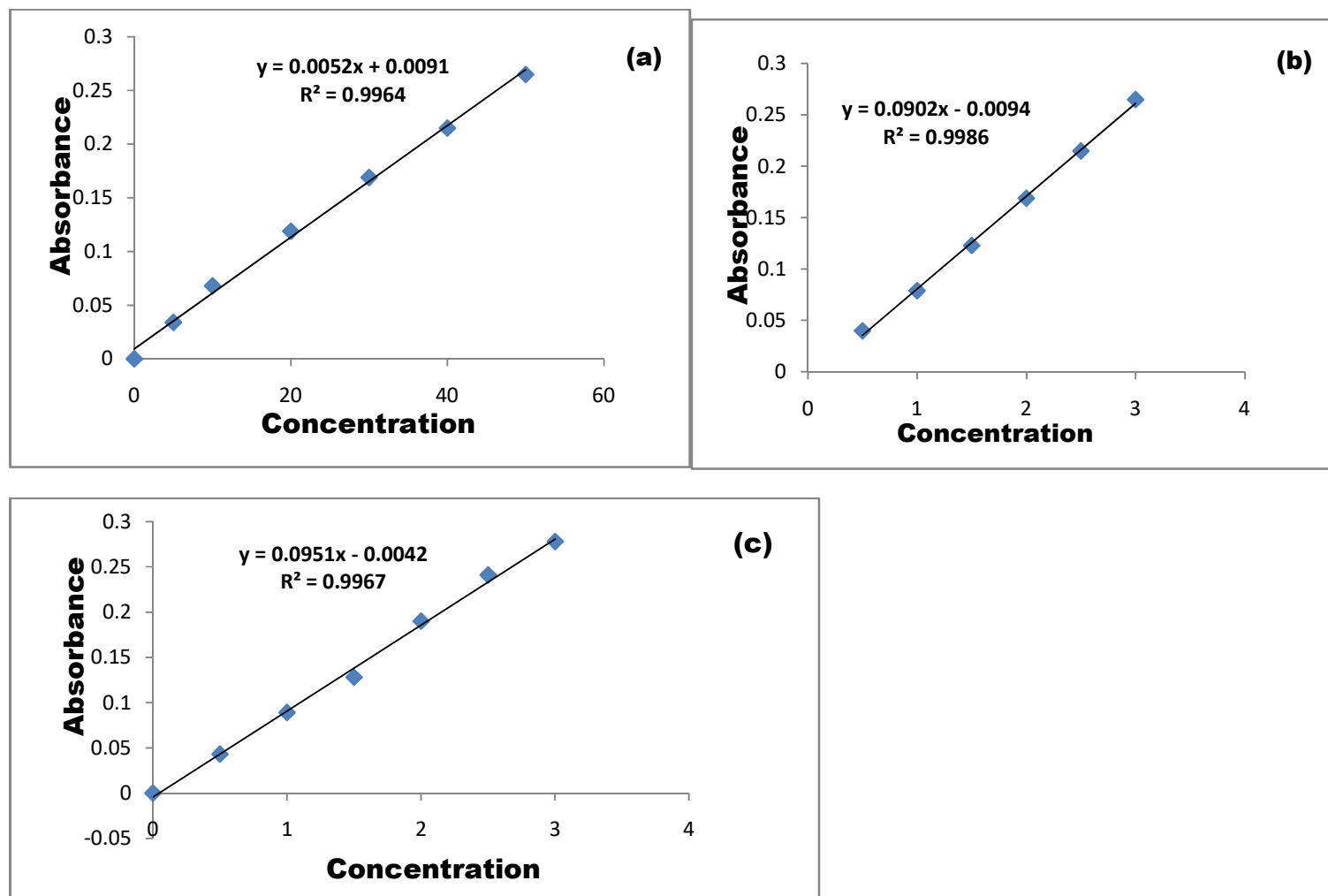
Appendix figure 1. Calibration curve of Malathion (a¹,a¹¹), 2,4-D (b¹,b¹¹) and mixture(c¹,c¹¹) for pH and contact time optimization, respectively.



Appendix figure 2. Calibration curve of Malathion (a¹,a¹¹), 2, 4-D (b¹,b¹¹) and mixture (c¹,c¹¹) for Agitation speed and Adsorbent dose optimization, respectively.



Appendix figure 3. Calibration curve of Malathion (a¹, a¹¹), 2, 4-D (b¹, b¹¹) and mixture (c¹, c¹¹) for initial concentration optimization and Adsorption isotherm, respectively.



Appendix figure 4. Calibration curve of Malathion (a), 2,4-Dm(b) and mixture (c) for kinetic studies.